Using Fractal Geometries to Understand Urban Drainage Networks and Green Stormwater Infrastructure Development

A Thesis

Submitted to the Faculty

of

Drexel University

by

Scott Martin Jeffers

in partial fulfillment of the

requirements for the degree

of

Doctor of Philosophy

June 2017

Dedications

This work is dedicated to my Mom for her unconditional love and support throughout my life and my Dad, who would sing, “Math and Science, Math and Science, go together in a nice Alliance!” whose passing during this dissertation process is a reminder to work towards a better world.

Acknowledgements

I would like to acknowledge the following for their support in enabling this work:

- The Boston Water Sewer Commission for providing sewer maps and flow data critical to the analysis
- Dr. Franco Montalto, my adviser for his continued guidance
- Dr. Paul Kirshen and Dr. Ellen Douglas of the University of Massachusetts Boston for facilitating a collaborative relationship between Drexel University, the University of Massachusetts Boston, and the Boston Water Sewer Commission
- My committee for providing meaningful feedback throughout this process including: Stephen Maakestad, Dr. Michael Waring, Dr. Patrick Gurian, and Dr. Charles Haas
- Dr. Ferdi Hellweger from Northeastern University who provided the Artificial Network Generator (ANGel) developed by Dr. Indrani Ghosh
- Computation Hydraulics International (CHI) for providing an education license to use PCSWMM software
- Consortium for Climate Risk in the Urban Northeast (CCRUN) for travel and logistical support

Table of Contents

LIST OF TABLES……………………………………………………………………………………viii

LIST OF FIGURES...…………………………………………………………………………………ix

ABSTRACT…...……………………………………………………………………………………xii

1 CHAPTER 1: INTRODUCTION ……………………………………………………………………1

1.1 The impact of urbanization on hydrology……………………………………………………1

1.2 Green Stormwater Infrastructure as a means of improving urban hydrology………………7

1.3 Modeling Urban Hydrology and GSI …………………………………………………………12

1.3.1 Traditional Methods……………………………………………………………………12

1.3.2 Hydrologic and Hydraulic Modeling……...……………………………………………13

1.3.3 GSI Modeling Techniques ………………………………………………………………13

1.3.4 Large Scale GSI Modeling………………………………………………………………15

1.3.5 Simplifications of Hydrologic Models ……………………………………………………15

1.4 Scaling and Self-Similarity in Hydrologic Systems …………………………………………17

1.4.1 Scaling Laws in Natural Systems ………………………………………………………17

1.4.2 Scaling Laws in Urban Systems…………………………………………………….25

1.4.3 Using Scaling Laws to create artificial networks…………………………………………26

1.5 Research Objectives and Purpose ……………………………………………………………30

1.6 Dissertation Structure …………………………………………………………………………32

1.7 List of References ………………………………………………………………………………33

2 CHAPTER 2: APPLYING RIVER BASIN SCALING LAWS TO URBAN CATCHMENTS……37

2.1 Abstract ………………………………………………………………………………………37

2.2 Introduction …………………………………………………………………………………38

2.2.1 Applications in urban systems …………………………………………………………44

2.2.2 Motivation ………………………………………………………………………………45

2.3 Methodology …………………………………………………………………………………47

2.3.1 Site Description …………………………………………………………………………47

2.3.2 Map analysis……………………………………………………………………………47

2.3.3 Testing Hack’s Law in urban sewersheds ……………………………………………47

2.3.4 Measuring the consistency of Horton order ratios at each scale ………………48

2.3.5 Additional Analysis ……………………………………………………………………48

2.4 Results…………………………………………………………………………………………50

2.5 Discussion 54
2.6 Conclusions....................56
2.7 List of References 57
3 CHAPTER 3: MODELING URBAN SEWERS WITH ARTIFICIAL FRACTAL GEOMETRIES....................59
3.1 Abstract 59
3.2 Introduction 61
3.3 Methodology 66
3.3.1 Site Description 66
3.3.2 Model Development 68
3.3.3 Further Model Considerations 70
3.3.4 Further Model Validation 71
3.4 Results....................73
3.5 Discussion....................81
3.5.1 Assessing Model Quality 81
3.5.2 Analysis of Network Resolution and the effect of Strahler Ordering 82
3.6 Conclusions....................87
3.7 List of References 89
4 CHAPTER 4: USING ARTIFICIALSEWER NETWORKS TO STUDY THE ROLE OF GREEN STORMWATER INFRASTRUCTURE IN REDUCING RUNOFF DURING BOTH HISTORIC AND FUTURE CHANGED PRECIPITATION 91
4.1 Abstract 91
4.2 Introduction....................93
4.2.1 Background 93
4.2.2 The case for a new model....................95
4.2.3 Research Objectives 98
4.2.4 GSI Development in East Boston....................99
4.3 Methodology....................100
4.3.1 GSI Scenarios 100
4.3.2 Effect of Climate Change....................102
4.3.3 Model Assumptions 102
4.4 Results 109
4.5 Discussion 116
4.5.1 GSI Scenarios 116

4.5.2 Spatial Analysis 117
4.5.3 Effect of Climate Change 117
4.6 Conclusions 123
4.7 List of References 125
5 CHAPTER 5: CONCLUSION 128
5.1 Significance 133
5.2 Limitation / Future Work 134
5.3 List of References 137
6 VITA 138

List of Tables

Table 2.1: Fractal parameters determined from 13 sites with areas greater than 200 km^2 (adapted from Rigon et al. 1996) ……43

Table 2.2: Horton Ratios observed in river basins (adapted from Marani et al. (1991) and Rosso et al. (1991))……44

Table 2.3: Description of urban catchments used in the study……49

Table 2.4: Hack's Law and Fractal Coefficients ……51

Table 2.5: Results from the Horton Analysis for all Sites. ……53

Table 2.6: Summary of average Horton order ratios in this study and other literature reviewed sources ……55

Table 3.1: Summary of the network geometries in the physically based and artificial fractal model……72

Table 3.2: Calibrated sensitive parameters in each model for Section 77……75

Table 3.3: Result from the April to May, 2016 simulation at Section 77. Events used in the calibration process are denoted with a * ……76

Table 3.4: Result from the April to May, 2016 simulation at Section 81……76

Table 3.5: Comparison of different Strahler order models……85

Table 3.6: Calibrated sensitive parameters in each Strahler order model for Section 77……85

Table 3.7: Comparison of different Strahler order models……85

Table 4.1: Summary of the network geometries in the physically based and artificial fractal model……105

Table 4.2: SWMM LID Control Input Parameters……106

Table 4.3: Summary of Green Stormwater Infrastructure Implementation Scenarios ……107

Table 4.4: Evaporation Rates used in the simulation from Logan Airport……108

Table 4.5: Extreme Events projected for East Boston (Reproduced from Climate Ready Boston, 2016) ……108

Table 4.6: Extreme event discharge reductions due to Case I greening scenario ……122

Table 5.1: Parameters to consider in a future analysis……135

List of Figures

Figure 1.1: Impervious cover in urban areas shifts the water budget largely in favor of runoff (US EPA, 2003) ……………………………………………………………………………………………2

Figure 1.2: Typical effect of urbanization on the rainfall-runoff response (Viessman and Lewis, 2002) ……………………………………………………………………………………………4

Figure 1.3: In normal dry weather, sanitary sewage enters into the sewer and is directed to the publically owned treatment works (POTW). During wet weather, stormwater enters and overburdens the system resulting in a combined sewer overflow (US EPA, 2004) ………………4

Figure 1.4: Diagram of combined sewer urban drainage and the potential of combined sewer overflow (Tchobanoglous et al., 2002) …………………………………………………………………5

Figure 1.5: Illustration of an oxygen sag curve. High nitrogen content produces nutrient loading and eutrophication. This in turn induces aerobic metabolism that leads to hypoxia which decreases dissolved oxygen levels (Davis and Masten, 2008) ………………………………………6

Figure 1.6: Water budget of a streetside bioswale. Runoff that enters the site will either infiltrate, be captured as storage, or leave the site if the site reaches capacity. The site will recharge after the storm through evapotranspiration or deep infiltration………………………………………………8

Figure 1.7: Areas in Philadelphia where infiltration potential is high, likely, or not recommended. To clarify potential, geotechnical investigation is recommended. (O'Rouke et al., 2012) ………11

Figure 1.8: Reference for various scales used in hydrology (Gleeson and Paszkowski, 2014) …17

Figure 1.9: Strahler ordering shown in a hypothetical river basin. When two first order streams meet a second order is form and so forth. ……………………………………………………………18

Figure 1.10: Hack's Law relates drainage area to stream length ($l \sim a^h$),In the example above, Hack's Law is consistent relating A1 to L1 and A2 to L2 ……………………………………………20

Figure 1.11: Drainage area related to basin length for a number of river basins ranging from hillside depressions to the world's largest rivers (Montgomery and Dietrich, 1992). ……………20

Figure 1.12: (Right Image): Measuring the coastline in 200 km increments yields about 2400 km (Left image): 50 km increments about 3400 km (Image from Wikicommons, 2005) ……………22

Figure 1.13: Dimensions are typically thought in terms of length (1st dimension), width (2nd), and depth (3rd) (left image) (reproduced from Ryan, 2007). Fractal dimensions can be between two dimensions illustrated with the Koch curve fractal (right image) (reproduced from Vassallo, 2005). As the fractal dimension increases, the density increases as it approaches the 2nd dimension. 22

Figure 1.14: Plan view of a river basin shows broken into geometric components for fractal analysis. This analysis is repeatable at each scale denoted by an apostrophe (Reproduced from Dodds and Rothman, 1998). ……………………………………………………………………………24

Figure 1.15: a) Binary dendritic fractal tree showing four Strahler stream orders b) The Tokunaga fractal method includes space filling branches more characteristic the drainage density found in natural stream networks (adapted from Turcotte and Newman, 1996) ……………………………28

Figure 2.1: Strahler ordering shown in a hypothetical river basin. When two first order streams meet a second order is form and so forth. ……………………………………………………………39

Figure 2.2: Hack's Law relates drainage area to stream length ($l \sim a^h$). In the example above, Hack's Law is consistent relating A1 to L1 and A2 to A2 41

Figure 2.3: Plan view of a river basin shows broken into geometric components for fractal analysis. This analysis is repeatable at each scale denoted by an apostrophe (Reproduced from Dodds and Rothman, 1999) 42

Figure 2.4: Strahler order applied to each of the drainage networks 49

Figure 2.5: Hack's Law applied over the urban catchments 52

Figure 3.1: a) Binary dendritic fractal tree showing four Strahler stream orders b) The Tokunaga fractal method includes space filling branches more characteristic the drainage density found in natural stream networks (adapted from Turcotte and Newman, 1996) 62

Figure 3.2: Dimensions are typically thought in terms of length (1st dimension), width (2nd), and depth (3rd) (left image) (reproduced from Ryan, 2007). Fractal dimensions can be between two dimensions illustrated with the Koch curve fractal (right image) (reproduced from Vassallo, 2005). As the fractal dimension increases, the density increases as it approaches the 2nd dimension. 62

Figure 3.3: Land use of East Boston Section 77...67

Figure 3.4: Images from PCSWMM showing the physically based (left) and artificial fractal (right) networks for Section 77. The regulator in this submodel is the lowest point. 69

Figure 3.5: DWF analysis from 4/15 to 4/23. Average DWF was 0.053 m^3/s. The NSE of the modeled DWF over the observed period was 0.73. 71

Figure 3.6: Images from PCSWMM comparing the physically based (left) and artificial fractal (right) networks for Section 81. The regulator in this submodel is the lowest point. 72

Figure 3.7: Sensitivity Analysis of the physically based and artificial simulated network in East Boston Section 71 for May 4th 12.45 mm event 74

Figure 3.8: Event Summary for the simulations in East Boston Section 77 77

Figure 3.9: Selected storms for the physically based and artificial fractal simulated networks in East Boston Section 77 78

Figure 3.10: Event Summary for the simulations in East Boston Section 81...........................79

Figure 3.11: Selected storms for the physically based and artificial fractal simulated network in East Boston Section 81 80

Figure 3.12: Different resolutions of the artificial network defined by Strahler order representing 1, 10, 24, and 173 subcatchments. 84

Figure 3.13: Hydrologic response of different modeled Strahler orders 86

Figure 4.1: Land use of the study catchment...104

Figure 4.2: Images from PCSWMM comparing the physically based (left) and artificial fractal (right) models 105

Figure 4.3: Summary of rain storms simulated ……………………………………………………107

Figure 4.4: Event based volumetric and peak flow reductions in the simulated GSI scenarios 111

Figure 4.5: Selected hydrographs the simulated GSI scenarios over varying rainfall depth……115

Figure 4.6: Volumetric and peak flow reductions of the simulated GSI scenarios……………….119

Figure 4.7: Spatial configurations of LID controls simulated in the artificial network. Presence of LID is shown in the lighter region of the network. GSI concentrated at the top of the catchment (left) resulted in 41% of the impervious treated by GSI and when concentrated on one side of the catchment (right) resulted in 38% treated. ……………………………………………………120

Figure 4.8: Volumetric and peak discharge reductions of various LID spatial configurations …121

Figure 4.9: Climate Adjusted Annual Rainfall under Case I and IV GSI scenarios………………122

Figure 5.1: The default fractal network (left) compared to the irregular network (right) (reproduced from Ghosh et al., 2006)……………………………………………………………………………134

Abstract

Using Fractal Geometries to Understand Urban Drainage Networks and Green Stormwater Infrastructure Development

Scott Martin Jeffers
Franco Montalto, Ph.D.

Human development significantly alters the hydrologic cycle. This change is most apparent in urban environments where infrastructure in many ways has replaced the natural ecosystem. In particular to cities, construction with impervious surfaces greatly increases runoff in the water budget. One contemporary way to manage urban runoff is through the use of green stormwater infrastructure (GSI). The impact of GSI on the urban hydrologic response can be assessed through modeling the drainage network based on the sewer layout, pipe diameter, inverts, catchment properties, and other physically based parameters. Developing physically based models can often be difficult given the limited availability of sewer plans and the time required to make a full resolution model. As a result, municipal drainage modelers often resort to simplifications that have (in certain circumstances) been shown to be less accurate than higher resolution models. Artificial sewer networks, based on fractal geometries typical of natural river basins, can help improve simplified models with accuracy similar to physically based models. This point is developed in three logical steps: 1) establish that fractal geometries exist in urban drainage networks in order to build confidence that they could be modeled as such, 2) develop artificial models to simulate urban drainage networks and compare the results to traditional physically based models in reproducing observed flow measurements, and 3) demonstrate applications of artificial models to address contemporary urban hydrologic challenges related to GSI. While previous research has, to a limited degree, revealed fractal geometries in urban drainage networks, there has been little attempt to apply fractal scaling laws developed in natural river basins to urban sewer systems. Additionally, artificial models incorporating fractal

geometries have not been validated against hydrologic observations. This research addresses this knowledge gap and shows that 1) fractal geometries exist in urban drainage networks as defined by Hack’s Law and Horton order in three study locations in East Boston, Massachusetts and the Bronx, New York, 2) in a 54 ha study catchment in East Boston, Massachusetts, over a one month duration of observed sewer flow both the artificial fractal based and physically based models when calibrated produced strong Nash-Sutcliffe model efficiency coefficients of 0.85, and 3) GSI when simulated with artificial models produces hydrologic simulations comparable to their physically based counterparts and can be used to address questions related to the practice such as effective levels of implementation, spatial layout of the systems throughout the catchment, and adaptation to increasing rainfall patterns associated with climate change.

Chapter 1: Introduction

The *Anthropocene* is the proposed name for our contemporary geological epoch, during which human activity has expanded rapidly in both scope and scale, to the point where it has come to play a significant (if not defining) role in shaping global ecosystems (Steffen et al., 2011). The term has steadily gained currency with commentators across a wide range of disciplines who observed that human infrastructure development, while creating many benefits for society, has dramatically and irrevocably transformed the natural world. These changes have been apparent in urban environments, where human infrastructure has most thoroughly displaced naturally functioning systems. Of particular importance to this study are the processes by which urban infrastructural development can substantially increase the 'impervious surface area' (most notably through transportation and building construction), which alters the hydrologic cycle dramatically and produces excessive stormwater runoff creating detrimental effects on both the built and natural environment.

This dissertation is rooted in improving methods to quantify urban hydrology and the implementation of stormwater mitigating strategies, in particular green stormwater infrastructure (GSI). In the introduction of this research, a background on the following fundamental topics are discussed:

1) *The impact of urbanization on hydrology:*

   A review of urban hydrology and the detrimental effects that motivate research into the subject.

2) *Green Stormwater Infrastructure (GSI) as a means of improving urban hydrology:*

   Implementation of GSI has shown promising results to improve urban hydrology. This section will provide a background on the engineering principles behind GSI and discuss ways that it is currently employed in the United States.

3) *Modeling Urban Hydrology and GSI:*

   Engineers and urban planners use computer enabled models to simulate urban hydrology. Contemporary approaches have implemented GSI into these models to better understand development. This section will review current practices.

4) *Scaling and Self-Similarity in Hydrologic Systems:*

In order to mitigate many of the issues relating to excessive urban stormwater with GSI, large scale implementation is required. This section will discuss how scale is traditionally viewed in natural hydrology. One of the main contributions of this research is an applications of these traditional hydrologic scaling laws in urban systems. In addition, these scaling laws can be applied to improve traditional modeling approaches.

At the conclusion of the introduction, the research objectives and purpose of the dissertation is discussed including the fundamental questions and corresponding hypotheses that will be tested. In addition, the dissertation structure of the subsequent chapters is presented.

The impact of urbanization on hydrology

In natural environments, the water budget of a rain event can be determined through the processes of infiltration, evapotranspiration, and runoff. In urban landscapes constructed with impervious materials such as concrete and asphalt (which hinder the processes of infiltration and evapotranspiration), the water budget is largely shifted towards runoff (Figure 1.1).

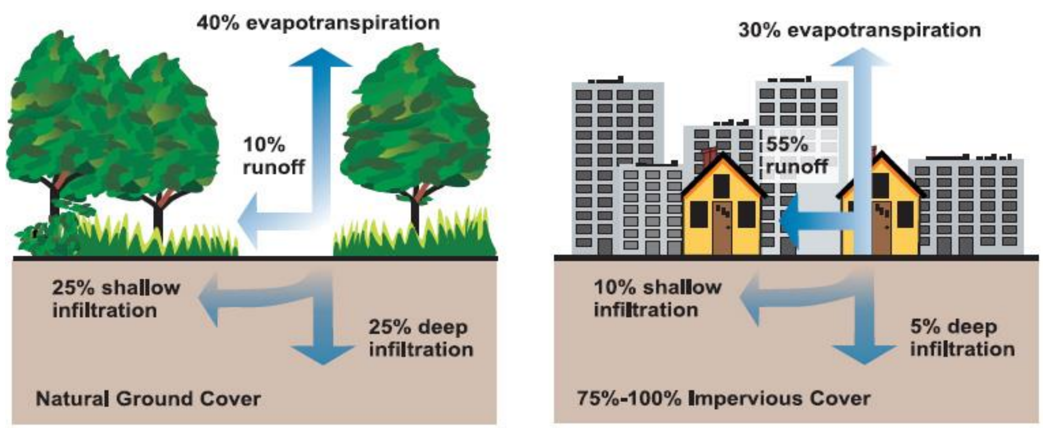

Figure 1.1: *Impervious cover in urban areas shifts the water budget largely in favor of runoff (US EPA, 2003).*

The excessive stormwater runoff brought on by construction with impervious materials has become a major concern for urban planners due to its detrimental effects on ecosystems, water quality, and sewer infrastructure. In comparison to natural landscapes, urban environments produce significantly more stormwater runoff during any given rain event, with peak discharges occurring faster as illustrated by Figure 1.2 (Viessman and Lewis, 2002). This increased 'flashiness' of the runoff translates into higher velocity flows, which accelerates the erosion of stream banks and hastens the degradation of surrounding ecosystems. Additionally, high-velocity runoff is more likely to pollute surrounding bodies of water as it washes away lawn fertilizers and chemicals, automotive petrochemicals, garbage, and a number of other toxins.

In order to address these issues, beginning in the 1970s, civil engineers began phasing out conventional designs for sewer conveyance systems (which were organized primarily to prevent flooding) in favor of designs that placed a greater emphasis on stormwater control structures such as detention basins as a means of mitigating the negative impacts to drainage networks (National Research Council, 2008). In 1987, when stormwater began to gain wider recognition as a significant source of pollution, the United States amended the Clean Water Act to control discharges under the National Pollutant Discharge Elimination Act (National Research Council, 2008). Since then, stormwater management priorities shifted towards local source control, flow attenuation, and treatment using constructed or natural landscape features (Niemczynowicz, 1999).

One type of legacy sewer system found in many older cities are 'combined sewer systems', meaning that sanitary sewage and stormwater runoff are collected together using a single collection system. Combined sewers are prone to overflowing from stormwater runoff during rain events that exceed a given depth, duration, and/or intensity. The result is a combined sewer overflow (CSO), in which the untreated sewage and stormwater are discharged directly into the local waterways including rivers and streams. A detailed schematic of this process is depicted in Figures 1.3 and 1.4 below.

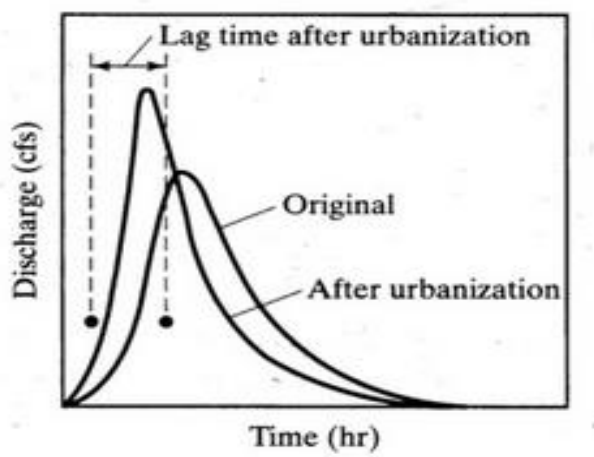

Figure 1.2: *Typical effect of urbanization on the rainfall-runoff response (Viessman and Lewis, 2002).*

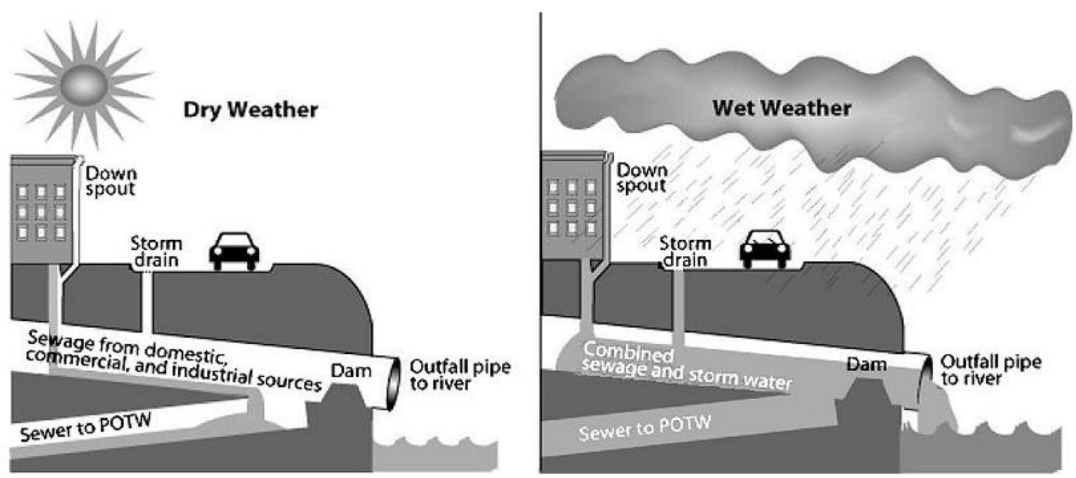

Figure 1.3: *In normal dry weather, sanitary sewage enters into the sewer and is directed to the publically owned treatment works (POTW). During wet weather, stormwater enters and overburdens the system resulting in a combined sewer overflow (US EPA, 2004).*

The severe pollution of waterways during a CSO poses acute risks to both natural ecosystems and public health, and has been linked to the ingestion of oocysts such as Cryptosporidium and Giardia—parasitic protozoan that can cause severe gastrointestinal illness in humans (Arnone et al. 2005). These parasites make their way into drinking water treatment plants that draw water from local sources and utilize water treatment processes that often fail to filter them from the supply of drinking water (Teunis et al., 1997). The public may also come into contact with these parasites during recreational use of the polluted waters. The EPA estimates that the exposure during recreational activity alone results in 3,500 to 5,500 gastrointestinal illnesses per year (Tibbetts, 2005).

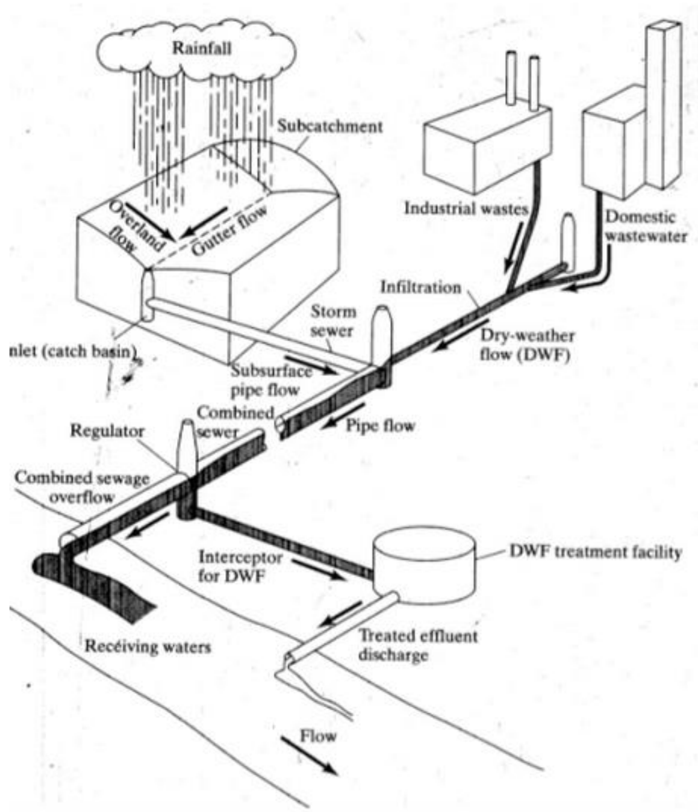

Figure 1.4: *Diagram of combined sewer urban drainage and the potential of combined sewer overflow (Tchobanoglous et al., 2002)*

Another potential consequence of CSOs is eutrophication, which can potentially offset entire ecosystems. During a CSO, nutrient-rich material may enter the receiving waters, thus increasing its biological oxygen demand (BOD). This can potentially result in a brief increase in the population of photosynthetic microorganisms, and thus higher concentrations of dissolved oxygen. Once this initial population begins to die off, hypoxia can occur as a result of increases in aerobic microorganisms that deplete the water's dissolved oxygen content—literally suffocating larger fauna such as fish. This effect is classically characterized by an oxygen sag curve and is depicted graphically in Figure 1.5. It is only kilometers downstream that these deleterious effects begin to dissipate and the water returns to its natural state (Davis and Masten, 2008).

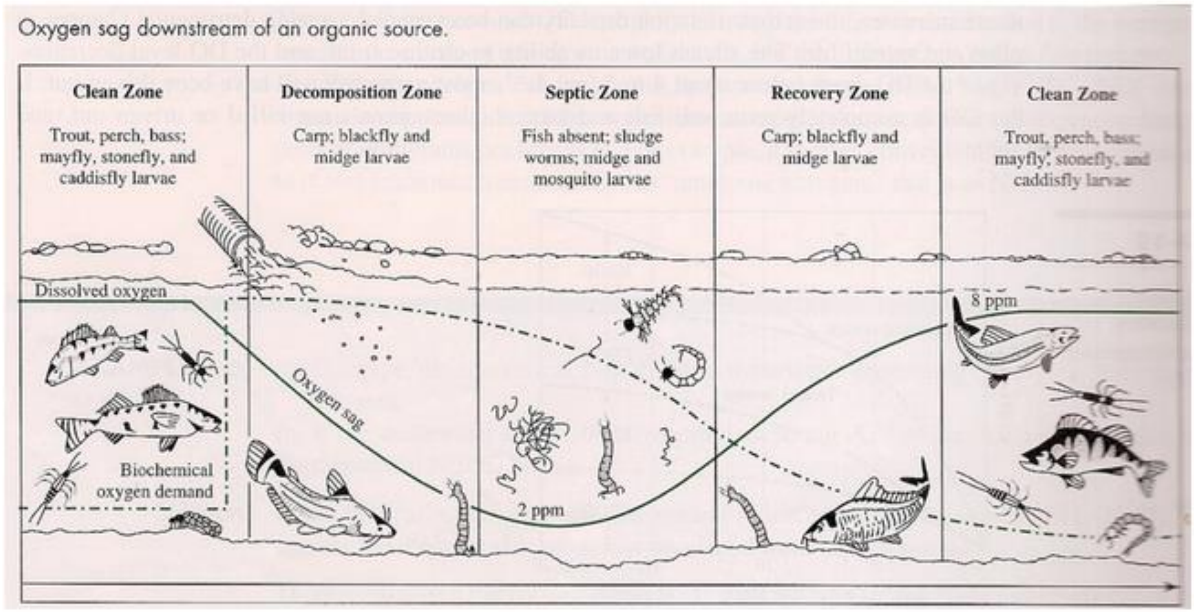

Figure 1.5: *Illustration of an oxygen sag curve. High nitrogen content produces nutrient loading and eutrophication. This in turn induces aerobic metabolism that leads to hypoxia which decreases dissolved oxygen levels (Davis and Masten, 2008)*

The EPA estimated that as much as 4,770 billion liters of untreated water from CSOs is released annually in the United States alone (US EPA, 2001). Furthermore, it has been estimated that more than 40 million Americans live in cities that rely on combined sewer systems with recorded CSOs (US EPA, 2001). In order to address the public health risks associated with combined sewer systems and CSOs, the EPA issued the Combined Sewer Overflow Control Policy in 1994, which mandated that communities relying on combined sewer systems establish long-term initiatives to reduce CSO pollution in accordance with the standards codified by the Clean Water Act (Tibbetts, 2005). Unfortunately, most of the affected communities have faced great difficulty meeting these standards due to logistical and economic restraints. The EPA has estimated a national cost of $50.6 billion using traditional ‘grey infrastructure’ approaches for controlling CSOs (US EPA, 2001).

Green Stormwater Infrastructure as a mean of improving urban hydrology

Due to insufficient funding for such an extensive ‘grey’ redevelopment plan, experts have proposed the implementation of green stormwater infrastructure (GSI) including bioretention basins, rain barrels, and porous pavement, and other approaches seeking to rebalance water budgets and approximating pre-urban hydrologic cycles by mimicking natural conditions. Implementation of GSI can reduce total runoff volumes, peak sewer flow rates, and the lag-to-peak duration times between peak rainfall intensity and peak sewer flow. By managing these key parameters, civil engineers can determine whether the conveyance capacity of a given system will be exceeded triggering a surcharge condition (Field et al., 1997).

A major impediment for GSI development initiative is a general lack of knowledge regarding the runoff reduction achieved by each system (US EPA, 2004). While it is understood that GSI will reduce some runoff, it is not easy to quantify by how much. In a 2008 action strategy, the EPA called for more comprehensive research as necessary to understanding GSI as a solution to CSOs (US EPA, 2008).

Documenting GSI performance at the facility scale is a fundamental step towards addressing its potential impact across larger geographic areas. At the scale of a single site, a GSI facility is typically designed to capture and slow stormwater runoff in order to reduce hydraulic loading on sewers and receiving waterways. In small catchments, GSI facilities can be positioned at points of low elevation in order to ensure that runoff from the drainage area will enter the site. Runoff from the contributing drainage area enters the site, it begins to infiltrate into the soil, and the soil voids and ponding area of the site provide storage to retain water. Water that is not captured by infiltration or storage leaves the site as runoff. After the storm subsides, evapotranspiration and deep infiltration recharge the system by freeing the storage voids. Additionally, runoff from the contributing drainage area that does not enter the site can be said to bypass the facility, which is most likely to occur during larger rain events.

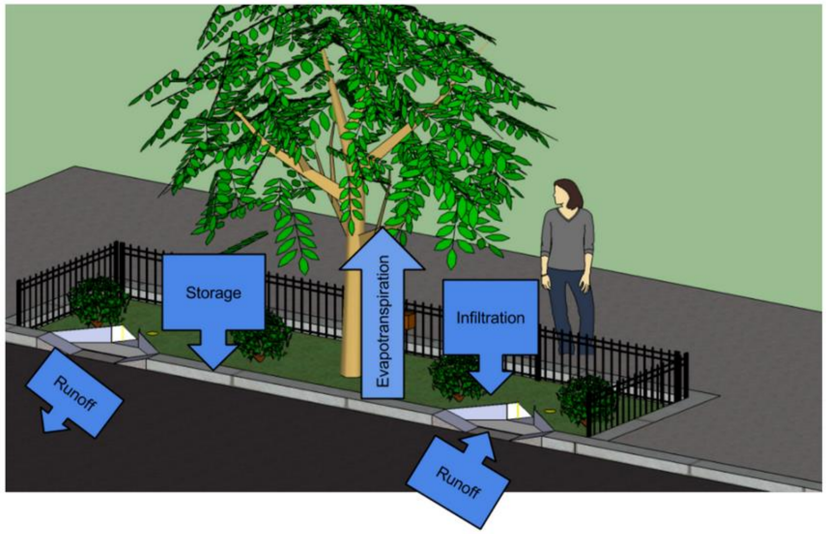

Figure 1.6: *Water budget of a streetside bioswale. Runoff that enters the site will either infiltrate, be captured as storage, or leave the site if the site reaches capacity. The site will recharge after the storm through evapotranspiration or deep infiltration.*

Urban areas throughout the United States are implementing GSI projects as part of larger, municipal stormwater management plans (SMPs). Citywide GSI development in the United States is typically conducted by municipal wastewater utilities under consent agreements with the U.S. EPA. For example, Washington, D.C. is required to retrofit 167 ha of impervious area to manage stormwater (Natural Resource Defense Council, 2011). Philadelphia, as another example, has committed $1.67 billion for GSI implementation to as part of a larger plan to reduce combined sewer flow by 85% (Philadelphia Water Department, 2011). Large scale planning can reduce overall costs due to economies of scale and the fact that multiple planning goals can be incorporated such as neighborhood development (or redevelopment), improved connectedness of open space and greenway trails, and social justice (Water Environment Federation, 2014). Evaluating the success of a GSI program can be assessed using the 'Triple Bottom Line' analysis, which analyzes social, economic, and environmental benefits; however, large-scale implementation efforts tend to be favored by regional sewer district authorities interested in capturing larger amounts of volume (Keeley et al., 2013).

Many urban stormwater plans strive to achieve the goals outlined under the Combined

Sewer Overflow (CSO) Control Policy (under the National Pollutant Discharge Elimination System permit (NPDES)) or in the Municipal Separate Storm Sewer System (MS4) permits. In Massachusetts and New Hampshire for example, these objectives translate to achieving a “condition of pre-development hydrology” and preventing runoff from 25.4 mm rainstorms (Water Environment Federation, 2014). In Philadelphia, PA, GSI is required to manage 38.1 mm rainstorms with a peak discharge rate into pre-existing sewers of 1.42 L/s (Philadelphia Water Department, 2015). Due to variations in climate and geologic characteristics, however, no one GSI plan fits all. Factoring in rainfall patterns and seasonal effects, such as varying soil moisture content affecting infiltration and evapotranspiration rate, can be critical factors in the success of a program. As an example, comparing the annual water budgets of Southern California to the Northeastern United States in undeveloped conditions, evapotranspiration amounts to 45% in the Northeast (Church et al., 1995) and 83-97% in Southern California (Ng and Miller, 1980).

The location and type of GSI implementation will have a dramatic impact on the success of a SMP, each type with its own unique advantages and challenges. In densely populated cities, GSI development is often done in the public right-of-way (ROW), typically in the form of green streets, porous streets, or roadside infiltration trenches. Development is typically designed based on site specific infiltration rates requiring geotechnical investigation such as boring and infiltration tests (Figure 1.7). In places with high bedrock, high water table, or low infiltration rates, the geological conditions may not be optimal for these types of systems. Designing systems with a factor of safety is recommend, as the function of these systems has been shown to reduce overtime. A study conducted by the U.S. EPA found that more than 50% of infiltration systems demonstrated significantly reduced performance after 5 years of service (US EPA, 1999). A survey of a various trenches conducted by Lindsey et al. (1991), demonstrated that 36% of systems were clogged. Galli (1992) surveyed 12 infiltration systems with pretreatment systems, all of which failed in the first two years. Additionally, ROW construction can be problematic, as it can conflict with pre-existing utilities that interfere with design and construction.

Due to a large majority of urban space being privately owned and managed, in order to achieve the ambitious goals set by SMPs, municipal governments should exercise flexibility and a willingness to consider other forms of GSI such as green roofs (Carter and Fowler, 2008). From a catchment perspective, because much of the urban landscape is occupied by rooftops, green roofs provide a means to reduce overall imperviousness. While green roof design varies, it is typically defined as either intensive or extensive. Intensive green roofs have deep soil layers (>100mm) to support large vegetation such as trees and bushes; extensive green roofs have a much shallower soil layer (generally 75-100mm) and normally support smaller vegetation such as succulent plants, herbs, grasses, and moss. (Berndtsson et al., 2009). Additionally, extensive green roofs tend to be more popular than intensive green roofs because they require less maintenance, are cheaper to build, and are much lighter (Carter and Fowler, 2008). To consider the potential of a large scale city-wide green roof SMP, one study simulated the effect of various roof greening scenarios throughout Washington, D.C. The study found that if every roof were greened in Washington, D.C., then there would be a 65-85% reduction in total rooftop runoff depending of the type of green roof used (CaseyTrees and LimnoTech, 2005). This study represents the upper bound of what could be expected from a city-wide green roof SMP because every possible rooftop was greened; however, realistic considerations, including costs and structural concerns, limit what is actually feasible. Carter and Jackson (2007) for example, discuss the importance of green roof location when considering large-scale implementation and suggested the most feasible candidates for development are flat roofed institutional buildings. This recommendation is also policy throughout many municipalities in North America where it is often a requirement for new government buildings to have green roofs when feasible (Carter and Fowler, 2008).

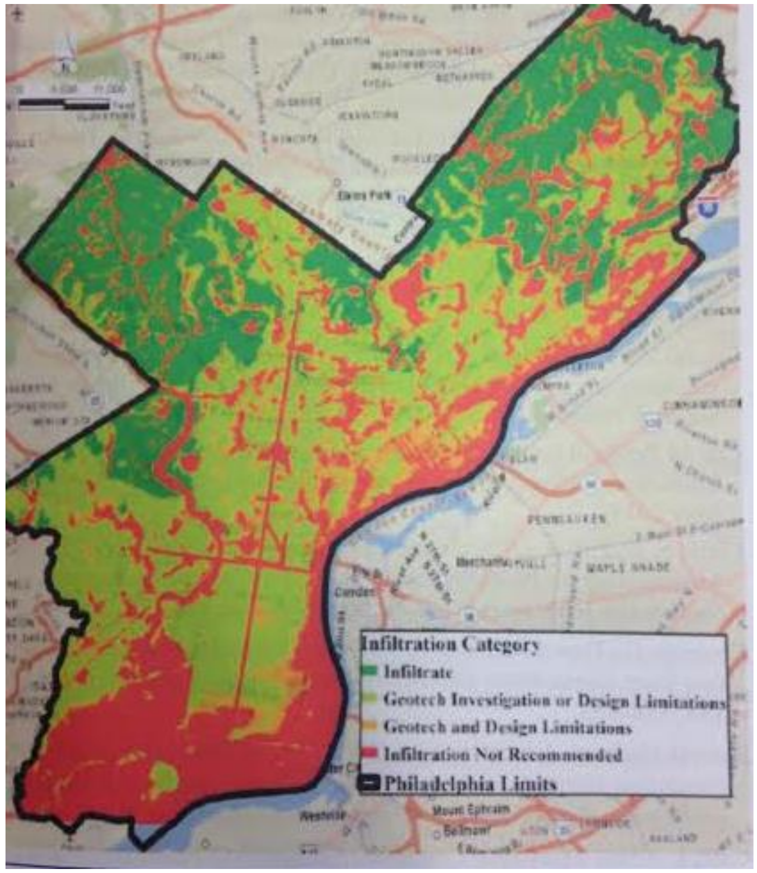

Figure 1.7: *Areas in Philadelphia where infiltration potential is high (green), likely (yellow), or not recommended (red). To clarify potential, geotechnical investigation is recommended. (O'Rouke et al., 2012)*

Modeling Urban Hydrology and GSI

There are a number of analytic tools to help quantify urban hydrologic and hydraulic systems. This section outlines some of the methods used by practicing engineers in sewer design in addition to contemporary approaches for GSI applications.

Traditional Methods

The two classical methods to quantify urban stormwater runoff are the Curve Number (CN) and Rational Method. Natural Resource Conservation Service (NRCS) Curve Number method can be used to calculate the total depth of runoff resulting from a discrete rain-event. Developed by the NRCS (previously named the Soil Conservation Service) in the 1950s for agricultural purposes, this empirically derived method can be used for analysis of small watersheds. Popular due to its simplicity and widespread (even global) use, the CN method has since been improved for application in urban catchments with the release of the Technical Release 55 (TR-55) (Natural Resource Conservation Service, 1986). While the goal of TR-55 was to extend the CN method to urban hydrology, questions remain on its applicability is small urban subcatchments. TR-55 defines CN use for urban and urbanizing small watersheds; although, many argue that due to the inherent limitations of the CN method (such as its inability to vary rain intensity and initial abstractions) the CN method is inaccurate and its use should be limited to rough estimations (Hawkins et al., 2009).

The other classic approach is the Rational Method and is a standard predictive method used for determining the peak runoff flow rate during rain-events. Developed in 1889 by Emil Kuichlin (Thompson, 2007) to quantify hydraulics of small catchments, its use has since become widely popular and is taught in contemporary hydrology textbooks for stormwater management design and hydrologic analysis (Viessman and Lewis, 2002) (Bedient et al., 2012)). Peak flow is determined through a multiplication of rainfall intensity, catchment area, and a runoff coefficient based on catchment imperviousness. This method assumes that rainfall intensity is uniform throughout the duration of the storm (e.g. block rainfall), such that there is no peak in rainfall intensity. The runoff coefficient is determined using similar methods to the curve number described above. In order to determine the C value for a heterogeneous catchment, a weighted average of C values by area is performed. The rational method is popular mainly due to its simplicity; however, this simplicity limits the scope to which it can be applied. For example, because the method does not factor details in topography and complexities of the catchment, applications are generally limited to catchments less than 81 ha. Additionally, results from the rational method can be skewed when using composite catchments where downstream areas are more developed than upstream areas (Akan and Houghtalen, 2003).

Hydrologic and Hydraulic Modeling

Hydrologic and hydraulic (H&H) modeling allows for more dynamic simulations of urban drainage networks. One of the most widely used methods for H&H modeling is the U.S. EPA's Storm Water Management Model (SWMM), described as a dynamic rainfall-runoff-subsurface runoff simulation model that can be used for both single-event and long-term simulation of surface and subsurface hydrology for both urban and suburban environments (US EPA, 2017). SWMM is a robust modeling method that is able to account for a wide range of hydrologic processes in urban areas. These include time-varying rainfall, evaporation of standing surface water, snow accumulation and melting, rainfall interception and depression storage, the infiltration of rainfall into unsaturated soil layers, the percolation of infiltrated water into groundwater layers, interflow between groundwater and the drainage system, nonlinear reservoir routing and overland flow, among other features. This ability was demonstrated in one study where a high resolution SWMM model was developed for an urban sewershed in Syracuse, NY. By comparing and calibrating the model to observed flow rates at the outlet of the system, the model uncertainty was analyzed. It was found that SWMM could actually predict flow rates and that SWMM could be calibrated efficiently based on combined total flow data and peak flows instead of intensive 5-minute monitored flow data (Sun et al., 2014).

GSI Modeling Techniques

Determining the effect that GSI will have on urban hydrology is typically assessed through a combination of hydrologic modeling and environmental monitoring. For example, the city of Milwaukee developed a Hydrologic Simulation Program - Fortran (HSPF) model to represent 2 ha of residential and city blocks to evaluate baseline sewer conditions followed by post-green conditions. This simulation showed that combining GSI implementation with rooftop downspout disconnections from the sewer would reduce peak sewer flows by 5-36% and reduce CSOs by 12-38% (Water Environment Federation, 2014). In 2009, the U.S. EPA updated SWMM with explicit low impact development (LID) controls such that it can now simulate LID devices such as bioretention cells, infiltration trenches, porous pavements, rain barrels, and vegetated swales. Selbig and Balster (2010) demonstrated that the updated SWMM with LID control can reasonably produce previously obtained results for both continuous and single event simulations and is capable of calibrating, validating, and evaluating GSI. Palla and Gnecco (2015) analyzed a 5.5 ha small urban catchment with a SWMM model implementing various degrees of LID controls. By first calibrating a SWMM model to observed catchment discharge, the authors were able to simulate levels of LID implementation including green roofs and permeable pavement based on LID control parameters calibrated based on lab test measurements. By greening all of the rooftops in the catchment and converting 16% of the parking lots and roads into permeable pavement, the 2-year rain event total discharge volume was reduced by 23% and the peak runoff rate reduced by 45%. Rosa et al. (2015) added more confidence to the LID controls showing that calibrated models could produce peak flows and total volume accurately compared to observed measurements ($R^2 > 0.8$ and 0.9 respectively). McCutcheon and Wride (2013) have recommended several action items in order to strengthen the confidence in using the SWMM models including the long term monitoring of GSI and LID devices so that they can be represented accurately in models, the establishment of an international database of performance data for engineering reference, the validation of all controls with a robust set of field data for both input parameters and model calibration performance from a wide variety of sites representing a diversity of field conditions, and an exploration of differences in calibrations by performing detailed sensitivity analyses.

Large Scale GSI Modeling

Large scale analysis of GSI implementation can be accomplished by employing SWMM based modeling with LID controls. In an analysis of a 784 hectare combined sewer drainage area in the Bronx, NY using a SWMM model, a 5% greening scenario over the entire catchment using various GSI systems showed a 14% reduction in annual CSOs (30 down from 35) (De Sousa et al., 2012). Similarly, Smullen et al. (2008) developed a SWMM model of the entire Philadelphia watershed to simulate various degrees of GSI implementations. They found that implementing GSI over the entire watershed would reduce total impervious runoff by 50% annually and CSO flow by nearly two-thirds. In 2012, Kansas City, MO completed a 40 ha pilot GSI program in a combined sewer area along the Middle Blue River Basin including development of green streets, bioswales, bioretention and porous pavements to capture runoff. In a joint effort between the U.S. EPA and the University of Missouri-Kansas City, runoff monitoring was maintained in the systems. Relative to a control watershed, the pilot project reduced flow by 76% based on SWMM modeling results (Kansas City Water Services, 2013) (Pitt et al. 2010).

Simplifications of Hydrologic Models:

The previous work cited above shows the role of modeling to understand the hydrologic and hydraulic effects of an urban GSI implementation project. In each case, the models were developed based on physical parameters (inverts, sizes, location, slopes, etc.) of the drainage system. However, developing these physically based models can be a difficult task due to limited public availability of sewer maps, the time required to construct a model, and limited observed sewer flow data used in calibrating a model. Additionally, a high resolution model is not always required for planning or research purposes where only a general strategy of GSI implementation is needed.

One method to simplify the modeling process is through model aggregation were high levels of resolution in subcatchments and pipe networks are combined in lower resolution models. Several researchers have already shown that models built based on simplifications of urban drainage networks can produce reasonable results. This literature focuses on subcatchment aggregation and conduit sketetonization. For example, Huber (2006) showed that for a 7 ha urban catchment, a physically based model that accounted for H&H processes on every parcel performed as well as a lower resolution model utilizing street blocks as the base hydrologic response unit (HRU) (118 versus 14 subcatchments). This result was repeated by Goldstein (2011) who showed that that a block scale SWMM model perform as well, if not better, than a high resolution physically based model when that incorporated all the pipes and features existing on one urban block. At greater modelled areas, low resolution can create error. This was shown by Cantone and Schmidt (2009) who created a physically based model of a 5.2 ha catchment using subcatchment resolution ranging from 44 to 1 and found that the most accurate predictions were obtained with 8 subcatchments. Modeling the entire catchment as one subcatchment resulted in a greater time of concentration and lower peak flows and the greatest error. This finding was replicated in a 341 ha catchment modeled with between 773 and 1 HRUs, again showing that the most accurate model had 65 subcatchments. The authors note that this result is worrisome because it is common for municipalities (in their case the City of Chicago) to utilize on these low resolution models for the reasons cited at the introduction of this paper.

Scaling and Self-Similarity in Hydrologic Systems

For larger watershed scale planning and modelling, it is important to understand the role of scale in hydrologic models especially when considering potential errors related to model aggregation. In this section, the concept of hydrologic scale will be introduced in its historic context related to natural river basins. These concepts are then discussed as they relate to urban drainage networks. Finally, applications of these scaling laws are explored towards improving current stormwater modeling techniques.

Scaling Laws in Natural Systems

Spatial scale is a fundamental concept in hydrology when considering the impact of little rain drops amounting to large rivers. One way to define scale within a hydrologic system is by the length of each hydrologic subset. While there are no strict categories for the various scale, Gleeson and Paszkowski (2014) show in Figure 1.8 one representation of the hydrologic scales.

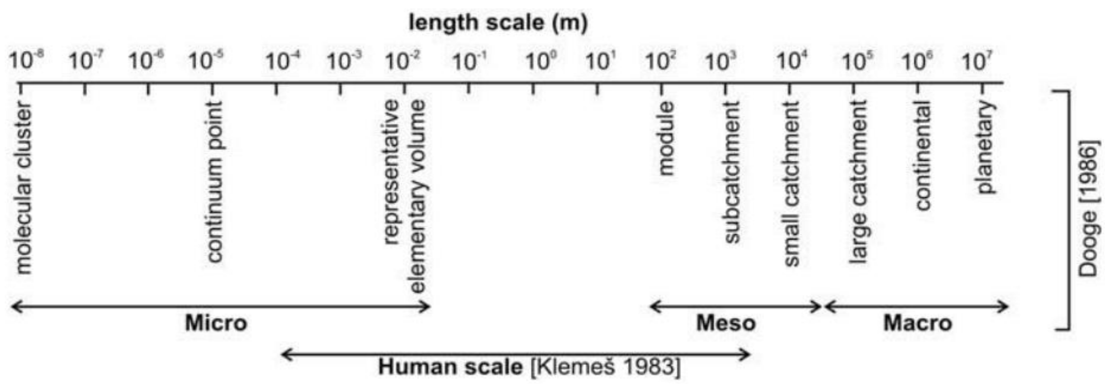

Figure 1.8: *Reference for various scales used in hydrology (Gleeson and Paszkowski, 2014)*

Typical watershed analysis deals within the Meso and Macro scales. One method for denoting the scaling process by which small tributaries form streams, creeks, and ultimately rivers was proposed by Robert Horton (1945) and later refined by Arthur Strahler (1952) which ranks the hierarchical structure of tributaries within a system. They ordered the network by assigning numbers to each tributary such that a first-order stream has no tributaries, a second-order is the joining of two first-orders, a third order is the combination of two second-orders, and so on (an example shown below is Figure 1.9).

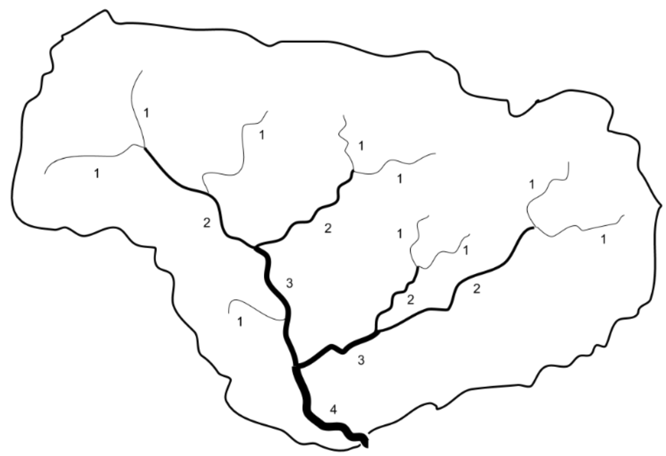

Figure 1.9: *Strahler ordering shown in a hypothetical river basin. When two first order streams meet a second order is form and so forth.*

Horton (1945) described a number of parameters to define river geometries including: the bifurcation ratio (R_B), used to describe the ratio of the number of streams (n_i) in order (i) to the number of streams (n_{i+1}) in the next highest order (i+1); the length-order ratio (R_L), used to describe the ratio of the average length ($\overline{l_{i+1}}$) of a stream order to the average length of the stream order below ($\overline{l_i}$); the area-order ratio (R_A), used to describe the ratio of the average area ($\overline{a_{i+1}}$) of a stream catchment to the average area ($\overline{a_i}$) of the stream order below; the drainage density (DD) ratio, denoting the ratio of one drainage density (defined as the total length of all the streams divided by the total drainage area) to the next higher order.

$$R_B = \frac{n_i}{n_{i+1}} \qquad R_L = \frac{\overline{l_{i+1}}}{\overline{l_i}} \qquad R_A = \frac{\overline{a_{i+1}}}{\overline{a_i}} \qquad DD = \frac{\frac{\sum l_i}{\sum a_i}}{\frac{\sum l_{i+1}}{\sum a_{i+1}}}$$

Horton (1945) also observed that these ratios were consistent at each scale throughout the basin, a geometric characteristic known as self-similarity or scale-invariance. As such, these ratios enable a river basin network to be structurally defined across each scale (Scheidegger, 1968).

John Hack (1957) of the United States Geological Survey also empirically determined a scale-invariant relationship between stream length and contributing drainage area in the Shenandoah Valley, Virginia now known as Hack's Law:

$$L = 1.4\, A^{0.6}$$

where L is the length (mile) of the longest stream measured from the top of the network to any point downstream and A is the area ($mile^2$) of the drainage network.

its general form:

$$L = C\, A^{h}$$

where C and h are constants calibrated for a unique network
with h generally 4/7 between a wide range of observed networks between 200-25,000km^2 (Birnir, 2008).

A visual representation of L and A used in Hack's Law is provided in Figure 1.10. Since 1957, other river basins have been analyzed with Hack's Law and the relationship was repeatedly affirmed (Montgomery and Dietrich, 1992) (Figure 1.11). One of the key differences between Horton order ratios and Hack's Law related back to scale-invariance is that Horton order ratios are discrete at each interval whereas Hack's Law is a continuous function.

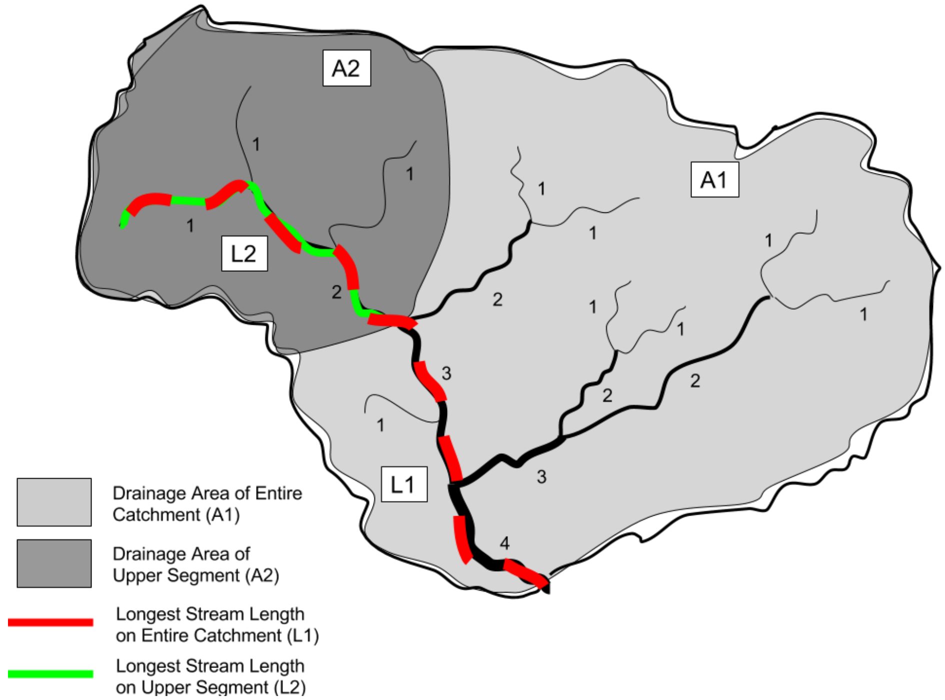

Figure 1.10: *Hack's Law relates drainage area to stream length ($l \sim a^h$). In the example above, Hack's Law is consistent relating A1 to L1 and A2 to L2.*

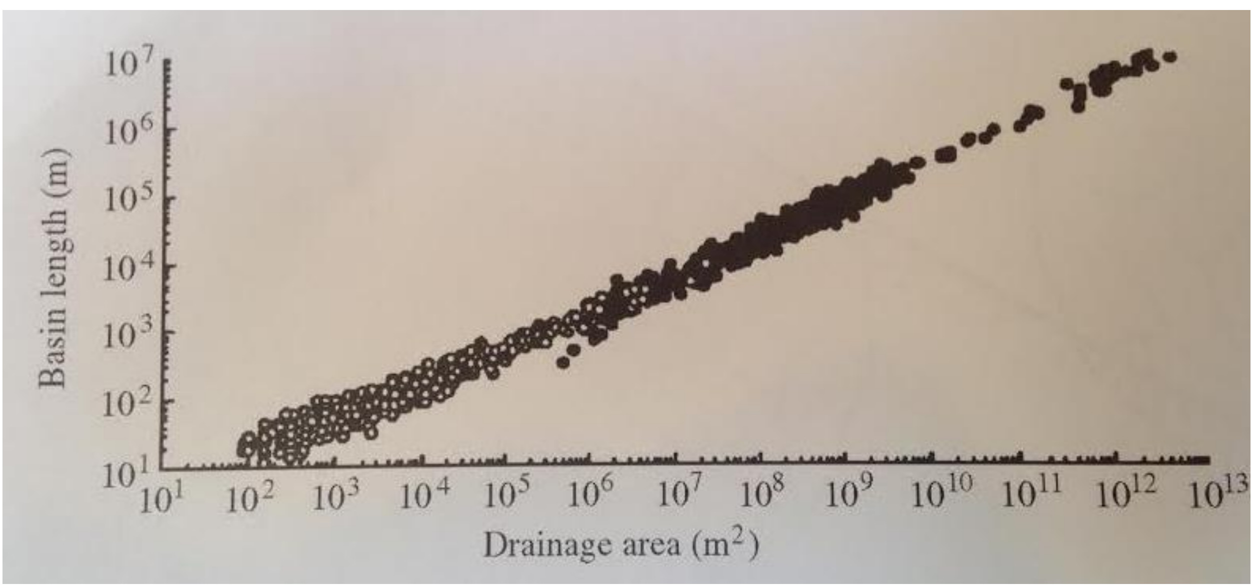

Figure 1.11: *Drainage area related to basin length for a number of river basins ranging from hillside depressions to the world's largest rivers (Montgomery and Dietrich, 1992).*

Luna Leopold et al. in 1964 expanded this idea relating drainage area to basin bankfull discharge (Leopold et al., 1995):

$$Q = C A^h$$

Purely derived empirically, Leopold et al. (1995) measured velocity, depth, and width measurements of a number of different rivers with the U.S. Geological Survey in conjunction with Manning's equation.

New insights into these relationships evolved with the emergence of fractal geometric analysis. In 1967, French mathematician Benoit Mandelbrot published his famous paper "How Long Is the Coast of Britain? Statistical Self-Similarity and Fractional Dimension" which illustrated the paradox of measuring the coastline of Britain. If using a yardstick to measure the coastline, one would get a smaller distance than if measured with a one-foot ruler (Figure 1.12) (Mandelbrot, 1967). As the measurement increments decrease, the measure distance of the coastline would paradoxically infinitely increase. Through this lens, Mandelbrot was able to mathematically explain the phenomena through the development of fractal geometry characterized by self-similar patterns. Recognizing this same self-similarity in river basins, Mandelbrot (1983) proposed that the Hack's Law exponent could be used to determine a basin's fractal dimension (D) which was later refined by Peckham (1995) through a relationship between the bifurcation ratio and total stream number as dimension D = 1/h ranging between 1 to 2, with higher values denoting denser systems. For fractal dimensions as they relate to river basins, D=1 represents a single dimension line (and no drainage area) and D=2 represents a completely filled 2-dimensional square (with maximum drainage density) (this is illustrated in Figure 1.13).

Figure 1.12: *(Right Image): Measuring the coastline in 200 km increments yields about 2400 km (Left image): 50 km increments about 3400 km (Image from Wikicommons, 2005)*

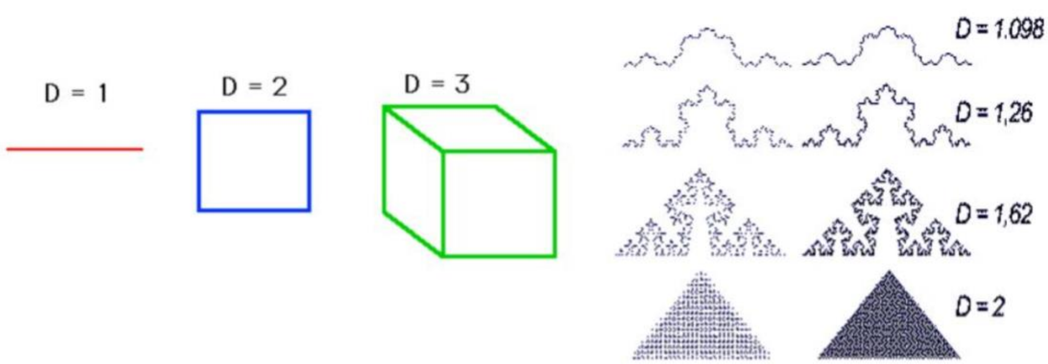

Figure 1.13: *Dimensions are typically thought in terms of length (1st dimension), width (2nd), and depth (3rd) (left image) (reproduced from Ryan, 2007). Fractal dimensions can be between two dimensions illustrated with the Koch curve fractal (right image) (reproduced from Vassallo, 2005). As the fractal dimension increases, the density increases as it approaches the 2nd dimension.*

A core concept of fractal geometry is the idea of scale-invariance (self-similarity) previously discussed. This means that the pattern seen at one scale will be identical to the pattern at both larger and smaller scales. Because the natural world rarely shows such perfect invariance, fractal models are best employed with stochastic variance. That is to say that probabilistic rules affecting a system will be the same at each scale, but the way the pattern manifests will have random elements governed by those rules (Veneziano and Langousis, 2010). Take for example a tree which is a natural manifestation of fractal geometry. While its shape is generally a fractal with the truck at its base branching into its smaller tributaries and ultimately leaves, the tree is affected by random elements in nature which can alter its shape. The main probabilistic rule governing the tree's shape will be sunlight and the desire to optimize this resource. In this regard, the tree would grow as a fractal yet its shape skewed in the direction towards the direction of sunlight. At each scale, the tree has an affinity for the invariant sunlight, yet is still influenced by the randomness inherent to the natural world and its own biology.

Dendritic fractal geometry (such as a tree, circulatory and respiratory system, or river basin) is common in nature because of the efficiency of its shape. In the case of the biological respiratory system for example, the dendritic geometry maximizes surface area for the transfer of oxygen to occur. In river basins, the dendritic geometry creates the path of least resistance for water flowing downhill. Mathematically, fractals can be represented by power laws as they display scale invariance. By combining fractal geometry with Horton stream ordering, a river network can be described mathematically. Rodriguez-Iturbe and Rinaldo (2001), in their book "Fractal River Basins: Chance and Self-Organization", describe the mathematics and fractal geometry inherent to river basins in the natural world and their effect on drainage networks. In their analysis, the authors start with a plan view of a natural river basin (Figure 1.14).

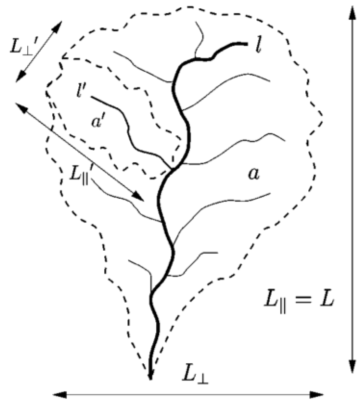

Figure 1.14: *Plan view of a river basin shows broken into geometric components for fractal analysis. This analysis is repeatable at each scale denoted by an apostrophe (Reproduced from Dodds and Rothman, 1998).*

They define the length of the entire basin by L_{II} (L) and the width as $L_\perp$ along with the length of the longest stretch of river (l) and the corresponding drainage area (a). $L_\perp$ is related by the Hurst exponent (H) as:

$$L_\perp \sim L_{II}^{H}$$

The stream length (*l*) is related to L_{II} by the scaling exponent, ϕ_L, using the following relationship:

$$l \sim L_{II}^{\phi_L}$$

From this the Hurst exponent is defined in relation to the Hack's Law exponent (h):

$$H = \frac{\phi_L}{h} - 1$$

Additionally, the elongation exponent, q, is defined:

$$q = 2 - \frac{\Phi_L}{h}$$

The Hurst exponent (H) represents the fractal nature of the system ranging from 0-1 with values closer to 1 relating to basins with more self-similarity between scales (Qian and Rasheed 2004). If q > 0 then the basin shows elongation at each scale consistent with fractal tendencies. Values less than 0 would show contractions.

Scaling Law in Urban Systems

These scaling and power law principles have since carried over into many urban studies as research develops to show self-similarity among human systems. Interestingly, cities can also be defined by scaling laws. By surveying over 500 cities in China, Chen and Zhou (2006) identified that city population and area fit to scaling law power function with an $R^2 > 0.98$. Chen continued in 2007 to show relationships between river systems and city systems illustrating that human systems are governed by the same geometric laws that govern the natural world (Chen and Zhou, 2008). Another example of this is shown in the work of Lu and Tang (2004) who demonstrated the application towards transportation networks successfully relating road length to population density in Texas.

In urban drainage networks, French scientist Serge Thibault conceptualized that Strahler stream ordering and fractal geometry could be applied to sewers in a similar way to how it is applied to natural river basins (Thibault, 1991). These ideas were applied by Joshua Canton who illustrated an application of Horton order ratios for a 316 ha urban catchment in Chicago, Illinois in addition to following new ratios for urban analysis (Cantone and Schmidt, 2011):

$$Ratio\ of\ conduit\ slopes\ (S_C) \qquad R_{Sc} = \frac{\overline{Sc_{\iota+1}}}{\overline{Sc_{\iota}}}$$

$$Ratio\ of\ conduit\ diameters\ (D) \qquad R_D = \frac{\overline{D_{\iota+1}}}{\overline{D_{\iota}}}$$

$$Ratio\ of\ overland\ slopes\ (S_O) \qquad R_{So} = \frac{\overline{So_{\iota+1}}}{\overline{So_{\iota}}}$$

$$\text{Ratio of overland region imperviousness} \qquad R_{imp} = \frac{\overline{imp_{i+1}}}{\overline{imp_i}}$$

In his analysis, the Horton order ratios were mostly consistent at each scale with the exception of the 1st order (smallest) showing self-similarity in the catchment. This breakdown at the smallest scale, he suggests, is most likely the result of smaller spatial scales found in urban networks relative to the natural networks which the Horton order ratios were developed. This claim is consistent with the work of Moussa and Bocquillon (1996) who showed that measured Horton order ratios of river basins would vary based on the resolution of the observation.

Another metric to define fractal geometry is the fractal dimension discussed earlier. In a recent publication related to urban sewer networks, Gires et al. (2016) analyzed sewer maps of 10 European urban networks (158-865 ha) and showed geometric scale invariance observing fractal dimensions ranging between 1.6 to 2. Additionally, the authors suggest potential to use scale invariance of urban networks to “fill gaps of missing data” if sewer map information is incomplete.

River basin scaling laws as applied to urban drainage systems is still in its infancy. Canton et al. (2011) was successful in applying his sewer Horton order ratios to an urban catchment, however, one catchment is not enough to show the universality of the claim. In addition, he did not include many of the Horton order ratios and Hack’s Law exponents typically applied in river basin analysis even being skeptical of their applicability. Likewise, Gires et al. (2016) added fractal dimensions and their relationship to urban density, however, fractal dimensions on only provide a limited perspective compared to the other scaling laws applied in river basins. This more thorough analysis was missing from the literature reviewed in this research.

Using Scaling Laws to create artificial networks

Scaling laws observed in both natural and urban drainage networks can be implemented to improve and simplify current hydrologic modeling methods. One of the most challenging aspects of sewer flow modeling is the availability of reliable sewer infrastructure plans from which to develop a physically-based model. In the conclusion of their analysis, Gires et al. (2016)

suggests that missing elements of sewer maps could be filled based on scale-invariant geometries. One current method to simulate artificial pipe networks is the Artificial Network Generator (ANGel) developed by Ghosh et al. (2006) allows for the creation of an artificial sewer network using Tokunaga fractal tree geometry defined as a dendritic tree with side-branching (Figure 1.15) (Turcotte and Newman, 1996) (Ghosh and Hellweger, 2012). The program creates pipes and nodes at various spatial scales and exports to a GIS shapefile which can then be imported to a SWMM model. Ghosh used this method to address the issue of scale effect in hydrologic models by comparing runoff of a large 4.66 km^2 catchment in the lower Charles River in Boston broken into 4, 18, and 401 subcatchments where models with more subcatchments had greater drainage densities. The results showed little difference in total runoff simulated by the different resolutions, but that peak runoff rates were significantly different at lower resolutions. There was a dual effect on peak flow rates in that larger storms in low resolution models tended toward less peak flow while smaller storms resulted in more peak flow. She surmised that the effect came from both the difference in the length of overland flow and conduit routing.

Möderl (2009) developed another method of generating artificial networks called the Case Study Generator (CSG). This method stochastically generates nodes and conduits based on Galton-Watson branching, another type of dendritic geometry typically associated with a family tree. Möderl used this tool to simulate 10,000 different artificial networks to analyze flooding and combined sewer overflows alongside two actual networks in Austria. Unlike the ANGel model, this method is able to simulate many different networks at one time whereas ANGel only generates one. However, the Galton-Watson geometry is less similar to urban networks than the Tokunaga geometry (with all branching occurring in generally one direction) and because the CSG currently is not georeferenced, it is less practical for GIS applications analyzing physical networks.

Ghosh and Möderl demonstrated the potential use of fractal scaling rules to develop artificial sewer networks for urban H&H modeling, but did not meaningfully characterize their precision through comparison to observations. While Ghosh was able to simulate comparable results to one observed storm (Ghosh reported no numerical analysis on accuracy), a more comprehensive evaluation of the approach would ideally consider multiple storms and multiple sewer networks with a thorough evaluation of the goodness of fit of the predictions to the observations. Likewise, Möderl only compared two storms to his model without any detailed analysis of the hydrologic response difference between the two, reporting only the surface ponding results as the only criteria for performance. Further, from a modeling perspective, understanding the sensitivity of the critical modeling parameters in the artificial networks is important for future implementation applying them to other unique networks.

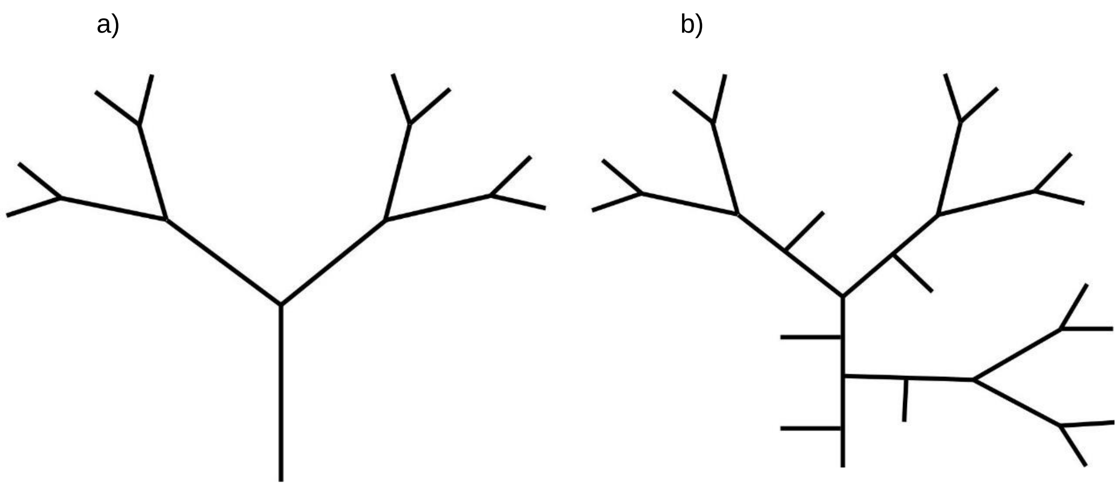

Figure 1.15:

a) Binary dendritic fractal tree showing four Strahler stream orders

b) The Tokunaga fractal method includes space filling branches more characteristic the drainage density found in natural stream networks

(adapted from Turcotte and Newman, 1996)

Using artificial networks has significant potential in answering other unique research questions related to GSI development. Ghosh et al. (2012), for example, originally developed ANGeL to demonstrate the effect of spatial resolution in SWMM models and understand the underlying mechanisms associated which could be applied to GSI implementation. Another example could address spatial design impacts by altering how each individual system is laid out throughout the catchment. Using a Netlogo based model, Zellner et al. (2016) showed that GSI dispersed across a catchment will manage stormwater more effectively than clustering the same amount of GSI to one central location. Although this model does not accurately predict runoff like SWMM, it illustrates how an artificial model can be used to address research based questions in a controlled model space with more symmetric geometries compared to the actual networks they represent.

Research Objectives and Purpose

This research serves to bridge the gap between fractal river basin analysis and urban hydrology. Urban hydrologists could benefit from these tools and gain insight into the fundamental structure of the systems they engineer. Grounding the research in the context of GSI gives the work contemporary appeal and offers alternatives to large scale implementation analysis outside of typical modeling. Additionally, by focusing on proposed projects currently underway in the U.S., it gives insight into the merits of the current plans to address the challenges of urban runoff while improving existing model performance.

The logical framework of this research is broken into three pieces. This first entails understanding the degree to which urban sewer networks resemble fractals. If it is true that urban drainage networks can be modeled with fractal geometry, then fractal geometries can be constructed to scale the results of smaller scale GSI implementation studies. This breaks down into the following fundamental questions and their corresponding testable hypotheses:

1. Are sewers fractals?
   a. Hack's Law is valid in urban sewersheds.
   b. Existing sewersheds can be geometrically define using Horton ordering.
2. Can the sewershed be hydrologically modeled with artificial fractal geometries?
   a. Artificial networks can simulate urban hydrology as well as traditional physically based models.
   b. Modeling a sewershed is more accurate using a high resolution fractal network than a lumped low resolution model.
3. Can GSI be modeled with artificial networks in urban catchments?
   a. Artificial networks can simulate GSI as well as physically based models.

Answering the previous questions builds the case that artificial models can be used to analyze large scale GSI performance in an urban catchment and using these models, the following questions can be addressed:

1. What types of GSI are most effective?
2. How much will various levels of implementations effect performance.
3. Does the spatial position of GSI facilities throughout the catchment matter?
4. What role can GSI play to manage extreme precipitation events and changing rainfall patterns associated with climate change?

Dissertation Structure

This chapters of this dissertation are structured in the form of three academic papers based around the research questions specified above.

Chapter 2: Applying river basin scaling laws to urban catchments:
Hack's Law and Horton river basin analysis in urban sewersheds

Chapter 3: Modeling urban sewers with artificial fractal geometries:
Comparing existing to synthetic sewer networks in simulating sewer flow compared to measured results

Chapter 4: Using artificial sewer networks to study the role of green stormwater infrastructure in reducing runoff during historic and future changed precipitation:
An analysis of urban sewer systems and the implementation of green stormwater infrastructure

These papers form the chapters of this dissertation and are structured as standalone documents with intent to ultimately publish each chapter in an academic journal. In the last chapter, the collective results of each chapter are discussed along with their practical implications. A detailed literature review is included in each chapter related to the topics cover in that chapter and as a result, there is some repetition from the literature review provided in the introduction.

List of References

Arnono, R. D., Borst, M., Walling, J. F. (May 15th 2005). "Investigation and evaluation of cryptosporidium and giardia in combined sewer overflow (cso) and stormwater runoff." *Proc., World Water & Environmental Resources Congress,* .

Bedient, P. B., Huber, W., Vieux, B. (2012). *Hydrology and Floodplain Analysis,* 5th Ed., Prentice Hall, .

Benoit Mandelbrot. (1967). "How Long is the Coast of Britain? Statistical Self-Similarity and Fractional Dimension." *Science,* 156(3775), 636-638.

Berndtsson, J. C., Bengtsson, L., Jinno, K. (2009). "Runoff Water Quality from Intensive and Extensive Vegetated Roofs." *Ecol. Eng.,* 35(3), 369-380.

Cantone, J., and Schmidt, A. (2011). "Improved Understanding and Prediction of the Hydrologic Response of Highly Urbanized Catchments through Development of the Illinois Urban Hydrologic Model." *Water Resour. Res.,* 47(8), W08538.

Cantone, J. P., and Schmidt, A. R. (2009). "Potential Dangers of Simplifying Combined Sewer Hydrologic/Hydraulic Models." *Journal of Hydrologic Engineering,* 14(6), 596-605.

Carter, T., and Fowler, L. (2008). "Establishing Green Roof Infrastructure through Environmental Policy Instruments." *Environmental Management,* 42(1), 151-164.

Carter, T., and Jackson, C. R. (2007). "Vegetated Roofs for Stormwater Management at Multiple Spatial Scales." *Landscape Urban Plann.,* 80(1), 84-94.

De Sousa, Maria R C, Montalto, F., Spatari, S. (2012). "Using Life Cycle Assessment to Evaluate Green and Grey Combined Sewer Overflow Control Strategies." *Journal of Industrial Ecology,* 16(6), 901-913.

Dodds, P. S., and Rothman, D. H. (1999). "Unified View of Scaling Laws for River Networks." *Phys. Rev. E,* 59(5), 4865-4877.

Fund, C. T. E., and LimnoTech. (2005). "Re-Greening Washington, DC: A Green Roof Vision Based on Quantifying Storm Water and Air Quality Benefits."

Casey Trees Endowment Fund, Washington, DC.Castleton, HF, Stovin, V., Beck, SBM, and Davison, JB (2010).“Green Roofs, , 1582-1591.

Ghosh, I., and Hellweger, F. L. (2012). "Effects of Spatial Resolution in Urban Hydrologic Simulations." *Journal of Hydrologic Engineering,* 17, 129-137.

Ghosh, I., Hellweger, F. L., Fritch, T. G. (2006). "Fractal generation of artificial sewer networks for hydrologic simulations." *Proc., Proceedings of the ESRI International User Conference, San Diego, California, August,* , 7-11.

Gires, A., Tchiguirinskaia, I., Schertzer, D., Ochoa Rodriguez, S., Willems, P., Ichiba, A., Wang, L., Pina, R., Van Assel, J., Bruni, G. (2016). "Fractal Analysis of Urban Catchments and their Representation in Semi-Distributed Models: Imperviousness and Sewer System." *Hydrology and Earth System Sciences & Discussions,* , 1-23.

Goldstein, A. (2011). "Comparison of a High and Low Spatial Resolution Model for an Urban Block and Implications for Depicting Low Impact Development." .

Hack, J. T., and Geological Survey, (U S). (1957). Studies of Longitudinal Stream Profiles in Virginia and Maryland, .

HORTON, R. E. (1945). "Erosional Development of Streams and their Drainage Basins; Hydrophysical Approach to Quantitative Morphology." *GSA Bulletin,* 56(3), 275.

Kansas City Water Services. (2013). Kansas City's Overflow Control Program: Middle Blue River Basin Green Solutions Pilot Project Final Report, .

Keeley, M., Koburger, A., Dolowitz, D. P., Medearis, D., Nickel, D., Shuster, W. (2013). "Perspectives on the use of Green Infrastructure for Stormwater Management in Cleveland and Milwaukee." *Environmental Management,* 51(6), 1093-1108.

Leopold, L. B., Wolman, M. G., Miller, J. P. (1995). *Fluvial Processes in Geomorphology,* Courier Corporation, .

Lu, Y., and Tang, J. (2004). "Fractal Dimension of a Transportation Network and its Relationship with Urban Growth: A Study of the Dallas-Fort Worth Area." *Environment and Planning B: Planning and Design,* 31, 895-911.

Mandelbrot, B. B. (1983). *The Fractal Geometry of Nature,* updated and augmented ed. Ed., Freeman, New York, NY.

McCutcheon, M., and Wride, D. (2013). "Shades of Green: Using SWMM LID Controls to Simulate Green Infrastructure." *Journal of Water Management Modeling,* .

Möderl, M., Butler, D., Rauch, W. (2009). "A Stochastic Approach for Automatic Generation of Urban Drainage Systems." *Water Sci. Technol.,* 59(6), 1137-1143.

Moussa, R., and Bocquillon, C. (1996). "Fractal Analyses of Tree-Like Channel Networks from Digital Elevation Model Data." *Journal of Hydrology,* 187(1-2), 157-172.

National Research Council. (2008). *Urban Stormwater Management in the United States,* The National Academic Press, .

Niemczynowicz, J. (1999). "Urban Hydrology and Water Management–present and Future Challenges." *Urban Water,* 1(1), 1-14.

Osman Akan, A., and Houghtalen, R. J. (2003). *Urban Hydrology, Hydraulics, and Stormwater Quality,* 1st Ed., Wiley, .

Palla, A., and Gnecco, I. (2015). "Hydrologic Modeling of Low Impact Development Systems at the Urban Catchment Scale." *Journal of Hydrology,* 528, 361-368.

Peckham, S. D. (1995). "New Results for Self-Similar Trees with Applications to River Networks." *Water Resour. Res.,* 31(4), 1023-1029.

Philadelphia Water Department. (2011). "Green City, Clean Waters: The City of Philadelphia's Program for Combined Sewer Overflow Control." .

Pitt, R., Voorhees, J., Clark, S. (2010). "Integrating Green Infrastructure into a Combined Sewer Service Area Model " *World Environment Water Resource Congress 2010: Challenges of Change,* .

Qian, B., and Rasheed, K. (2004). "Hurst Exponent and Financial Market Predictability." *IASTED Conference on Financial Engineering and Applications ,* .

Rodríguez-Iturbe, I., and Rinaldo, A. (2001). *Fractal River Basins,* 1. paperback ed. Ed., Cambridge Univ. Press, Cambridge [u.a.].

Rosa, D. J., Clausen, J. C., Dietz, M. E. (2015). "Calibration and Verification of SWMM for Low Impact Development." *JAWRA Journal of the American Water Resources Association,* 51(3), 746-757.

Ryan, B. (2007). "Fractaldimensionexample.PNG." Wikimedia Commons.

Scheidegger, A. E. (1968). "Horton's Law of Stream Numbers." *Water Resources Research,* 4(3), 655.

Schellekens, J., Brolsma, R. J., Dahm, R. J., Donchyts, G. V., Winsemius, H. C. (2014). "Rapid Setup of Hydrological and Hydraulic Models using OpenStreetMap and the SRTM Derived Digital Elevation Model." *Environmental Modelling & Software,* 61, 98-105.

Selbig, W. R., and Balster, N. (2010). "Evaluation of Turf-Grass and Prairie-Vegetated Rain Gardens in a Clay and Sand Soil, Madison, Wisconsin, Water Years 2004-08." *U.S. Geological Survey Scientific Investigations Report 2010,* .

Smullen, J. T., Myers, R. D., Reynolds, S. K., Maimone, M. (2008). "A Green Approach to Combined Sewer Overflow Control: Source Control Implementation on a Watershed Scale " *11th International Conference on Urban Drainage, Edinburgh, Scotland, UK,* .

Steffen, W., Grinevald, J., Crutzen, P., McNeill, J. (2011). "The Anthropocene: Conceptual and Historical Perspectives." *Philosophical Transactions of the Royal Society of London A: Mathematical, Physical and Engineering Sciences,* 369(1938), 842-867.

Strahler, A. N. (1957). "Quantitative Analysis of Watershed Geomorphology." *Eos, Transactions American Geophysical Union,* 38(6), 913-920.

Teunis, P., Medema, G. J., Kruidenier, L., Havelaar, A. H. (1997). "Assessment of the Risk of Infection by Cryptosporidium Or Giardia in Drinking Water from a Surface Water Source." *Water Research,* 31(6).

Thibault. (1991). "Fractals Et Structure Des Réseaux Urbains D'Assainissement Eau Pluviale." *Flux,* 7(4), 5-14.

Thompson, D. (2007). "The Rational Method." *R.O. Anderson Engineering,* .

Turcotte, D. L., and Newman, W. I. (1996). "Symmetries in Geology and Geophysics." *Pnas,* 93(25), 14295-14300.

United States Environmental Protection Agency. (2017). "Storm Water Management Model (SWMM)." (5.1), .

Vassallo, C. (2005). "Notion of fractal dimension." <http://charles.vassallo.pagesperso-orange.fr/en/art/dimension.html> .

Veneziano, D., and Langousis, A. (2010). "Scaling and Fractals in Hydrology." *Databased Approaches for Hydrologic Modeling and Forecasting,* .

Wayne C Huber. (2006). BMP Modeling Concepts and Simulation .
Wikicommons. (2005). "Britain-Fractal-Coastline-50km.Png." .

Wisconsin Department of Natural Resources. (2012). "Recarga model." <http://dnr.wi.gov/topic/stormwater/standards/recarga.html> .

Zarriello, P. J. (1998). "Comparison of Nine Uncalibrated Runoff Models to Observed Flows in Two Small Urban Watersheds." *U.S. Geological Survey,* .

Zellner, M., Massey, D., Minor, E., Gonzalez-Meler, M. (2016). "Exploring the Effects of Green Infrastructure Placement on Neighborhood-Level Flooding Via Spatially Explicit Simulations." *Computers, Environment and Urban Systems,* 59, 116-128.

Chapter 2: Applying river basin scaling laws to urban catchments

Hack's Law and Horton river basin analysis in urban sewersheds

Abstract

Hack's Law and Horton ordering ratios numerically define natural river basin geomorphology and geometry throughout different scales of the network. Hack's Law relates the length of a stream to its receiving drainage area and Horton ordering ratios relate basin characteristics such as stream diameter, length, drainage density, and stream bifurcation between scales. Developed traditionally for use in natural river basins, these scaling laws can be applied to urban drainage networks because they resemble the dendritic geometric structure found in nature. This application is demonstrated by analyzing sewer network layouts of three highly impervious residential urban drainage networks in East Boston, Massachusetts (54 and 64 ha) and Bronx, New York (149 ha) serviced by either combined or separate stormwater sewers. The correlation between sewer length and contributing drainage area was strong (R^2>0.86) for all three networks predicted with Hack's Law. In natural river basins Horton ordering ratios tend to be similar between consecutive stream orders, a characteristic called self-similarity or scale invariance. The urban networks surveyed showed, on average, similar scale invariance expected in natural networks with most inconsistencies found at the smallest observed scale. In addition, this research demonstrates that Horton ordering ratios can be used to describe the structure of a sewer network in the same way they are used to describe natural stream networks. The potential applications of these relationships to urban drainage models is discussed.

Introduction

The Anthropocene is a term used to describe the Earth's current epoch in which human advancement and expansion plays a dominant role in global ecosystems (Steffen et al. 2011). Human infrastructure development, while creating many societal benefits, has dramatically altered the natural landscape. This change is most apparent in urban environments where built infrastructure has, in many ways, replaced natural ecosystem services. In particular, the watershed in the most urbanized areas has nearly been completely replaced by a sewershed where stormwater is conveyed through channels and pipes rather than streams and creeks. Hydrologists over many years have developed empirically-derived scaling rules to define the geometry of natural watersheds and ultimately predict their geomorphic characteristics such as length, drainage area, width, and geometric layout (Dodds and Rothamn, 1999). However, it is unclear how successfully these analytical methods can be applied to an urbanized sewershed (Cantone and Schmidt, 2011). The goal of this work is to apply these principles to an urban sewershed to assess their applicability and usefulness in characterizing urban drainage systems.

Hydrologic scaling laws are a core concept in characterizing a drainage system denoting the scaling relationship from streams to rivers. A method to define hydrologic scale was proposed by Robert Horton (1945) and later refined by Arthur Strahler (1952), which ranks the hierarchical structure of tributaries within a system. The network is ordered by assigning numbers to each tributary such that a first-order stream has no tributaries, a second-order is the joining of two first-orders, a third order is the combination of two second-orders, and so on (Figure 2.1).

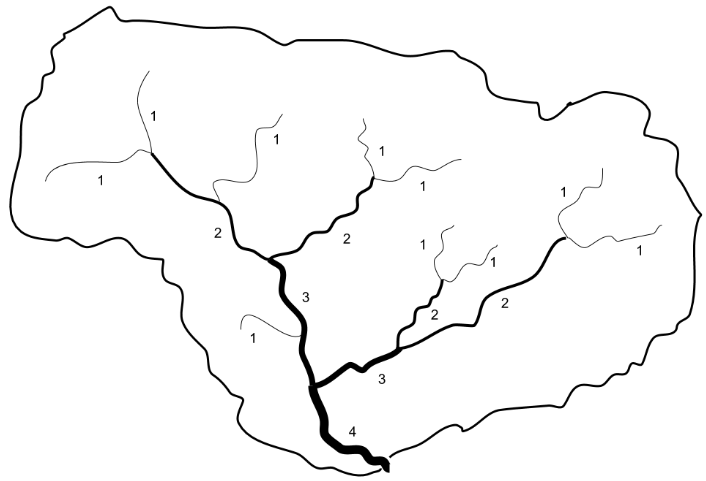

Figure 2.1: *Strahler ordering shown in a hypothetical river basin. When two first order streams meet a second order is form and so forth.*

Horton (1945) described a number of parameters to define river geometries including: the bifurcation ratio (R_B), used to describe the ratio of the number of streams (n_i) in order (i) to the number of streams (n_{i+1}) in the next highest order (i+1); the length-order ratio (R_L), used to describe the ratio of the average length ($\overline{l_{\iota+1}}$) of a stream order to the average length of the stream order below ($\overline{l_\iota}$); the area-order ratio (R_A), used to describe the ratio of the average area ($\overline{a_{\iota+1}}$) of a stream catchment to the average area ($\overline{a_\iota}$) of the stream order below; the drainage density (DD) ratio, denoting the ratio of one drainage density (defined as the total length of all the streams divided by the total drainage area) to the next higher order. These relationships are defined mathematically below:

$$R_B = \frac{n_i}{n_{i+1}} \quad (1) \qquad R_L = \frac{\overline{l_{\iota+1}}}{\overline{l_\iota}} \quad (2) \qquad R_A = \frac{\overline{a_{\iota+1}}}{\overline{a_\iota}} \quad (3) \qquad DD = \frac{\frac{\sum l_i}{\sum a_i}}{\frac{\sum l_{i+1}}{\sum a_{i+1}}} \quad (4)$$

Horton (1945) also observed that these ratios were consistent at each scale throughout the basin, a geometric characteristic known as self-similarity or scale-invariance. As such, these ratios enable a river basin network to be structurally defined across each scale (Scheidegger, 1968).

John Hack (1957) of the United States Geological Survey also empirically determined a scale-invariant relationship between stream length and contributing drainage area in the Shenandoah Valley, Virginia now known as Hack's Law:

$$L = 1.4\, A^{0.6} \qquad (5)$$

where L is the length (mile) of the longest stream measured from the top of the network to any point downstream and A is the area ($mile^2$) of the drainage network upstream of that point.

its general form:

$$L = C\, A^{h} \qquad (6)$$

where C and h are constants calibrated for a unique network
with h typically converging to a mean value of 4/7 over a wide range on observed networks between 200-25,000 km^2 (Birnir, 2008).

The most striking feature of Hack's Law is that it is applicable regardless of where in the network the measurement point was chosen. For example, if a point was chosen halfway down a stream network, the relationship was identical to a point chosen at the end (example in Figure 2.2). This relationship was repeatedly affirmed in other networks by Montgomery and Dietrich (1992) illustrating the self-similarity of the basin geometry uniform through all scales.

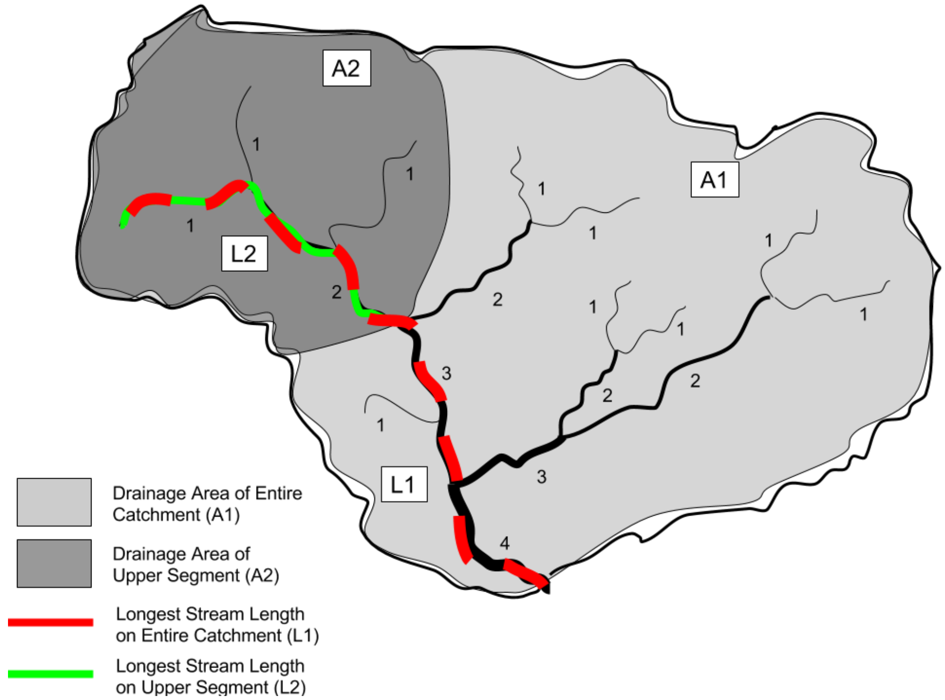

Figure 2.2: *Hack's Law relates drainage area to stream length ($l \sim a^h$). In the example above, Hack's Law is consistent relating A1 to L1 and A2 to L2.*

New insights into these relationships evolved with the emergence of fractal geometric analysis. In 1967, French mathematician Benoit Mandelbrot published his famous paper "*How Long Is the Coast of Britain? Statistical Self-Similarity and Fractional Dimension*" which illustrated the paradox of measuring the coastline of Britain. If using a yardstick to measure the coastline, one would get a smaller distance than if measured with a one-foot ruler (Mandelbrot, 1967). As the measurement increments decrease, the measure distance of the coastline would paradoxically infinitely increase. Through this lens, Mandelbrot was able to mathematically explain the phenomena through the development of fractal geometry characterized by self-similar patterns. Recognizing this same self-similarity in river basins, Mandelbrot proposed that the Hack's Law exponent could be used to determine a basin's fractal dimension (D) which was later refined by Peckham (1995) through a relationship between the bifurcation ratio and total stream number as dimension D = 1/h ranging between 1 to 2, with higher values denoting denser systems (Mandelbrot, 1983).

In river basins, the dendritic fractal geometry of river basins creates the path of least resistance for water flowing downhill. Mathematically, fractals can be represented by power laws as they display scale invariance. By combining fractal geometry with Horton stream ordering, a river network can be described mathematically. Rodriguez-Iturbe and Rinaldo (2001), in their book "*Fractal River Basins: Chance and Self-Organization*", describe the mathematics and fractal geometry inherent to natural river basins and their effect on drainage patterns. In their analysis, the authors start with a plan view of a natural river basin (Figure 2.3).

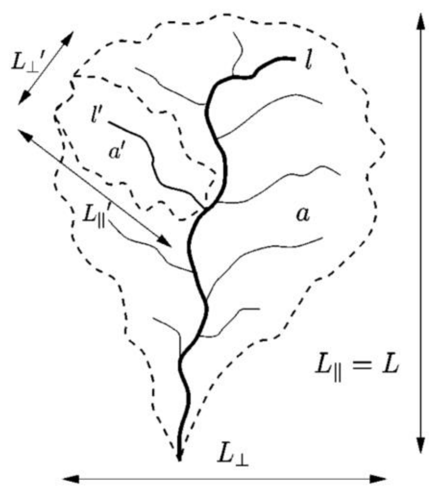

Figure 2.3: *Plan view of a river basin shows broken into geometric components for fractal analysis. This analysis is repeatable at each scale denoted by an apostrophe (Reproduced from Dodds and Rothman, 1999).*

They then define the length of the entire basin by L_{II} (L) and the width as $L_\perp$ along with the length of the longest stretch of river (l) and the corresponding drainage area (a). $L_\perp$ is related by the Hurst exponent (H) as:

$$L_\perp \sim L_{II}{}^{H} \qquad (7)$$

The stream length (*l*) is related to L_{II} by the scaling exponent, ϕ_L, using the following relationship:

$$l \sim L_{II}^{\phi_L} \qquad (8)$$

From this the Hurst exponent is defined in relation to the Hack's Law exponent (h):

$$H = \frac{\phi_L}{h} - 1 \qquad (9)$$

Additionally, the elongation exponent, q, is defined:

$$q = 2 - \frac{\phi_L}{h} \qquad (10)$$

The Hurst exponent (H) represents the fractal nature of the system ranging from 0-1 with values closer to 1 relating to basins with more self-similarity between scales (Qian and Rasheed, 2004). If q > 0 then the basin shows elongation at each scale consistent with fractal tendencies. Values less than 0 would show contractions.

Natural river basin scaling laws and Horton order ratios have been observed in many different river basins around the world. Using digital terrain models to survey and analyze 34 river basins around the United States, Rodriguez-Iturbe and Rinaldo (2001) determined q values > 0 for all basins showing elongation and the fractal nature of Hack's Law. In addition, Rigon et al. (1996) determined scaling coefficients of 13 catchments greater than 200 km^2 with results reproduced in Table 2.1. Marani et al. (1991) and Rosso et al. (1991) accumulated Horton order ratios observed in natural river basins from many different studies and their results are reproduced in Table 2.2.

Table 2.1: *Fractal parameters determined from 13 sites with areas greater than 200 km^2 (adapted from Rigon et al. 1996)*

	ϕ_L	h	H
Average	1.05	0.55	0.93
Max	1.07	0.6	1.01
Min	1.02	0.52	0.75

Table 2.2: *Horton order ratios observed in river basins (adapted from Marani et al. (1991) and Rosso et al. (1991)).*

River	R_B	R_L	R_A
Alto Liri Basin *(standard error reported)*	4.75 ± 0.24	2.50 ± 0.30	5.13 ± 0.46
Hacking River	4.81	2.97	5.35
Beech Creek	3.69	2.61	4.05
Vermillon River	3.11	2.07	2.80
Kaskaska River	3.76	2.63	4.35
Daddy's Creek	4.1	2.18	4.71
Davidson River	3.96	2.41	4.80
Querecual	4.2	1.75	4.5
Ilice Creek	2.7	2.0	5.1
Virginio Creek	3.9	2.3	4.5
Bisenzio	4.1	2.3	4.6
Elsa	4.4	1.8	4.2
Sieve	4.9	2.5	4.6
Sagamon River	3.13	1.82	3.29

Dodds and Rothman (1999) compiled these governing laws and related equations relating to self-similarity and scaling laws in river networks. In this work they reiterate the following assumptions as they apply to rivers: 1) networks are structurally self-similar, 2) single channels are self-affine (meaning that they scale differently in the x and y directions), and 3) drainage density is uniform. In short, this compilation shows the fundamental framework of fractal geometry present in natural systems and reaffirms the work of over half a century that has built on that claim.

Application to urban systems

French scientist Serge Thibault (1991) conceptually showed how Strahler stream ordering and fractal geometry could be applied to sewers in a similar way to how it is applied to natural river basins. These ideas were applied 20 years later by Cantone and Schmidt (2011), who illustrated an application of Horton order ratios for a 316 ha urban catchment in Chicago, Illinois. This research also introduced new ratios specifically for urban analysis:

$$\text{Ratio of conduit slopes } (S_C) \qquad R_{Sc} = \frac{\overline{Sc_{\iota+1}}}{\overline{Sc_\iota}} \tag{11}$$

$$\text{Ratio of conduit diameters } (D) \qquad R_D = \frac{\overline{D_{\iota+1}}}{\overline{D_\iota}} \tag{12}$$

$$Ratio\ of\ overland\ slopes\ (S_O) \qquad R_{So} = \frac{\overline{So_{i+1}}}{\overline{So_i}} \tag{13}$$

$$Ratio\ of\ overland\ region\ imperviousness \qquad R_{imp} = \frac{\overline{imp_{i+1}}}{\overline{imp_i}} \tag{14}$$

Cantone and Schmidt (2011) found that Horton order ratios were mostly consistent at each scale with the exception of the 1st order (smallest), demonstrating self-similarity in the catchment. The authors explain that in urban network analysis the smallest observed scale is smaller than the smallest observed scale in natural networks which the Horton order ratios were developed. This claim is consistent with the work of Moussa and Bocquillon (1996) who showed that measured Horton order ratios of river basins would vary based on the resolution of the observation.

Another metric to define fractal geometry is the fractal dimension discussed earlier. In a recent publication related to urban sewer networks, Gires et al. (2016) analyzed sewer maps of 10 European urban networks (158-865 ha) and showed geometric scale invariance observing fractal dimensions ranging between 1.6 to 2. Additionally, the authors suggest potential to use scale invariance of urban networks to “fill gaps of missing data” if sewer map information is incomplete.

Motivation

While previous research has demonstrated fractal tendencies in urban drainage networks, there are few studies that address the topic especially when compared to the wide range documenting natural river basins. Gires et al. (2016) showed repeating fractal dimensions at various scales building promise to the endeavor, however fractal dimensions only provide limited information regarding the actual structure of a sewer network. Cantone and Schmidt (2011) were successful in applying his sewer Horton order ratios to an urban catchment, however, one catchment is not enough to show the universality of the claim. In addition, he did not include many of the Horton order ratios and Hack’s Law exponents typically applied in river basin analysis even being skeptical of their applicability. This more thorough analysis was missing from the literature reviewed in this research. To advance this research foundation, the following hypotheses will be tested: 1) Urban sewersheds can be modeled using Hack’s Law, and

2) Horton order ratios are consistent at each scale throughout the network.

Methodology

Site Descriptions

Sewer maps were obtained for parts of New York City and Boston. These maps show sewer location, size, manhole inverts, and catchment area. Using these maps, three study areas are considered and shown in Figure 2.4 with their properties summarized in Table 2.3. The first, HP009 is a 149 ha combined sewer catchment in Bronx, NY located in a heavily urbanized residential neighborhood. The second in East Boston, Massachusetts (designated as Section 77) is also located in a heavily urbanized 54 ha area serviced by a combined sewer. East Boston is unique from HP009 as it is located on a peninsula with much of its developed land on historic fill. In addition, East Boston has a unique diversity of sewer infrastructure with recent additions of separate storm sewers and a large interceptor pipe network to reduce combined sewer overflows. Section 77 was chosen because it is a purely combined sewer network that drains to a single point. The third site is a 65 ha separate stormsewer network also located in East Boston (immediately east of Section 77). This area was chosen because it is the largest purely stormwater network that drains to a single outfall in East Boston.

Map analysis

The maps were analyzed using ESRI ArcMap 10.2 (Environmental Systems Research Institute, 2013) in order to determine lengths and areas required to calculate Horton order ratios and Hack's Law exponents. In urban networks, a single line of pipe can change in size at each manhole junction, so in order to make the analysis consistent with river network analysis, these pipes were joined as single units averaging their characteristics including pipe diameter.

Testing Hack's Law in urban sewersheds

Hack's Law relates the length of a drainage network to the contributing area as discussed above. In a fractal, Hack's Law is applicable at all scales within a network. The stream length was determined as the longest contributing pipe length feeding into a given junction. The drainage area was the total area contributing to that given point. The smallest resolution for computing drainage area was one urban block. Using the relationship between the measured area and length, the coefficients (h and C) of the power law were determined to best fit the data at all hierarchical levels. Using these coefficients and the power equation, predicted lengths were calculated at all scales. Goodness of fit (R^2) from of the observed results to the predicted results was calculated to assess the network's consistency with Hack's Law.

Measuring the consistency of Horton order ratios at each scale

Self-similarity is determined by consistent Horton order ratios at each scale. In this analysis, Strahler order was applied throughout the network such that the combination of two 1st order pipes resulted in a 2nd order pipe. The pipe length, diameter, slope, and contributing area were measured for each pipe and defined by order. Using this data, the bifurcation ratio R_B, the length-order ratio R_L, the area-order ratio R_A, the conduit diameter-order ratio R_D, and the drainage density DD were calculated at each for each order. Horton order ratios relate mean values, so standard errors of each measured mean were propagated to determine the standard deviation of each ratio (Ku, 1966). The results are compared to Horton order ratios observed in natural river basins summarized in Table 2.2.

Additional Analysis

In addition to the above calculations, the following fractal parameters were calculated: Hurst exponent (H), scaling exponent (ϕ_L), elongation exponent (q). These will be determined using the equations 7,8,9 and 10 described above by measuring basin length (L_{II}) and basin width ($L_{\perp}$) for each order above 1. For comparison with other studies, the fractal dimensions of the networks are also calculated from the Hack's Law coefficient. These values, in addition to the Hack's coefficients, were compared to values observed in river basins determine the similarity to natural systems (Table 2.1).

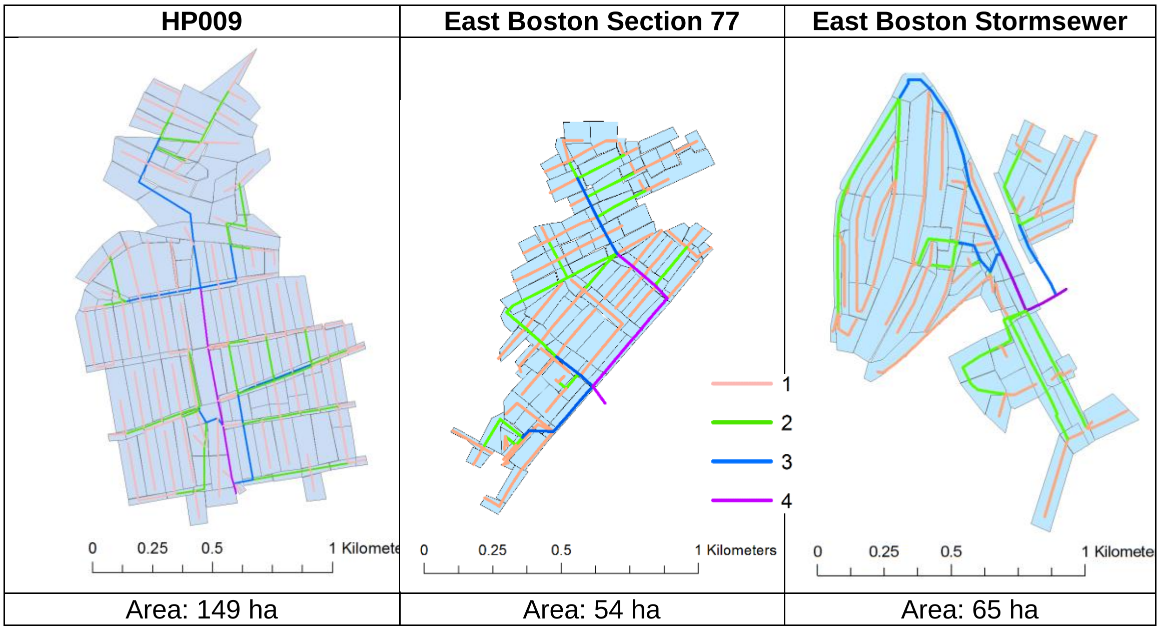

Figure 2.4: *Strahler order applied to each of the drainage networks.*

Table 2.3: *Description of urban catchments used in the study*

	HP009	East Boston Section 77	East Boston Stormwater
Area (ha)	149	54	65
Majority Soil Type (NRCS, 2017)	Till substratum	Silty Loam	Silty Loam
Topographic Slope (NRCS, 2017)	0-8%	3-15%	0-25%
Estimated Population Density (per ha) (US Census Bureau, 2010)	220	201	66
Sewer Type	Combined	Combined	Stormwater
Total Pipe Length (m)	20375	10502	13170

Results

Sewer length and contributing drainage area were plotted on log-log scale for each network individually and together in Figure 2.5. The R^2 linear regression to Hack's for HP009, East Boston Combined Sewer (Section 77), and the East Boston Stormwater Sewer were 0.94, 0.86, and 0.88 respectively. The R^2 was 0.81 when combining the results of all three sites on one plot. In all cases, most deviation from Hack's Law was observed higher in the catchment when stream length and drainage area are low. As the stream length and drainage area increase, each system begins to move closer toward the expected result as determined by the Hack's Law power equation.

A summary of the scaling law coefficients is compiled in Table 2.4. The scaling exponent ϕ_L was determined to be between 1.07-1.09 for all three sites with a standard deviation between 0.05-0.08). The Hack's Law exponent (h) observed over the three sites was between 0.54-0.56 with a standard deviation of 0.01 in each case. The Hurst exponent varied from 0.87-0.94. The calculated elongation coefficient (q) was 0.12-0.13. The Hack's Law coefficient (C) was 0.50 in HP009, 0.99 in the East Boston Combined Sewer, and 1.28 in the East Boston Separate Sewer. The fractal dimension (D) varied from 1.79-1.85.

The results from the Horton order ratio analysis are compiled in Table 2.5. The 3rd order was the highest observed order in the three sites. R_B, R_L, R_A, DD, and R_D are listed at each order for each site in addition to the averages of each site. The associated standard deviation with each measurement is also presented.

Table 2.4: *Hack's Law and Fractal Coefficients.*

	HP009	East Boston Section 77	East Boston Stormwater	From Rigon et al. in River Basin
ϕ_L	1.07	1.08	1.09	1.05
Std Dev	0.05	0.08	0.08	
h	0.54 ± 0.01	0.55 ± 0.01	0.56 ± 0.01	0.55
H	0.87	0.94	0.92	0.93
q	0.13	0.12	0.13	
C	0.50	0.99	1.28	
Fractal Dimension, D	1.85	1.82	1.79	1.82
R^2 to Predicted	0.94	0.86	0.88	

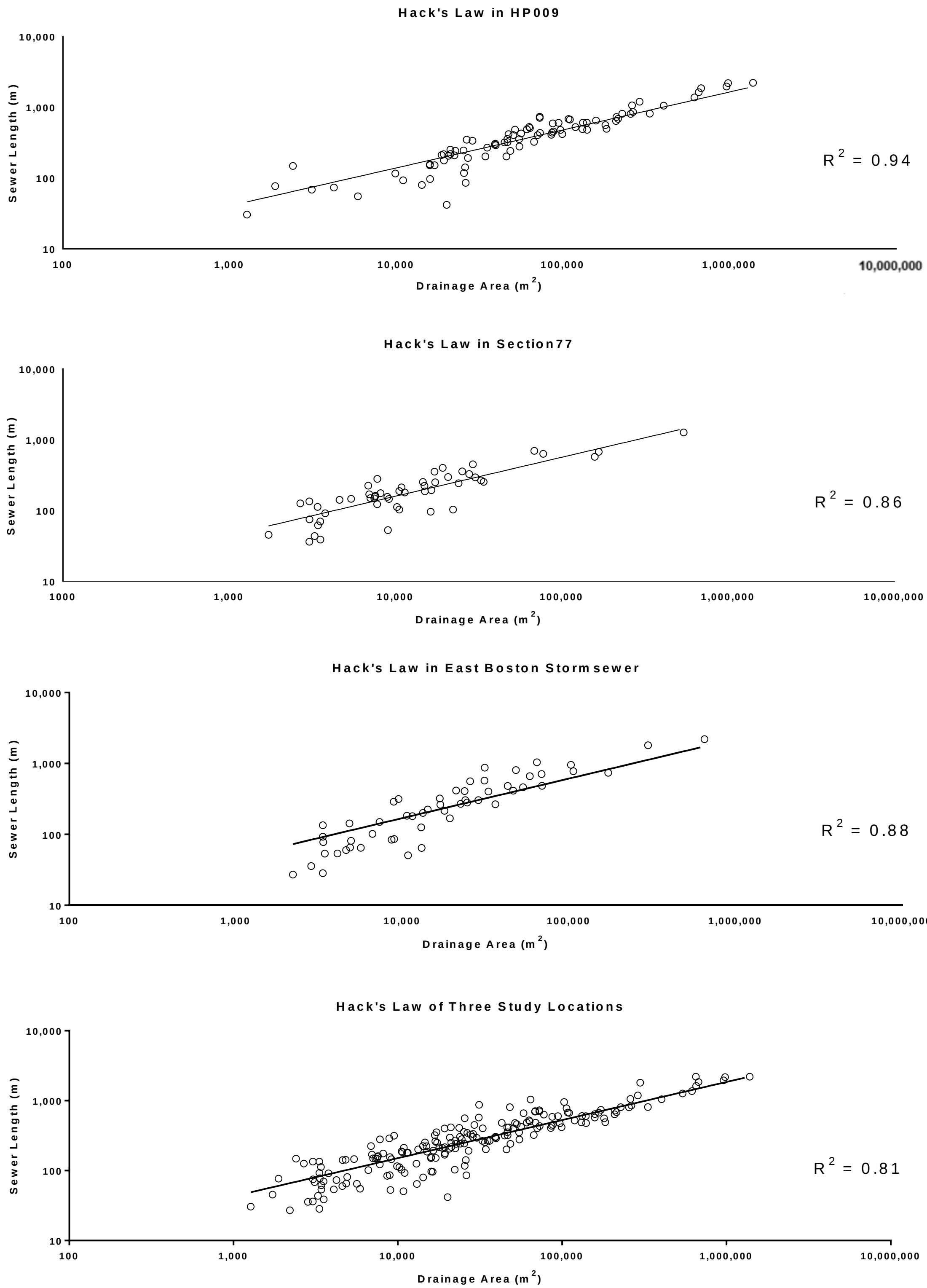

***Figure 2.5:** Hack's Law applied over the urban catchments.*

Table 2.5: *Results from the Horton Order Analysis for all Sites.*

		HP009		East Boston Section 77		East Boston Stormwater		Average	
R_B			Std Dev		Std Dev		Std Dev		Std Dev
	1st Order	4.89	-	4.08	-	3.33	-	4.1	-
	2nd Order	3.60	-	4.33	-	4.00	-	3.98	-
	3rd Order	5.00	-	3.00	-	3.00	-	3.67	-
	Average	4.50	0.78	3.80	0.71	3.44	0.51	3.91	0.66
R_L									
	1st Order	3.08	0.32	2.35	0.37	3.03	0.59	2.82	0.43
	2nd Order	2.17	0.62	2.22	0.32	1.90	0.65	2.10	0.53
	3rd Order	2.31	0.29	1.96	0.11	1.99	0.63	2.09	0.34
	Average	2.52	0.41	2.18	0.27	2.31	0.62	2.33	0.43
DD									
	1st Order	1.91	-	2.05	-	1.24	-	1.73	-
	2nd Order	2.23	-	2.18	-	2.07	-	2.16	-
	3rd Order	2.18	-	2.11	-	1.70	-	2.00	-
	Average	2.11	0.17	2.11	0.07	1.67	0.42	1.96	0.22
R_A									
	1st Order	4.68	0.93	3.19	0.66	3.56	0.72	3.81	0.77
	2nd Order	4.84	1.44	4.86	1.45	3.92	1.30	4.54	1.40
	3rd Order	5.05	1.24	4.13	0.99	3.39	0.99	4.19	1.07
	Average	4.86	1.20	4.06	1.03	3.62	1.00	4.18	1.08
R_D									
	1st Order	2.10	0.42	1.47	0.15	1.56	0.19	1.71	0.25
	2nd Order	2.24	0.59	1.58	0.32	1.66	0.47	1.83	0.46
	3rd Order	1.51	0.31	1.32	0.24	1.81	0.47	1.55	0.34
	Average	1.95	0.44	1.46	0.24	1.67	0.38	1.69	0.35

Discussion

Hack's Law, while generally holding true for all the networks showed significant inconsistencies higher in the network when total drainage area and stream length were low. This result was also evident in river networks as the inherent variability of the network is most pronounced at its individual nodes (Montgomery and Dietrich, 1992). Additionally, the fractal coefficients and exponents of the urban networks were consistent with the results from Rigon et al. (1996) even though the networks in that study were all greater than 200 km^2, much larger than the 3 sites used in this study.

A perfect fractal would have Horton order ratios equivalent at each order. The following summarizes each of the calculated ratios in the analysis and relates the values observed in natural rivers basins shown in Table 2.2. As a more concise reference, the average results from this study and reproduced along with the results from previous literature reviewed studies in Table 2.6:

- R_B: The bifurcation ratio ranged between 3-5 in the networks of this study. This is consistent when compared to natural river basins which ranged from 2.7-4.81. Additionally, Rosso et al. (1991) reported a standard error of 0.24 in the Alto Liri Basin compared to a standard error between 0.29-0.45 observed in the three sewers (calculated standard deviations were converted to standard error for comparison purposes).
- R_L: The ratio of the network lengths ranged from 1.9 to 3.08 with more consistency found in the higher orders. This is the result of the heterogeneity of the first order systems which average out over the total length of the network. Natural river basins observed were between 1.75-2.97. Rosso et al. (1991) reported a standard error of 0.30 compared to the 0.16-0.30 in the sewers.
- DD: The drainage density of the networks ranged from 1.24-2.23 and was fairly consistent which is expected due to the positive correlation of Hack's Law.
- R_A: The area order ratio ranged from 3.19-5.05 and had the greatest standard deviation due again to the heterogeneity of the first order systems. In natural river basins this ratio

ranged between 2.80-5.28 and Rosso et al. (1991) reported a 0.46 standard error compared with a standard error between 0.58-0.69 in the sewers.

- R_D: The pipe order ratio ranged from 1.34-2.23 and showed the most consistency with low standard deviations and consistent values in East Boston. In the Bronx, the pipe size tended to increase more by order than in East Boston. This may be telling of the design techniques employed by a different municipality.

When comparing each order to one another in the same network, there was significant variance between scales. On average, however, each of the Horton order ratios analyzed in this research showed consistency between orders. Horton order ratios showed similar results as predicted by Cantone et al. (2011), with most inconsistency at the lower orders. At higher orders the network appeared to be most predictable in terms of conduit diameter and sewer length. Another interesting result from this analysis was that the fractal dimensions found in each network were between 1.79 and 1.85 compared to 1.82 typically found in natural river basins.

Table 2.6: *Summary of average Horton order ratios in this study and other literature reviewed sources.*

	Bronx	**East Boston Combined Sewer**	**East Boston Separate Sewer**	**Average**	**River Basin Ave.**	**Marani et al. (1991)**	**Sewer Std. Error**	**Cantone and Schmidt (2011)**
R_B	4.50±0.78	3.80±0.71	3.44±0.51	3.91±0.66	3.97	4.75±(0.24)	(0.29-0.45)	2.73±1.54
R_L	2.52±0.41	2.18±0.27	2.31±0.62	2.33±0.43	2.27	2.50±(0.30)	(0.16-0.30)	
R_A	4.86±1.20	4.06±1.03	3.62±1.00	4.18±1.08	4.43	5.13±(0.46)	(0.58-0.69)	
R_D	1.95±0.44	1.46±0.24	1.67±0.38	1.69±0.35				1.60±0.56

Conclusions

In natural river basins, scaling laws were developed through analyzing many different systems across many different topographies. While this research contributes to the scope of sewershed fractal geometry, in order to create general rules that could be applied universally, more sewer network should be analyzed to understand how these rules should be applied throughout different municipal systems. Additionally, in the case of East Boston which is located on a peninsula and nearly entirely surround by water, the network is unable to branch out along water boundaries. For these reasons, when assessing the entirety of East Boston, it is difficult to assess the network orders greater than 4 despite orders of 5 and potentially 6 existing in East Boston as a result of combined sewer interceptor pipes which service most of the combined sewer portion of the area.

Regardless of the inconsistent Horton ordering throughout the network, there is value in using this method to define their geometric characteristics. Using simple Horton order ratios of a sewer system, the general structure of a system, its density, and relative pipe sizes can be defined and compared to another. According to British mathematician Michael Barnsley (1988), “Fractal geometry is a new language. Once you can speak it, you can describe the shape of a cloud as precisely as an architect can describe a house”. Despite the coarseness of a sewer layout relative to clouds, developing this mode of analytical thinking could have broad applications across many other human systems.

List of References

Barnsley, M. F. (1988). *Fractals Everywhere,* Corr. print. Ed., Acad. Press, Boston [u.a.].

Benoit Mandelbrot. (1967). "How Long is the Coast of Britain? Statistical Self-Similarity and Fractional Dimension." *Science,* 156(3775), 636-638.

Birnir. (2008). "Turbulent Rivers." *Quarterly of Applied Mathematics,* 66(3), 565-594.

Cantone, J., and Schmidt, A. (2011). "Improved Understanding and Prediction of the Hydrologic Response of Highly Urbanized Catchments through Development of the Illinois Urban Hydrologic Model." *Water Resour. Res.,* 47(8), W08538.

Dodds, P. S., and Rothman, D. H. (1999). "Unified View of Scaling Laws for River Networks." *Phys. Rev. E,* 59(5), 4865-4877.

Environmental Systems Research Institute. (2013). "ArcGIS." (10.2), .

Gires, A., Tchiguirinskaia, I., Schertzer, D., Ochoa Rodriguez, S., Willems, P., Ichiba, A., Wang, L., Pina, R., Van Assel, J., Bruni, G. (2016). "Fractal Analysis of Urban Catchments and their Representation in Semi-Distributed Models: Imperviousness and Sewer System." *Hydrology and Earth System Sciences & Discussions,* , 1-23.

Hack, J. T., and Geological Survey, (U S). (1957). *Studies of Longitudinal Stream Profiles in Virginia and Maryland,* .

HORTON, R. E. (1945). "Erosional Development of Streams and their Drainage Basins; Hydrophysical Approach to Quantitative Morphology." *GSA Bulletin,* 56(3), 275.

Ku, H. H. (1966). "Notes on the use of Propagation of Error Formulas." .

Mandelbrot, B. B. (1983). *The Fractal Geometry of Nature,* updated and augmented ed. Ed., Freeman, New York, NY.

Montgomery, D., and Dietrich, W. (1992). "Channel Initiation and the Problem of Landscape Scale." *Science,* 255, 826-830.

Moussa, R., and Bocquillon, C. (1996). "Fractal Analyses of Tree-Like Channel Networks from Digital Elevation Model Data." *Journal of Hydrology,* 187(1-2), 157-172.

National Resource Conservation Service. (2017). "Web Soil Survey." .

Peckham, S. D. (1995). "New Results for Self-Similar Trees with Applications to River Networks." *Water Resour. Res.,* 31(4), 1023-1029.

Qian, B., and Rasheed, K. (2004). "Hurst Exponent and Financial Market Predictability." *IASTED Conference on Financial Engineering and Applications ,* .

Rigon, R., and Rinaldo, A. (1991). "A Note on Fractal Channel Networks." *Water Resour. Res.,* 27(12), 3041-3044.

Rigon, R., Rodriguez-Iturbe, I., Maritan, A., Giacometti, A., Tarboton, D. G., Rinaldo, A. (1996). "On Hack's Law." *Water Resour. Res.,* 32(11), 3367-3374.

Rodríguez-Iturbe, I., and Rinaldo, A. (2001). *Fractal River Basins,* 1. paperback ed. Ed., Cambridge Univ. Press, Cambridge [u.a.].

Rosso, R., Baslassare, B., Barbera, P. (1991). "Fractal Relation of Mainstream Length to Catchment Area in River Networks." *Water Resour. Res.,* 27(3), 381-387.

Scheidegger, A. E. (1968). "Horton's Law of Stream Numbers." *Water Resources Research,* 4(3), 655.

Steffen, W., Grinevald, J., Crutzen, P., McNeill, J. (2011). "The Anthropocene: Conceptual and Historical Perspectives." *Philosophical Transactions of the Royal Society of London A: Mathematical, Physical and Engineering Sciences,* 369(1938), 842-867.

Strahler, A. N. (1957). "Quantitative Analysis of Watershed Geomorphology." *Eos, Transactions American Geophysical Union,* 38(6), 913-920.

Thibault. (1991). "Fractals Et Structure Des Réseaux Urbains D'Assainissement Eau Pluviale." *Flux,* 7(4), 5-14.

U.S. Census Bureau. (2010). "2010 Census." .

Chapter 3: Modeling urban sewers with artificial fractal geometries

Comparing existing to synthetic sewer networks in simulating sewer flow compared to measured results

Abstract

Sewer models are used to simulate complex urban hydrology. However, the development of physically based models can be difficult given the limited availability of sewer plans and the time required to incorporate the actual system layout including pipe locations, sizes, inverts, and catchment characteristics. By contrast, fractal geometries could potentially be used to overcome some of these constraints. In this study, a highly impervious residential urban catchment (54 ha) serviced by a combined sewer in East Boston, Massachusetts is modeled using Storm Water Management Model (SWMM). Two different modeling techniques are compared. The first is a physically based model developed from the physical characteristic of the network obtained from municipal sewer maps; the second is an artificial model developed based on fractal scaling laws often used to describe natural river basins. Both models were calibrated to one month of empirical 5-minute interval sewer flow measurements and predicted similar total discharge volumes and peak flows over the course of 10 observed rainfall events (0.5-12.7 mm) with Nash-Sutcliffe model efficiency coefficient (NSE) values of 0.85 over the duration of observed flow. In a neighboring 24 ha catchment, this process was repeated creating a second comparison between a physically and artificially based model using pipe and catchment model parameters obtained from the previous calibration and evaluated to a second set of observed flow over the same period. Again, both models predicted similar total discharge volumes and peak flows, although, over the duration of the observed flow, the physically based model was more accurate than the artificial model (NSE of 0.85 and 0.75 respectively). In both cases, the models were most accurate at simulating storms larger than 5 mm with most deviation in smaller events. Model resolution was tested by simulating the 54 ha catchment as 1, 10, 24, and 173 subcatchments and showed that accurate simulations could be produced in all of the resolutions

however, caution should be taken when employing low resolution aggregated models as suggested from previous academic research.

Introduction

Stormwater runoff is a major concern for cities due to its detrimental effects on ecosystems, water quality, and sewer infrastructure. Descriptions of the hydrologic and hydraulic (H&H) flow processes of urban drainage systems can be accomplished with computer models and simulations. One of the most widely used methods for H&H modeling is the United States Environmental Protection Agency's (US EPA) Storm Water Management Model (SWMM), a dynamic rainfall-runoff-subsurface runoff simulation model that can be used for both single-event and long-term simulation of surface and subsurface hydrology for both urban and suburban environments (US EPA, 2017). SWMM is a robust modeling method that is able to account for a wide range of hydrologic processes including time-varying rainfall, evaporation of standing surface water, snow accumulation and melting, rainfall interception and depression storage, infiltration of rainfall into unsaturated soil layers, percolation of infiltrated water into groundwater layers, interflow between groundwater and the drainage system, nonlinear reservoir routing and overland flow, and the capture and retention of rainfall and runoff with various types of low impact development (LID) practices (US EPA, 2017).

Development of accurate reliable sewer models can, however, be challenging due to the availability of sewer infrastructure plans, the amount of time required to create a detailed H&H model, and limited availability of sewer flow data with which to calibrate a model. The use of artificial sewer models could help to circumvent these issues provided they can produce reasonable results without full calibration to observed flows. Artificial networks could be designed based on fractal geometries extensively analyzed in natural river basins (Jeffers and Montalto, 2017, Cantone and Schmidt, 2011).

Natural river basins generally take the shape of a dendritic tree. A typical binary dendritic fractal tree geometry will have one trunk branching out into two half sized branches repeated for a number of generations. Tokunaga modified this binary tree to include more branches to increase the drainage density and be more representative of natural geometries, an example shown in Figure 3.1 (Turcotte and Newman, 1996). The drainage density of the network can be defined by the fractal dimension (D), where D=1 represents a single dimension line (and no drainage area) and D=2 represents a completely filled 2-dimensional square (with maximum drainage density) (Figure 3.2).

a) b)

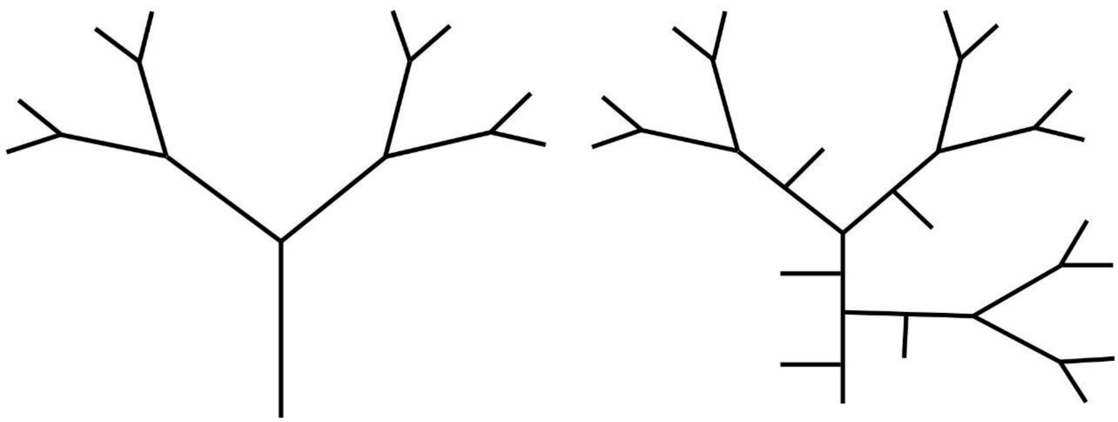

Figure 3.1:

a) Binary dendritic fractal tree showing four Strahler stream orders

b) The Tokunaga fractal method includes space filling branches more characteristic the drainage density found in natural stream networks

(adapted from Turcotte and Newman, 1996)

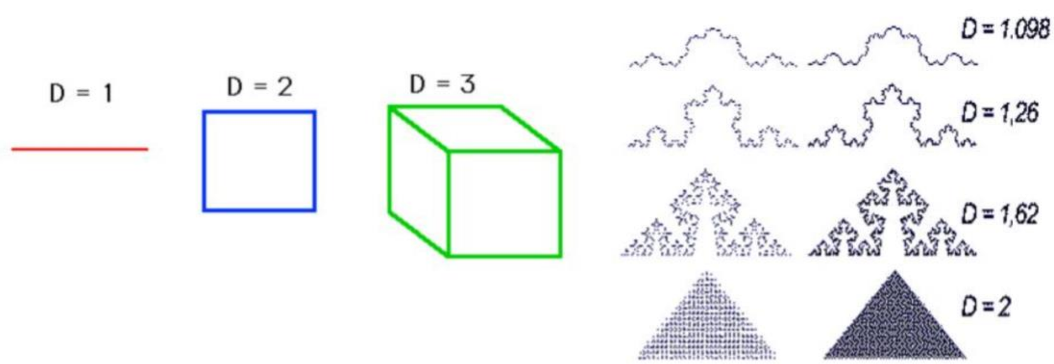

Figure 3.2: *Dimensions are typically thought in terms of length (1st dimension), width (2nd), and depth (3rd) (left image) (reproduced from Ryan, 2007). Fractal dimensions can be between two dimensions illustrated with the Koch curve fractal (right image) (reproduced from Vassallo, 2005). As the fractal dimension increases, the density increases as it approaches the 2nd dimension.*

Mathematically, fractals can be represented by power law expressions because they display scale invariance between geometric scales. Scale invariance means that the pattern observed at a given scale will be identical to the pattern at both larger and smaller scales. In 1957, John Hack of the United States Geological Survey empirically determined scale invariant power law relationships that relate a river basin's length to the contributing drainage area, now known as Hack's Law (1957). In 1967, French mathematician Benoit Mandelbrot began implementing and refining power law geometry in natural systems with fractals (1967). Traditionally, river basin geometry is defined using Strahler stream ordering, a classification scheme whereby each tributary is numerically ranked such that a first-order stream has no tributaries, a second-order is the joining of two first-orders, and so on. By combining Strahler ordering with fractal power laws, Rodriguez-Iturbe and Rinaldo (2001) in their book "Fractal River Basins: Chance and Self-Organization," introduce methods to analyze natural river basins geometries and the effect they have on the drainage networks. Because the natural world rarely shows such perfect invariance, fractal models are best employed with stochastic-variance. That is to say that probabilistic rules affecting a system will be the same at each scale, but the way the pattern manifests will have random elements governed by those rules (Veneziano and Langousis, 2010).

These methods have previously been applied to generate artificial sewer networks. The Artificial Network Generator (ANGel) developed by Ghosh et al. (2006) allows for the stochastic creation of an artificial sewer network using Tokunaga fractal geometry. The program creates pipes and nodes at various spatial scales. Ghosh (2006) used this method to investigate scale effects in hydrologic models by comparing predicted runoff of a large 4.66 km^2 catchment in the lower Charles River in Boston broken into 4, 18, and 401 subcatchments with increasing drainage densities (total pipe length). The results showed little difference in predicted total runoff volume simulated at the different resolutions, but the predicted peak runoff rates were significantly different at lower resolutions. There was also a dual effect on peak flow rates: larger storms in low resolution models tended toward less flow while smaller storms resulted in more flow when comparing the results of the models to each other. Ghosh surmised that the effect came from the difference in both the length of overland flow and conduit routing (Ghosh and Hellweger, 2012). In this analysis, there were no observed results, only modeled predictions.

Möderl (2009) developed another method of generating artificial networks called the Case Study Generator (CSG). This method stochastically generates nodes and conduits based on Galton-Watson branching, another type of dendritic geometry typically associated with a family tree. Möderl used this tool to simulate 10,000 different artificial networks to analyze flooding and combined sewer overflows alongside two actual networks in Austria. Unlike the ANGel model, this method is able to simulate many different networks at one time whereas ANGel only generates one. However, the Galton-Watson geometry is less similar to urban networks than the Tokunaga geometry (with all branching occurring in generally one direction) and because the CSG currently is not georeferenced, it is less practical for GIS applications analyzing physical networks.

Ghosh and Möderl demonstrated the potential use of fractal scaling rules to develop artificial sewer networks for urban H&H modeling, but did not meaningfully characterize their precision through comparison to observations. While Ghosh was able to simulate comparable results to one observed storm (Ghosh reported no numerical analysis on accuracy), a more comprehensive evaluation of the approach would ideally consider multiple storms and multiple sewer networks with a thorough evaluation of the goodness of fit of the predictions to the observations. Likewise, Möderl only compared two storms to his model without any detailed analysis of the hydrologic response difference between the two, reporting only the surface ponding results as the only criteria for performance. Further, from a modeling perspective, understanding the sensitivity of the critical modeling parameters in the artificial networks is important for future implementation applying them to other unique networks.

One of the main motivations for developing artificial sewer networks is to simplify the urban H&H modeling process. Several researchers have already shown that models built based on simplifications of urban drainage networks can produce reasonable results. This literature focuses on subcatchment aggregation and conduit sketetonization. For example, Huber (2006) showed that for a 7 ha urban catchment, a physically based model that accounted for H&H processes on every parcel performed as well as a lower resolution model utilizing street blocks as the base hydrologic response unit (HRU) (118 versus 14 subcatchments). This result was repeated by Goldstein (2011) who showed that that a block scale SWMM model perform as well, if not better, than a high resolution physically based model when that incorporated all the pipes and features existing on one urban block. At greater modelled areas, low resolution can create error. This was shown by Cantone and Schmidt (2009) who created a physically based model of a 5.2 ha catchment using subcatchment resolution ranging from 44 to 1 and found that the most accurate predictions were obtained with 8 subcatchments. Modeling the entire catchment as one subcatchment resulted in a greater time of concentration and lower peak flows and the greatest error. This finding was replicated in a 341 ha catchment modeled with between 773 and 1 HRUs, again showing that the most accurate model had 65 subcatchments. The authors note that this result is troublesome because it is common for municipalities (in their case the City of Chicago) to utilize on these low resolution models for the reasons cited at the introduction of this paper.

The focus of this paper is to test the accuracy of artificial sewer models built with fractal scaling laws urban watersheds. This goal will be accomplished by using Tokunaga fractal geometries found in natural river basins to represent urban catchments using the ANGel program. The hydrologic response of the artificial networks will be analyzed based on multiple storms and observed catchment discharge for two sewersheds. Additionally, a sensitivity analysis will be conducted to help inform the model calibration. Evidence supporting the application of fractal geometries to urban catchments can be found in a companion paper (Jeffers and Montalto, in preparation).

Methodology

Site Description

East Boston is a neighborhood in Boston, Massachusetts serviced by both separate and combined sewers. The study area in this analysis included two sections of the combined sewer network. The first section of the sewer network analyzed services a 54 ha highly impervious (land use shown in Figure 3.3) combined sewer in a mostly urban residential area (201 people per ha) which will be referred to as East Boston Section 77 (US Census Bureau, 2010). Based on soil survey data from the Natural Resource Conservation Service, the typical soil profile is defined by silty loam with a deep infiltration rate of 0.71 cm/hr with topographic slopes ranging from 3-15% (NCRS, 2017). The second section analyzed is a 22 ha area, referred to as East Boston Section 81. It is similar to Section 77 in that it is an immediately adjacent, highly impervious residential catchment, serviced by a combined sewer. Due to its prolixity to Section 71, its soil survey was the same as Section 77. Both Section 77 and Section 81 were chosen because they drain to a single point at a regulator were observed sewer data was available.

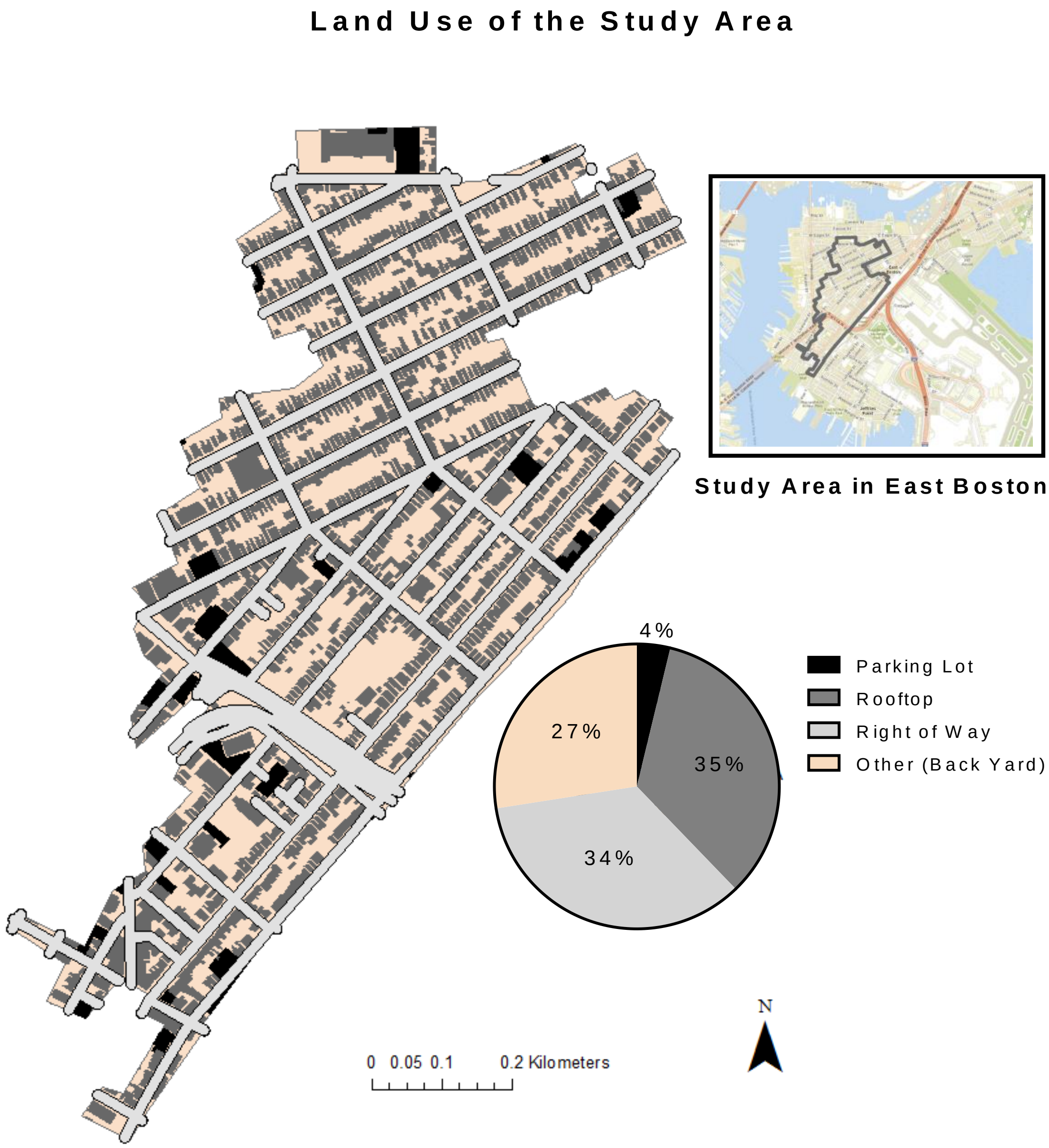

Figure 3.3: *Land use of East Boston Section 77.*

Model Development

A physically based model of the area was developed with PCSWMM 2017 (with SWMM engine version 5.1.011 (US EPA, 2017)) using GIS data provided from the Boston Water Sewer Commission. The model included pipe sizes, inverts, manhole and catch basin locations, topography, and all special sewer points including regulators based on the map details. One month of 5-minute interval sewer flow data from April 15 to May 15, 2016 was obtained at the downstream regulator for use in calibrating and validating the model. Subcatchments were modeled at the block scale. The model was run over the course of the observed sewer flow period using rainfall data from a tipping bucket rain gage on a 15-minute interval located I Charlestown roughly 1.5 km away from the catchment. This period included 10 rain events ranging from 0.51-12.7 mm. The results from the simulated network were calibrated to the observed flow by adjusting the most sensitive parameters discussed later in this section. SWMM simulations were run under dynamic wave routing, Horton infiltration (max rate of 76.2 mm/hr and min rate of 12.7 mm/hr), 5-minute time steps routed at 5 seconds, dampen inertial terms, both normal flow criteria, and the Hazen-Williams force main equation.

A second artificial model was developed based on fractal scaling laws using the ANGel program. ANGel version 1.0 was provided by Dr. Ferdi Hellweger from Northeastern University. In the user interface of the ArcGIS plugin ANGel, first a shapefile is imported into ArcGIS, in this case the outline of the East Boston drainage area. Using ANGel, the start and end points of the network are defined. Next, the number of generations is defined equivalent to the maximum Strahler stream order in the system. ANGel employs the Tokunaga fractal tree such it begins with a main truck then branches out at 90,180, and 270 degrees. The pattern is repeated at each branch based on the stream order selected. ANGel also allows for irregularity in the fractal such that there are stochastically generated irregular bends in the Tokunaga branching deviating from perfect geometry. This option was enable in the network generation using the default value of 30. Additionally, the shape of the network can be restricted by the catchment boundary shapefile such that all pipes are contained in the catchment. Based on the artificial HRUs generated this way, manholes, pipes, and/or subcatchments are exported to a GIS enabled SWMM model using the ArcGIS built-in export tool (Ghosh et al. 2006). Manhole inverts in the artificial network were assumed based on a 2% pipe slope with the outfall of the network as the lowest point. Pipe diameters were selected to eliminate all flooding and surcharge of the sewer network to avoid additional complexity that could arise from under-sizing the network. The resulting networks from the two models are shown in Figure 3.4 below.

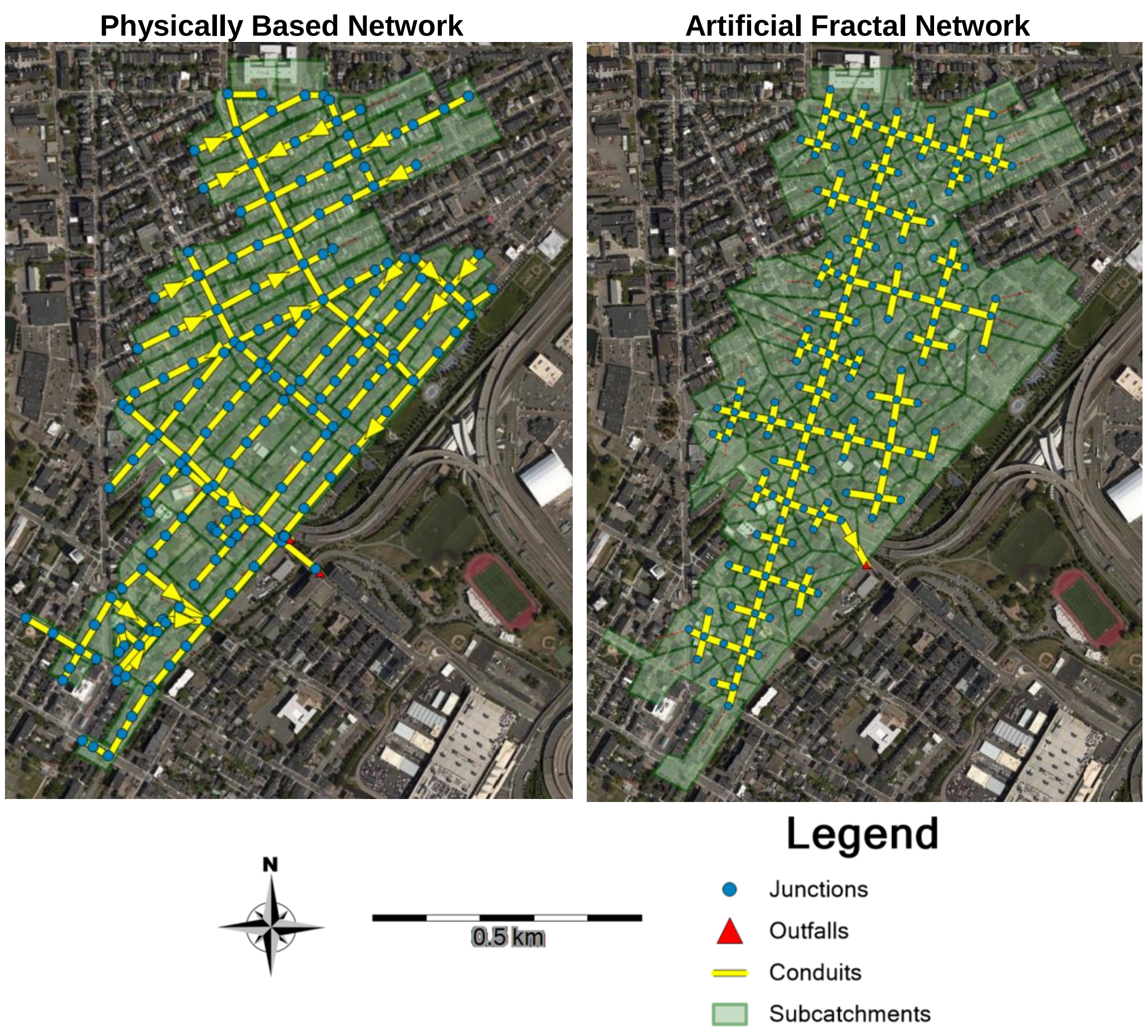

Figure 3.4: *Images from PCSWMM showing the physically based (left) and artificial fractal (right) networks for Section 77. The regulator in this submodel is the lowest point.*

Further Model Considerations

This section of East Boston is serviced by a combined sewer such that sanitary and stormwater combined in one pipe. As a result, there is dry weather flow (DWF) in the system at all times. DWF was estimated from a week of observed DWF using the sewer flow monitoring data. In SWMM, DWF can be implemented as a weekly time pattern multiplied by an average flow and applied to nodes within the simulation. DWF was added to both the actual network and artificial models at each outfall. The applied time pattern was calculated using PCSWMM and the average DWF was determined over the observed period shown in Figure 3.5. The average DWF was 0.053 m^3/s and the modeled DWF had a NSE of 0.73 over the observed period.

Calibration of the models was accomplished by varying the subcatchment slope, % imperviousness, storage, length, the conduit roughness, and baseline DWF. The SWMM model is run multiple times using the PCSWMM SRTC calibration tool to adjust each parameter on a sliding scale. This tool was used to linearly adjust each parameter in increments of 25% of its original value to examine the effect on total discharge and peak discharge rate for the May 4th 12.45 mm event. A sensitivity analysis was performed on the following parameters: subcatchment slope, percent imperviousness, surface roughness, subcatchment length (directly related to catchment width), sewer pipe Manning's roughness, and DWF baseline flow. Both models were simulated multiple times to characterize the sensitivity of the predicted peak flow and total volumetric storm discharge at the section outfall. Each parameter was independently adjusted ±100% its original value over intervals of 25%.

The models were calibrated based on two events over the observed period by manually adjusting parameters to optimize peak flows and total discharge. The remaining eight storms were used to validate the model. Several methods were employed to assess model accuracy. Moriasi et al. (2007) recommend statistics including the Nash-Sutcliffe efficiency coefficient (NSE) in addition to graphical analysis based upon an extensive literature review of watershed simulations that compared simulations to observed results. In a technical code of practice for hydraulic modeling of sewer systems, the Wastewater Planning Users Group (2002) also developed criteria to assess model quality. Using a minimum of three observed storms, the peak flow rates should be in the range of +25% and -15% while the total volume should be +20% and -10%. Additionally, the percent error between the predicted an observed total and peak discharges is presented.

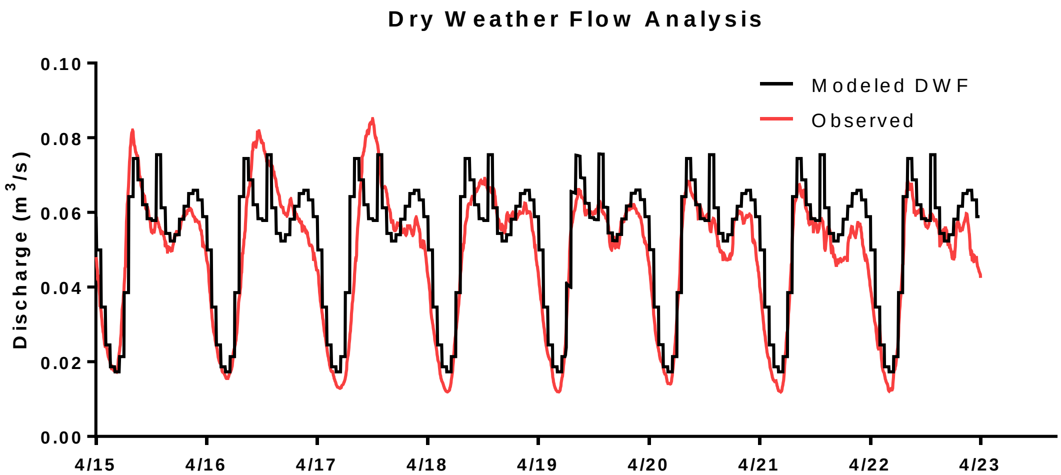

Figure 3.5: *DWF analysis from 4/15 to 4/23. Average DWF was 0.053 m³/s. The NSE of the modeled DWF over the observed period was 0.73.*

Further Model Validation

The subcatchment and conduit parameters determined from the Section 77 artificial model calibration process were applied to another artificial model developed to simulate Section 81. The purpose of this exercise was to determine the replicability of the findings without a direct calibration. A physically based model of Section 81 was developed for comparison to the artificial network. Properties from the subcatchments and conduits in the physically based model were determined from the previous Section 77 calibration. The model was simulated over the same 10 events as Section 77 and compared to observed sewer flow at the outfall. The two models are shown in Figure 3.6 below. A summary of the total pipe lengths, number of junctions, and subcatchments in each model is summarized in Table 3.1.

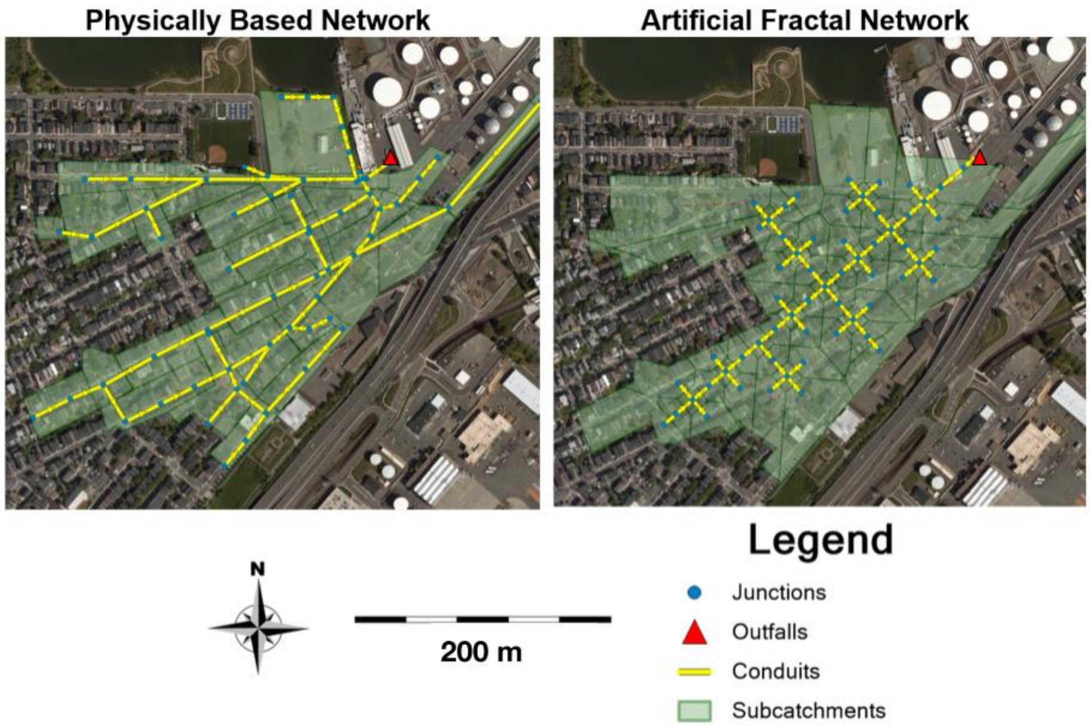

Figure 3.6: *Images from PCSWMM comparing the physically based (left) and artificial fractal (right) networks for Section 81. The regulator in this submodel is the lowest point.*

Table 3.1: *Summary of the network geometries in the physically based and artificial fractal model.*

Network Summary

Section 77	**Total Pipe Length (m)**	**# of Junctions**	**# of Subcatchments**	**Total Area (ha)**	**Longest Flow Path (m)**
Physically Based	10502	183	128	54	1377
Artificial Fractal	6889	173	173	54	1234
Section 81					
Physically Based	4394	65	35	22	818
Artificial Fractal	2195	60	59	22	695

Results

The results of the sensitivity analysis are shown in Figure 3.7 for the physically based and artificial fractal models. The only sensitive parameters for total catchment discharge were the % imperviousness and baseline DWF and both models were equally sensitive. Baseline DWF and % impervious were also highly sensitive parameters in both models for predicting peak discharge. A key difference between the two models was that the physically based model was more sensitive to conduit roughness than the fractal model. The final selected calibrated parameters used in the simulations are shown in Table 3.2.

Descriptions of the 10 simulated rainfall events in Section 77, which ranged from 0.51-12.7 mm of total precipitation, are summarized in Table 3.3. This table shows the date, rainfall depth, and duration of each of the storms in addition to the total discharge and peak flow rate of the observed, physically based model, and artificial fractal model. The percent error and NSE are listed for both models relative to the observed flow. Figure 3.8 provides a similar event summary graphically comparing the simulated to observed total discharge and peak flow for the physically based and artificial fractal models. The results are plotted within the bounds of the Wastewater Planning Users Group criteria for good model performance. Select hydrographs are shown in Figure 3.9 for April 26th (6.68 mm), May 1st (12.5 mm), May 4th (12.45 mm), and May 5th (3.81 mm). The observed and simulated flows in both models are shown along the rainfall time-series.

The results for Section 81 are formatted in the same way as Section 77. The summary of events for Section 81 is shown in Table 3.4. These results are graphically represented in Figure 3.10. Select hydrographs are shown in Figure 3.11.

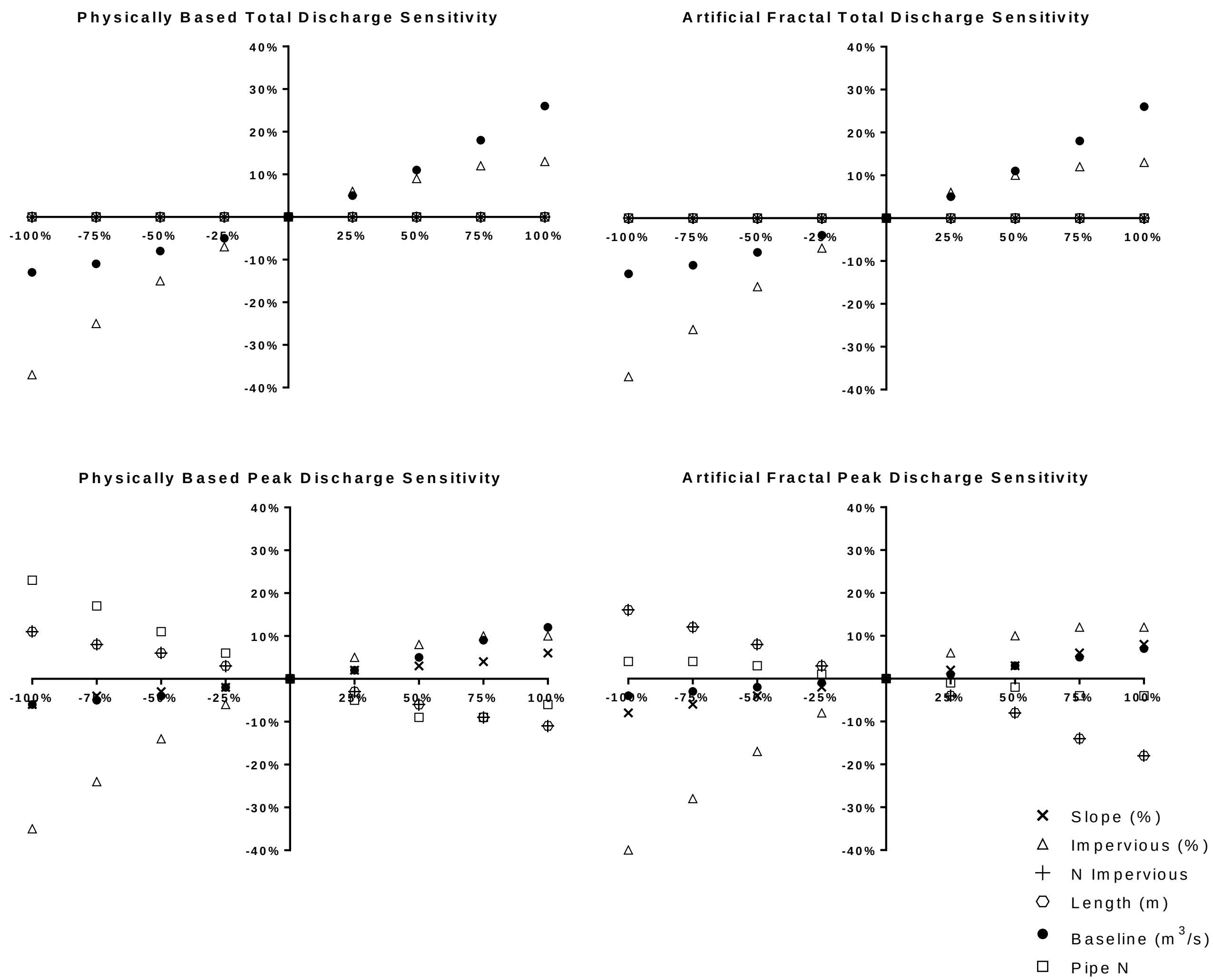

Figure 3.7: *Sensitivity Analysis of the physically based and artificial simulated network in East Boston Section 71 for May 4th 12.45 mm event.*

Table 3.2: *Calibrated sensitive parameters in each model for Section 77.*

Calibrated Parameters						
	Slope (%)	**% Impervious**	**n Impervious**	**Catchment Length**	**Pipe n**	**DWF**
Artificial Fractal	3.7	71.2	0.01	251 m	0.005	0.053 m^3/s
Physically Based	3	73.3	0.01	244 m	0.003	0.053 m^3/s

Table 3.3: *Result from the April to May, 2016 simulation at Section 77. Events used in the calibration process are denoted with a **

Rain Events				Observed		Physically Based Model					Artificial Fractal Model				
Event	Date	Rainfall (mm)	Duration (h)	Total Discharge (m^3)	Peak (m^3/s)	Total Discharge (m^3)	% Error	Peak (m^3/s)	% Error	NSE	Total Discharge (m^3)	% Error	Peak (m^3/s)	% Error	NSE
1	4/19	0.51	6	1111	0.07	1194	7.5%	0.07	13.4%	0.85	1192	7.3%	0.08	13.7%	0.85
2	4/23	2.29	17	3412	0.10	3523	3.2%	0.11	9.9%	0.7	3540	3.7%	0.09	-9.1%	0.74
3*	4/26	6.86	8	4010	0.58	4171	4.0%	0.62	6.6%	0.96	4202	5.0%	0.57	1.4%	0.94
4	5/1	12.70	27	9002	0.69	10203	13.3%	0.85	22.2%	0.88	10647	18.3%	0.88	27.2%	0.88
5	5/3	2.54	13	3398	0.12	3877	14.1%	0.14	9.4%	0.71	3973	16.9%	0.14	11.5%	0.57
6*	5/4	12.45	11	7139	0.50	6887	-3.5%	0.58	16.8%	0.89	7297	2.2%	0.48	-2.1%	0.89
7	5/5	3.81	13	3579	0.11	2939	-17.9%	0.10	-3.0%	0.48	2999	-16.2%	0.10	-7.9%	0.63
8	5/6	2.29	9	2047	0.13	2194	7.2%	0.22	72.0%	0	2211	8.0%	0.17	33.3%	0.23
9	5/8	0.51	6	1943	0.11	1454	-25.2%	0.10	-13.7%	0	1461	-24.8%	0.09	-21.5%	0
10	5/13	2.54	10	2095	0.12	3070	46.5%	0.19	56.0%	0	3160	50.8%	0.16	28.9%	0

Table 3.4: *Result from the April to May, 2016 simulation at Section 81*

Rain Events				Observed		Physically Based Model					Artificial Fractal Model				
Event	Date	Rainfall (mm)	Duration (h)	Total Discharge (m^3)	Peak (m^3/s)	Total Discharge (m^3)	% Error	Peak (m^3/s)	% Error	NSE	Total Discharge (m^3)	% Error	Peak (m^3/s)	% Error	NSE
1	4/19	0.51	6	294	0.02	260	-16.7%	0.01	-16.7%	0.43	263	-10.5%	0.01	-20.0%	0.50
2	4/23	2.29	17	1006	0.04	824	-18.1%	0.02	-38.5%	0.54	925	-8.0%	0.03	-30.0%	0.72
3	4/26	6.86	8	1192	0.25	1329	11.5%	0.23	-10.1%	0.87	1442	21.0%	0.22	-15.6%	0.62
4	5/1	12.70	27	2491	0.31	3081	23.7%	0.34	11.0%	0.90	3180	27.7%	0.32	3.5%	0.83
5	5/3	2.54	13	733	0.03	1074	46.5%	0.05	58.3%	0.56	1105	50.7%	0.05	25.0%	0.68
6	5/4	12.45	11	2031	0.18	2194	8.0%	0.23	28.1%	0.84	2347	15.6%	0.17	-4.9%	0.79
7	5/5	3.81	13	764	0.03	799	4.7%	0.03	10.0%	0.80	817	6.9%	0.03	0.0%	0.85
8	5/6	2.29	9	510	0.08	584	14.5%	0.07	-13.3%	0.06	603	18.2%	0.05	-57.9%	0.04
9	5/8	0.51	6	358	0.02	405	13.0%	0.03	71.4%	0.08	400	11.7%	0.03	30.0%	0.11
10	5/13	2.54	10	469	0.03	899	91.5%	0.07	100%	0.11	929	97.8%	0.05	33.3%	0.12

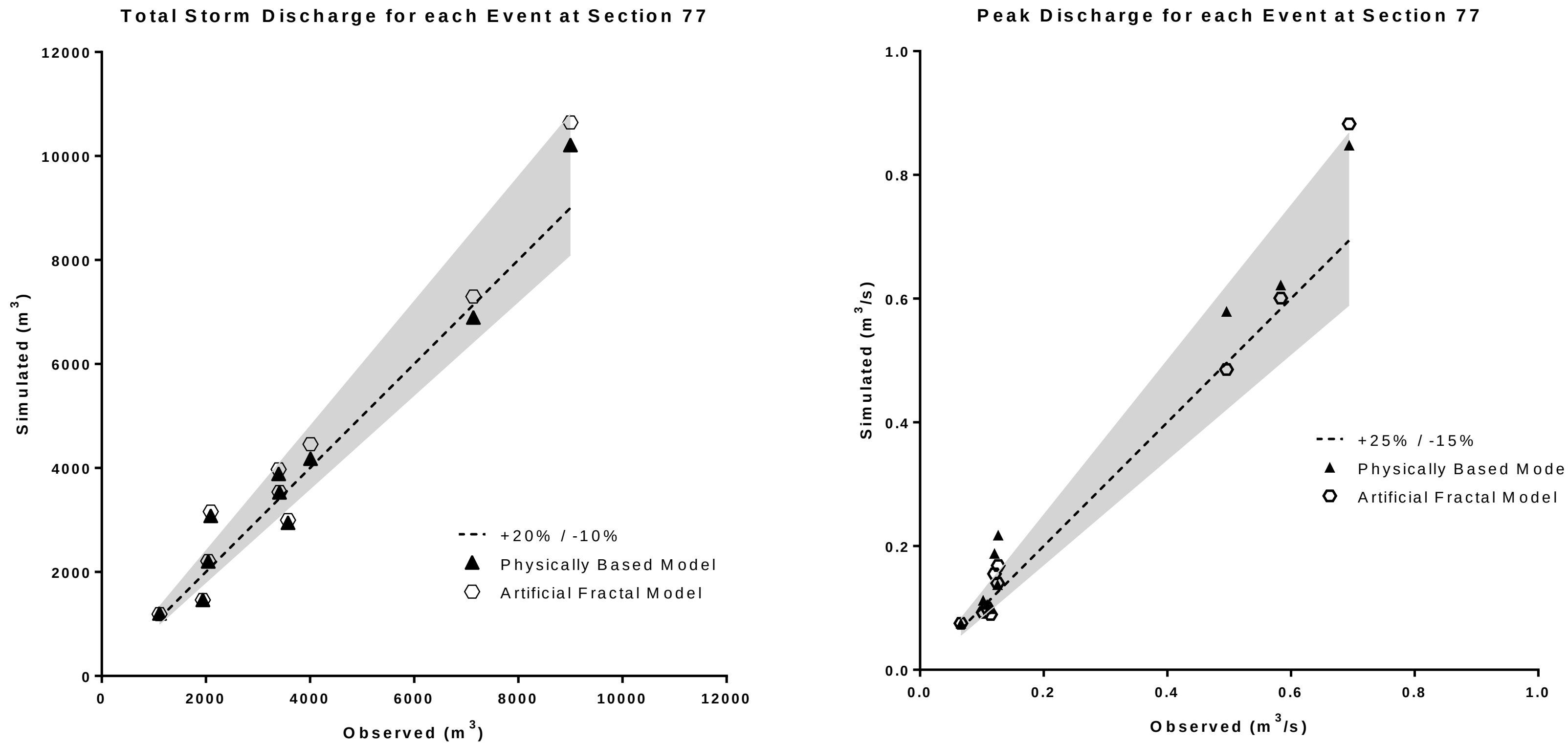

Figure 3.8: *Event Summary for the simulations in East Boston Section 77*

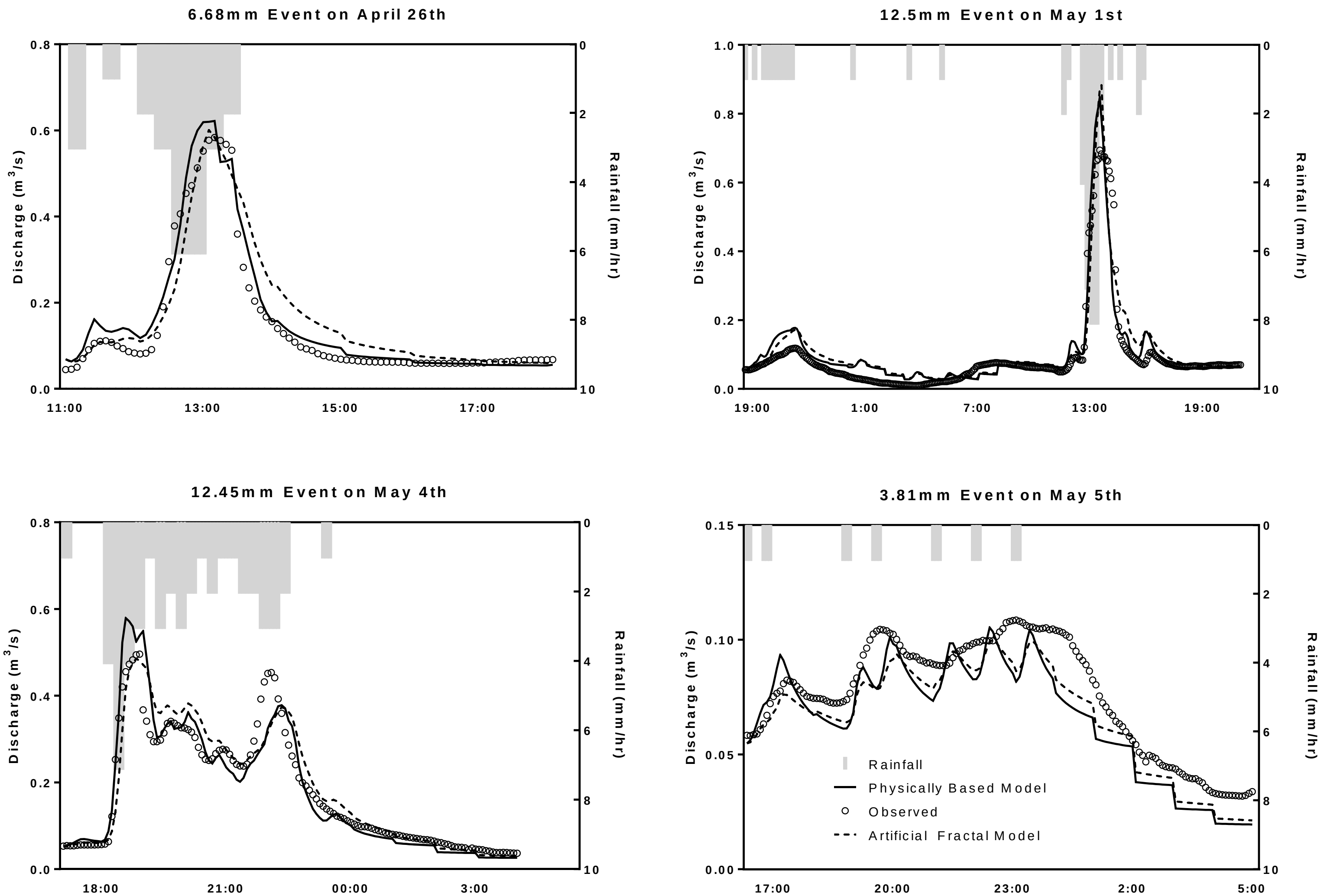

Figure 3.9: *Selected storms for the physically based and artificial fractal simulated networks in East Boston Section 77*

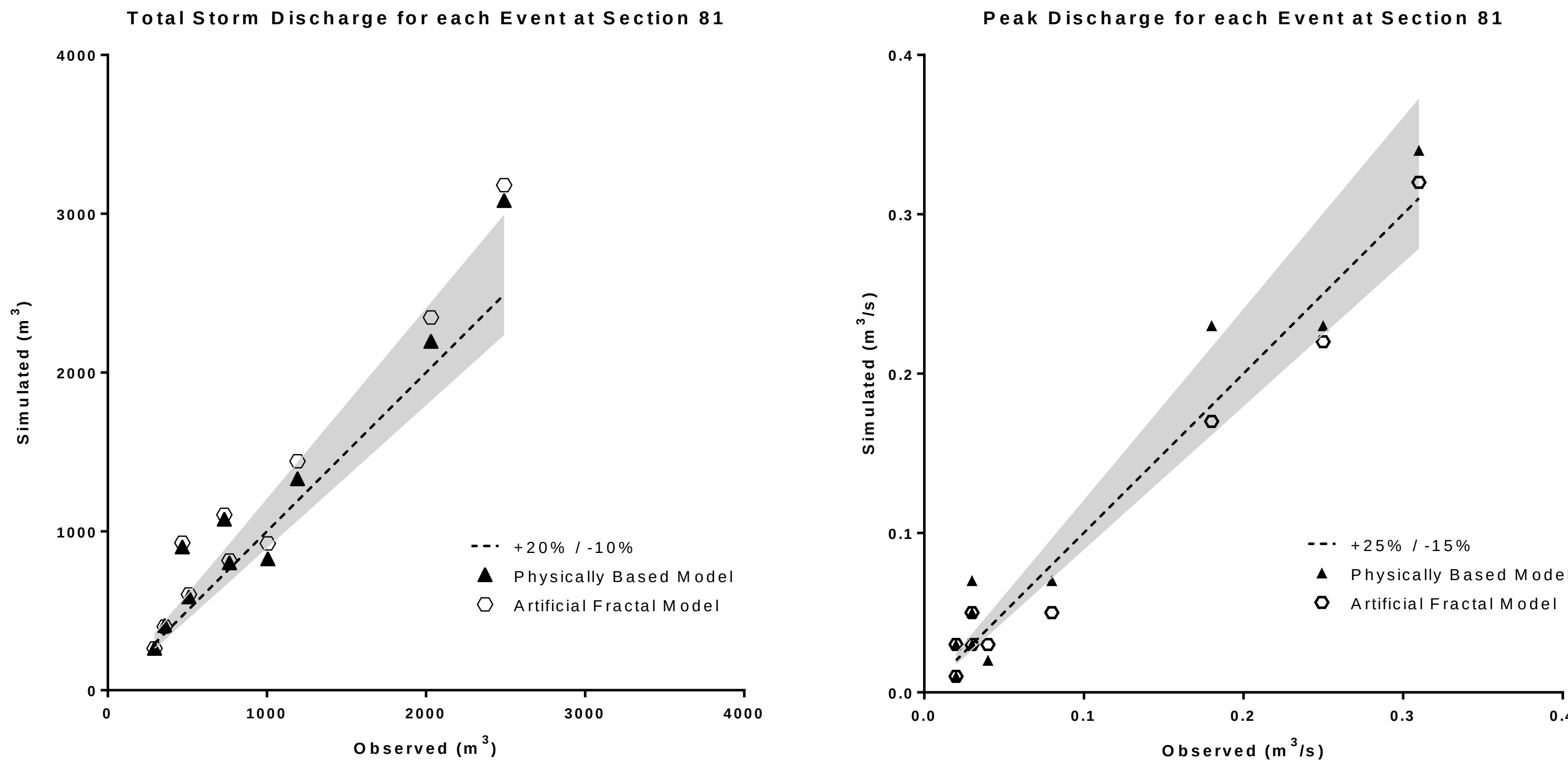

Figure 3.10: *Event Summary for the simulations in East Boston Section 81*

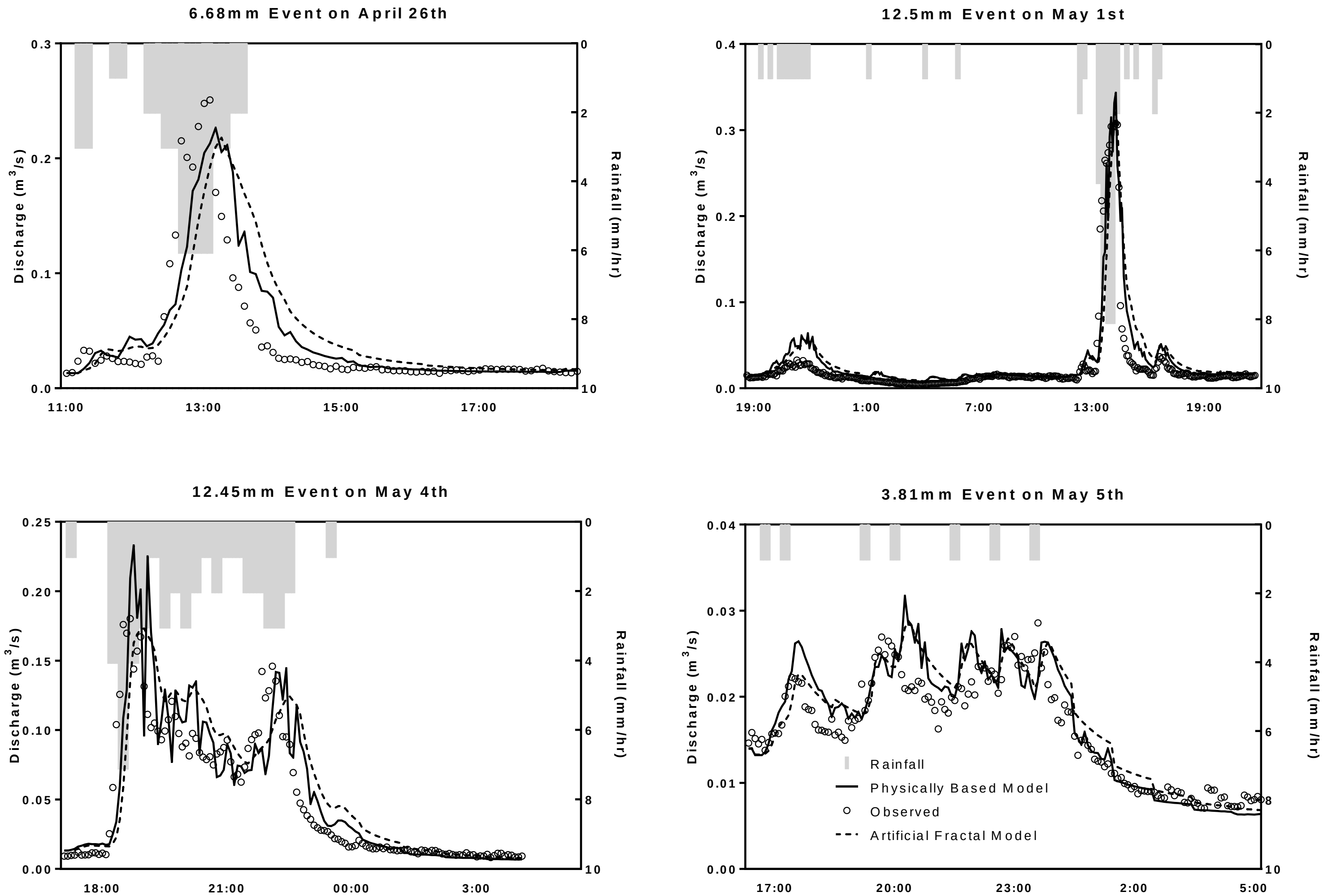

Figure 3.11: *Selected storms for the physically based and artificial fractal simulated network in East Boston Section 81*

Discussion

Assessing Model Quality

When assessing the quality of the physically based and artificial models in Section 77, in both cases smaller events were less accurate than larger events with the physically based model NSE between 0.88-0.96 and the artificial fractal model NSE between 0.88-0.89 for storms > 5 mm with some smaller events < 5 mm having no correlation. NSE values > 0.75 are considered very good with values > 0.5 satisfactory (Moriasi et al., 2007). The largest storm in the simulation period was 12.7 mm on May 1st. Both models over-predicted total flow and, most noticeably, peak flow. This could be a limitation of the models underrepresenting the storage capacity of the catchment, or perhaps, because the peak occurs relatively quickly, the sewer flow monitoring device at a 5-minute sampling interval did not sample the highest peak flow. Despite the differences in the observed flow, when comparing the total discharge volume and peak discharge rate to the observed results throughout the study period, both models fit the Wastewater Planning Users Group (2002) criteria for good model performance defined in the methods section.

The model comparison in Section 81 had similar results to the calibrated model in Section 77 (physically based model NSE between 0.84-0.90 and fractal based model NSE between 0.62-0.89 for storms > 5mm with some smaller events < 5mm having no correlation). Both the models tended to over-predict total discharge volumes with the artificial model predicting slightly more than the actual model. The modeled peak flows were significantly lower than the observed peak flows. While the results of this uncalibrated simulation were expectedly less accurate than the calibrated model, both models produced comparable simulations of the observed period. When viewing the time series as a whole, both models had strong correlations to observed flows with a NSE of 0.85 and 0.86 for the physically based and artificial fractal models respectively in Section 77, and a NSE of 0.85 for the physically based model and 0.75 for the artificial model in Section 81.

One source of the differences in the two model could be the result of the artificial network having less drainage density than the physically based resulting in a more delayed hydrologic response. Another source of error could be the approximation of DWF. Three small events (<

2.5 mm) where DWF is a larger component of total discharge compared to large storms produced unsatisfactory results. This could be because DWF was derived as a function of observed flow patterns, there is some error associated with applying an average DWF pattern through the simulation period that will be most pronounced in the smallest events. This is illustrated in the May 5th event which shows the effect on the sinusoidal DWF pattern applied to the simulated models. In comparison, the observed flow is steadier than the model predicts.

Analysis of Network Resolution and the effect of Strahler Ordering

As previous discussed, a main motivation to employ artificial networks is to simplify the modelling process. As noted by Cantone and Schmidt (2009), aggressive aggregation of subcatchments in low resolution models can produce inaccurate simulations relative to observed flows (as the result of shorter pipe lengths and longer periods of overland flow where infiltration can occur) and can be avoided by preserving resolution. In addition, they stress the need to incorporate resolution in municipal stormwater models that often employ these low resolutions models. Artificial networks in this regard can provide this level of resolution more readily than their physically based counterparts.

To explore this concept, ANGel was used to generate artificial models for Section 77 based on Strahler orders of 1, 2, and 3 in addition to the 4th. These models featured 1, 10, 24, and 173 subcatchments respectively. The models were each calibrated to observed flow and compared based on NSE, total volume, and peak flow. These networks are shown in Figure 3.12, their physical parameters shown in Table 3.5, and their calibrated parameters in Table 3.6.

Results are shown in Table 3.7. A selected hydrograph is showed in Figure 3.13. Considering the effect of scale, the all of the orders showed strong correlations to the observed flow with NSE values > 0.84 over the course of the April 26th 6.68 mm event. The calibrated model parameters in the 4th order model were closer to that of the physically based model (which is a 4th order network itself). The main difference between the orders were the total pipe length, length of overland flow, and slope. Because the smaller orders have less pipe, more overland flow length is required for the time of the hydrologic response to be consistent with observed flow.

In addition, because overland flow is more of a factor, increasing slope can cause more flashiness in the hydrologic response.

Cantone and Schmidt (2008) and Ghosh and Hellweger (2011) showed a much greater difference in their lowest lumped resolution models. This could be because their catchment sizes were much bigger and had more pervious area. Cantone and Schmidt (2008) has a 341 ha catchment and modeled the subcatchments as 50% imperviousness in general and 80% impervious if the subcatchments were primarily roads. Ghosh and Hellweger (2011) modeled the 466 ha area of the Faneuil Brook Sub-Basin (a tributary to the lower Charles River) and although no level of imperviousness is listed, the area is less developed than the 54 ha area of East Boston used in this study. Based on this analysis, for future implementation of artificial networks particular interest should be given to the size of the modeled catchment and the level of imperviousness. If the catchment is larger than 54 ha and/or there is an imperviousness less than 73% the other factors discussed in the previously discussed research can come into play. These potential issues can be avoided using artificial models.

Different Levels of Strahler Order Modeled

Figure 3.12: *Different resolutions of the artificial network defined by Strahler order representing 1, 10, 24, and 173 subcatchments.*

Table 3.5: *Comparison of different Strahler order model network characteristics.*

Network Summary				
Section 77	**Total Pipe Length (m)**	**# of Junctions**	**# of Subcatchments**	**Total Area (ha)**
Physically Based	10502	183	128	54
Artificial 4th Order	6889	173	173	54
3rd Order	2647	24	24	54
2nd Order	2231	10	10	54
1st Order	381	1	1	54

Table 3.6: *Calibrated sensitive parameters in each Strahler order model for Section 77.*

	Calibrated Parameters				
Strahler Order	**Slope (%)**	**% Impervious**	**n Impervious**	**Catchment Length**	**Pipe n**
One	9.5	73	0.01	1237 m	0.003
Two	8.6	71.4	0.02	266 m	0.004
Three	4.6	73.5	0.016	317 m	0.006
Four	3.7	71.2	0.01	251 m	0.005
Physically Based	3	73.3	0.01	244 m	0.003

Table 3.7: *Comparison of different Strahler order models.*

	One	**Two**	**Three**	**Four**	**Observed**
Overall NSE	0.86	0.85	0.84	0.86	-
April 26th NSE	0.94	0.91	0.95	0.94	-
April 26th Total (m^3)	4326	4366	3792	4202	4010
April 26th Peak (m^3/s)	0.60	0.61	0.52	0.57	0.58

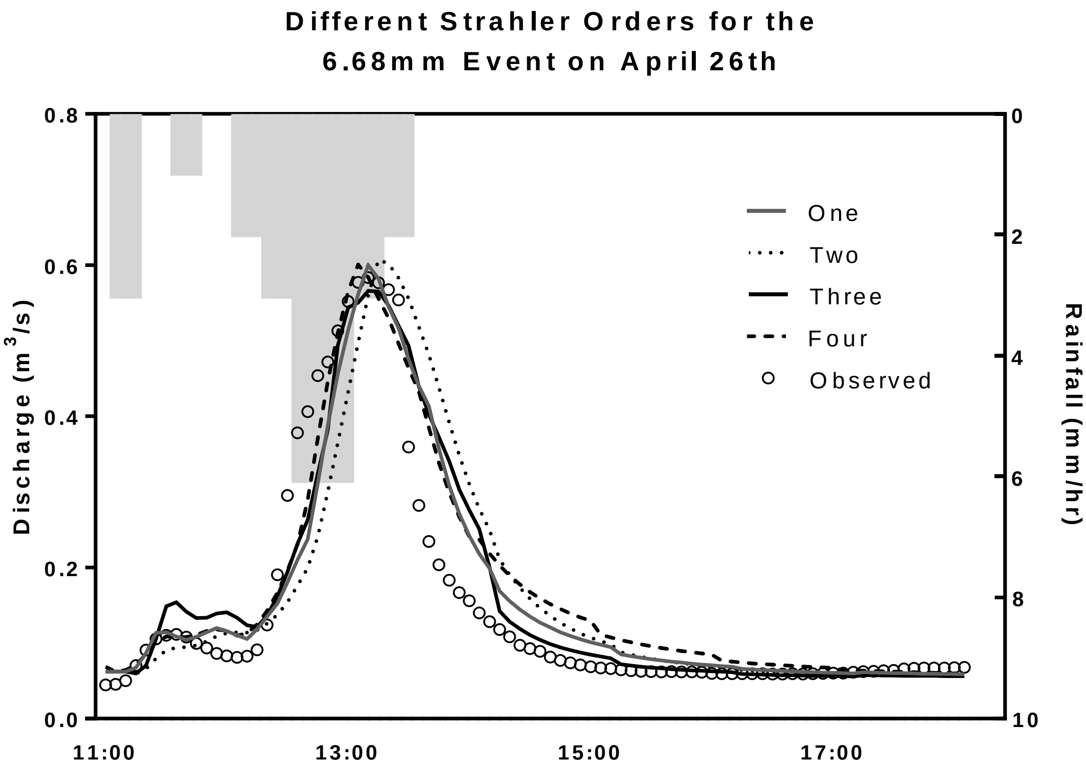

Figure 3.13: *Hydrologic response of different modeled Strahler orders*

Conclusions

This study demonstrates an application of an artificial fractal based in a highly urban residential catchment. While it is unclear how applicable artificial fractal models are in less urbanized areas or places with less homogenous topography, their implementation can add resolution to existing models and avoid issues related to model aggregation. Because many sewer modelers rely on aggregated low resolutions models (with catchment often much larger than the 54 ha area in this study), this method provides a relatively simple method to potentially improve model accuracy.

Developing this methodology for urban catchments enables many practical applications of sewer management and urban planning. One example relates to the large scale implementation of green stormwater infrastructure (GSI) to mitigate issues relating to flooding and combined sewer overflows. Alterations to an urban catchment using SWMM LID controls can be modeled relatively quickly using artificial sewer models and quantitative assessments made. In addition, creating high resolution models enable a spatial analysis on the effect of GSI placement throughout the network not possible in lower resolution aggregated models. Future work with this method will focus on GSI implementation as a demonstration of the practical applications in the engineering and research fields.

One of the main critiques of the fractal models used in this study is that they do not incorporate topological characteristics of the catchment to define conduit and catchment slopes and widths. In this regard, Digital Elevation Models (DEMs) have shown promising applications in urban hydrologic modeling as they are able to take topographic information and create drainage networks based on elevation gradient (J. Schellekens et al., 2014). However, because urban drainage networks often do not follow the elevation gradient as is expected in natural river basins, generating a model based on a DEM can produce misleading results and requires information regarding the structure of the network. In one study built on applied fractal river basin analysis developed by Rodriguez et al. (2005), a DEM was implemented alongside sewer pipe location data to generate a model with accurate results for a large urban catchment in France (Rossel et al., 2014). Likewise, Blumensaat et al. (2012) developed a method to use a DEM to generate artificial sewer pipe layouts that were relatively similar to actual layouts with assumed pipe diameters based on catchment characteristics with SWMM simulation results comparable to observed flow (NSE 0.51-0.73). It is possible that implementing a DEM alongside a fractal artificial sewer network generating tool such as ANGel would produce more realistic catchment parameters and conduit slopes and thus generate more accurate results particularly related to peak flow.

List of References

Benoit Mandelbrot. (1967). "How Long is the Coast of Britain? Statistical Self-Similarity and Fractional Dimension." *Science,* 156(3775), 636-638.

Blumensaat, F., Wolfram, M., Krebs, P. (2012). "Sewer Model Development Under Minimum Data Requirements." *Environ Earth Sci,* 65(5), 1427-1437.

Cantone, J., and Schmidt, A. (2011). "Improved Understanding and Prediction of the Hydrologic Response of Highly Urbanized Catchments through Development of the Illinois Urban Hydrologic Model." *Water Resour. Res.,* 47(8), W08538.

Cantone, J. P., and Schmidt, A. R. (2009). "Potential Dangers of Simplifying Combined Sewer Hydrologic/Hydraulic Models." *Journal of Hydrologic Engineering,* 14(6), 596-605.

Computational Hydraulics International. (2017). "PCSWMM." (7.0.2330), .

Ghosh, I., and Hellweger, F. L. (2012). "Effects of Spatial Resolution in Urban Hydrologic Simulations." *Journal of Hydrologic Engineering,* 17, 129-137.

Ghosh, I., Hellweger, F. L., Fritch, T. G. (2006). "Fractal generation of artificial sewer networks for hydrologic simulations." *Proc., Proceedings of the ESRI International User Conference, San Diego, California, August,* , 7-11.

Goldstein, A. (2011). "Comparison of a High and Low Spatial Resolution Model for an Urban Block and Implications for Depicting Low Impact Development." .

Hack, J. T., and Geological Survey, (U S). (1957). *Studies of Longitudinal Stream Profiles in Virginia and Maryland,* .

Jeffers, S., and Montalto, F. (2017). "Applying River Basin Scaling Laws to Urban Catchments." Unpublished material.

Möderl, M., Butler, D., Rauch, W. (2009). "A Stochastic Approach for Automatic Generation of Urban Drainage Systems." *Water Sci. Technol.,* 59(6), 1137-1143.

Moriasi, D. N., Arnold, J. G., Van Liew, M. W., Bingner, R. L., Harmel, R. D., Veith, T. L. (2007). "Model Evaluation Guidelines for Systematic Quantification of Accuracy in Watershed Simulations." *American Society of Agricultural and Biological Engineers,* 50(3), 885-900.

National Resource Conservation Service. (2017). "Web Soil Survey." .

Rodriguez, F., Cudennec, C., Andrieu, H. (2005). "Application of Morphological Approaches to Determine Unit Hydrographs of Urban Catchments." *Hydrol. Process.,* 19(5), 1021-1035.

Rodríguez-Iturbe, I., and Rinaldo, A. (2001). *Fractal River Basins,* 1. paperback ed. Ed., Cambridge Univ. Press, Cambridge [u.a.].

Ryan, B. (2007). "Fractaldimensionexample.PNG." Wikimedia Commons.

Schellekens, J., Brolsma, R. J., Dahm, R. J., Donchyts, G. V., Winsemius, H. C. (2014). "Rapid Setup of Hydrological and Hydraulic Models using OpenStreetMap and the SRTM Derived Digital Elevation Model." *Environmental Modelling & Software,* 61, 98-105.

Turcotte, D. L., and Newman, W. I. (1996). "Symmetries in Geology and Geophysics." *Pnas,* 93(25), 14295-14300.

U.S. Census Bureau. (2010). "2010 Census." .

US EPA (2017). "Storm water management model (SWMM)." <https://www.epa.gov/water-research/storm-water-management-model-swmm> (Mar 22, 2017).

Vassallo, C. (2005). "Notion of fractal dimension." <http://charles.vassallo.pagesperso-orange.fr/en/art/dimension.html> .

Veneziano, D., and Langousis, A. (2010). "Scaling and Fractals in Hydrology." *Databased Approaches for Hydrologic Modeling and Forecasting,* .

WASTEWATER PLANNING USERS GROUP. (2006). *GUIDE TO THE QUALITY MODELLING OF SEWER SYSTEMS;* .

Wayne C Huber. (2006). "*BMP Modeling Concepts and Simulation", US EPA*.

Chapter 4: Using artificial sewer networks to study the role of green stormwater infrastructure in reducing runoff during both historic and future changed precipitation

An analysis of urban sewer systems and the implementation of green stormwater infrastructure.

Abstract

This paper simulates the effect of green stormwater infrastructure (GSI) using an artificial sewer model based on the fractal geometry of urban drainage systems. In this research, GSI is simulated in a 54 ha urban residential catchment in East Boston, Massachusetts using artificial sewer networks modeled in the Storm Water Management Model (SWMM) and compared to a physically based model created from the actual layout of the system including pipe locations, inverts, diameters, and catchment properties calibrated to observed sewer flow data. These models are then used to show the effect of various GSI implementation scenarios including green roof and right-of-way infiltration based systems and evaluated on reductions in total storm discharge volume, peak flow, and cost. The scenarios investigated the effect of varying levels of implementation and the spatial placement of GSI. Over the course of an annual 15-minute interval rainfall pattern, the artificial network in this analysis predicted the volumetric event discharges equivalent (R^2>0.99) to predictions from traditional physically based model. More difference (R^2>0.97) was seen comparing the peak event flow rates with the artificial model for larger storms although are still comparable. The four simulated GSI scenarios showed annual discharge of the study area could be reduced 30-54%. The most effective scenario was to maximize the impervious area treated by GSI with a combination of green roofs and infiltration based systems. Spatial analysis showed the volumetric reductions are maximized by evenly distributing the systems throughout the network; however, more unique clustering of systems could reduce peak flows more significantly in some larger events. When considering the effect of

climate change, the annual rainfall pattern was adjusted to 2045-2074 projections resulting in a 7% increase in annual precipitation. This increase in precipitation resulted in a 7-11% increase in annual runoff depending on the GSI scenario, and suggests that GSI implementation is an adequate strategy to address changes in the typical annual rainfall pattern. For larger 10-year return extreme events, however, the results showed that even that most intensive level of GSI implementation would only reduce event discharge by 12-19% and peak flow rates by 23-27%.

Introduction

Background

Urban areas throughout the United States are implementing green stormwater infrastructure (GSI) projects as part of larger stormwater management plans (SMPs) to reduce runoff potential and adapt to increasing precipitation due to climate change (Water Environment Federation, 2014). Citywide GSI implementation in the United States is typically done by municipal organizations under consent agreements with the U.S. Environmental Protection Agency (EPA) based under the Combined Sewer Overflow (CSO) Control Policy as part of the National Pollutant Discharge Elimination System permit (NPDES)) or Municipal Separate Storm Sewer System (MS4) permits. For example, Washington, D.C. is required to retrofit 167 ha of impervious area to manage stormwater (Natural Resource Defense Council, 2011). Philadelphia, as another example, has committed $1.67 billion for GSI implementation as part of a larger plan to reduce combined sewer flow by 85% (Philadelphia Water Department, 2011).

The effect that GSI will have on urban hydrology is assessed both through monitoring and hydrologic and hydraulic (H&H) modeling. For example, the city of Milwaukee developed a Hydrologic Simulation Program - Fortran (HSPF) model to represent 2 ha of residential and city blocks to evaluate baseline sewer conditions followed by post-green conditions. This simulation showed that combining GSI implementation with rooftop downspout disconnections from the sewer would reduce peak sewer flows by 5-36% and reduce CSOs by 12-38% (Water Environment Federation, 2014). In 2012, Kansas City, MO completed a 40 ha pilot GSI program in a combined sewer area along the Middle Blue River Basin including development of green streets, bioswales, bioretention and porous pavements to capture runoff. In a joint effort between the U.S. EPA and the University of Missouri-Kansas City, sewer flow monitoring was performed in the affected catchment. Using this sewer flow data, a calibrated XPSWMM model was developed to simulate design storms. Relative to pre-existing conditions, the pilot project reduced the total volume of a 36 mm design storm by 36% and peak flow by 76% (Kansas City Water Services, 2013).

One of the most widely used H&H modeling tool for urban catchments is the U.S. EPA's Storm Water Management Model (SWMM). In 2009, the U.S. EPA updated SWMM to include low impact development (LID) controls that can be used to simulate GSI devices such as bioretention cells, infiltration trenches, porous pavements, rain barrels, and vegetated swales. Selbig and Balster (2010) demonstrated that the LID controls can reasonably reproduce observations in both continuous and single event simulations. Rosa et al. (2015) showed that calibrated models with LID controls in place reasonably the rate of and volume of runoff compared to observed measurements (R^2 > 0.8 and 0.9 respectively). Palla and Gnecco (2015) used SWMM to analyze a 5.5 ha small urban catchment various levels of GSI in place. The calibrated SWMM model was used to simulate implementation of green roofs and permeable pavement based, the properties of which were calibrate to laboratory measurements. By greening all of the rooftops in the catchment and converting 16% of the parking lots and roads into permeable pavement, the 2-year rain event total discharge volume was reduced by 23% and the peak runoff rate reduced by 45%. In a SWMM analysis of a much larger 784 ha combined sewer drainage area in the Bronx, NY, a 5% greening scenario featuring various GSI systems yielded a 14% reduction in annual CSOs (30 annual occurrences down from 35) (De Sousa et al., 2012). Similarly, Smullen et al. (2008) developed a SWMM model of the entire Philadelphia watershed to simulate various degrees of GSI implementations, finding that GSI could reduce total runoff by 50% annually and CSO flow by nearly two-thirds.

The effect of climate change (in particular increasing rainfall patterns) could increase the amount of investment require to mitigated CSOs (US EPA, 2014a). By simulating projected rainfall patterns in SWMM, Denault et a. (2006) predicted that the 10-year design storm peak flow rates would double by 2050 based on a 1975 baseline in a 440 ha 45% impervious urbanized basin in North Vancouver, British Columbia. GSI can provide a means of climate change adaptation and can be incrementally developed to provide benefits as necessary (US EPA, 2014a). In one site scale example, De Sousa (2015) observed that a bioretention basin in Queens, NY was able to consistently perform during extreme precipitation events from 2011 to 2014 and only the largest hurricane level event (163 mm) caused overflow in the system and only for a brief period. One of the primary reasons that the bioretention basin in De Sousa (2015) performed so well in extreme events was that the hydraulic loading rate (HLR) (a term used to describe the ratio of drainage area to bioretention area) was so low (3.8:1). In contrast, sites with higher HLRs are more susceptible to decreases in performance related to increasing rainfall patterns. This was observed by Hathaway et al. (2014) in two bioretention basins in North Carolina where annual overflows of the GSI sites would nearly double by 2055 (each had hydraulic loading rates (HLR) of 24:1 and 19:1).

To help H&H modelers address climate change, the EPA in 2014 released the SWMM Climate Adjuster Tool (SWMM-CAT) which can adjust the rainfall input parameters in SWMM to projected futures levels derived from the Couple Model Intercomparison Project Phase 3 (CMIP3) (US EPA, 2014b). One study that employed SWMM-CAT observed a constructed wetland in Flushings, NY, Frazier (2016) and demonstrates that annual stormwater retention would reduce 8% from baseline 2008 conditions when projected to 2045-2074. Similar methods are also used to analyze the effect on the watershed scale. Alexanderson and Bradbury (2013) developed a H&H model for the Los Angeles River Basin and simulated varying GSI levels throughout the watershed depending on land use (5-80% of total land area serviced). The authors projected based on CMIP3 ‘business as usual’ projections for 2095 that peak flow rates would increase 22-72% and the GSI implementation could only reduce that peak by 3%. In a related study, Radavich (2015) focused on one 33150 ha 61% impervious section of the Los Angeles River Basin (Ballona Creek) and simulated a 6% increase in precipitation using SWMM-CAT projected to 2045-2074 resulting in a 3% increase in annual flow. Based on a few large scale GSI implementation scenarios throughout the catchment (ranging from 77-85% of all impervious land serviced by GSI), Radavish (2015) demonstrated that annual reductions would vary between 42-78% depending on the type and level of GSI implementation.

The case for a new model

The work cited above reveals the role that modeling can play in evaluating the hydrologic and hydraulic effects of an urban GSI programs. In each case, the models were developed based on physical characteristics (inverts, sizes, location, slopes, etc.) of the actual drainage system. However, such characteristics are not always readily available. Even when they area, the time required to construct physically based models is significant and actual observed sewer flow data is not always available to calibrate the model. Moreover, a high resolution physically based model is not always required for planning or research purposes where only a general strategy of GSI implementation is needed.

GSI decisions can be made more efficient by simplified modelling strategies, and researchers have sought methods to do this for some time. Huber (2006) showed that for a 7 ha catchment a high resolution model that accounted for every parcel performed as well as a lower resolution model broken into urban blocks (118 versus 14 subcatchments). This result was repeated by Goldstein (2011) who showed that that a low resolution SWMM model performed just as well if not better (depending on the storm) than a high resolution model when comparing predicted to measured sewer flow in a small urban catchment (one urban block) (reporting 11.4% and 8.4% volumetric error for the low and high resolution model respectively over 5 months). This is, however, not always the case when the catchment size is large or subcatchment resolution becomes too low. Cantone and Schmidt (2009) modeled a 5.2 ha catchment using subcatchment resolution ranging from 44 to 1 and found that the lowest resolution to produce accurate sewer flow compared to observed measurements was 8 subcatchments and that modeling the entire catchment as one subcatchment resulted in a greater time of concentration and lower peak flows. This finding was repeated in a 341 ha catchment in a series of models with 773 to 1 hydrologic response units (HRUs). The result showed that the most accurate model had 65 subcatchments, with greater errors occurring at the lower levels of resolution. The authors note that this result is problematic because it is common for municipalities (in their case the City of Chicago) to rely on low resolution models. Krebs et al. (2013) suggested that higher resolution models were easier to calibrate since the model was less sensitive any one variable.

Artificial networks can be used to reduce the time required to create an urban H&H model without detailed physical parameters. One method to design an artificial network is with fractal scaling laws. Classical work in natural river basins has been extended recently to urban contexts

(Cantone and Schmidt, 2011 and Jeffers and Montalto, in preparation). The Artificial Network Generator (ANGeL) developed by Ghosh et al. (2006) can be used to generate artificial sewer networks based on Tokunaga fractal geometries. Ghosh and Hellweger (2012) used ANGeL to model a 4.66 km^2 catchment in the lower Charles River, using as 4, 18, and 401 subcatchments respectively to study the effect that resolution has in SWMM. They found that in low resolution models, large storms tended towards less peak flows and small storms tended towards more peak flow. In another example, Möderl et al. (2009) created the Case Study Generator to stochastically generate SWMM models based on Galton-Watson geometries (another type of dendritic geometry). Möderl et al. (2009) used this model to simulate 10,000 different artificial models to represent two actual networks in Austria and demonstrated the model could predict observed surface flooding.

It is noteworthy that in both these cases, the SWMM models were not validated with observed sewer flow measurements. In the companion piece to this research "*Modeling urban sewer with artificial fractal geometries,"* (Jeffers and Montalto, in preparation), artificially generated sewer networks using ANGeL were shown to simulate flows as accurately as their physically based counter-parts. Flow from a 54 ha urban residential catchment in East Boston, Massachusetts was modeled using artificial fractal based networks and calibrated to observed flow with a Nash-Sutcliffe efficiency coefficient (NSE) of 0.85. The same method was applied to an uncalibrated neighboring 22 ha catchment with a NSE of 0.75 to observed flow. NSE values > 0.75 are considered very good with values > 0.5 satisfactory (Moriasi et al., 2007).

Artificial models offer significant potential in answering other unique research questions related to GSI development such as the selection of GSI types, their distribution across the watershed, and evaluating their performance during historic and projected future changed prepictation. In one example, Zellner et al. (2016) developed a Netlogo based model to simulate GSI spatial distribution across a catchment and showed that GSI evenly distributed would manage stormwater more effectively than clustering the same amount of GSI to one central location. Although this model does not predict realistic quantities of runoff, it illustrates how an artificial model can be used to address research based questions in a controlled model space with more symmetric geometries compared to the actual networks they represent.

Research Objectives

This research seeks to build upon previous work developing artificial networks to simulate urban drainage networks by introducing LID controls and demonstrating applications related to urban stormwater management and climate change adaptation. Despite the success of many early adopters of GSI, one of the key reasons why adoption of GSI management practices has been slow is due to skepticism by engineers and planners that GSI will work in their particular climate or soil condition or that the wide-spread implementation will give the promised benefits (Roy et al., 2008). GSI policy decisions are typically made at the municipal scale and there is a need to develop modelling approaches that can be rapidly employed to support decision making. Methods exist to simplify the process with artificial networks, but no model found in this review had both the sophistication level of a high resolution SWMM model and LID control.

As such, this work is twofold: 1) demonstrate the creation of an artificial model with LID controls and 2) show how the model can be applied for planning and research purposes. Using the highly urban residential East Boston neighborhood in Massachusetts, a detailed physically based model is developed. This model is then compared to an artificial model developed based on fractal relations to compare runoff reductions achieved by this approach for a range of GSI scenarios. The specific GSI scenarios that are modeled were developed to manage the impervious area in East Boston using various levels of right-of-way (ROW) and green roof GSI. In addition, different layout configurations of GSI are tested to understand optimal placement on a limited budget. Both continuous and event based simulation is performed based on a typical annual rainfall year obtained from the local municipal water utility, the Boston Water and Sewer Commission, used in planning purposes. The effect of increases in precipitate related to climate change is also investigated using SWMM-CAT projections. Extreme events are considered based on baseline 10-year design storms along with projected increases to 2100.

GSI Development in East Boston

The research was enabled in large part due to collaborative efforts with the Boston Water Sewer Commission (BWSC). Like many municipal utilities, BWSC is regulated by the EPA NPDES regulations. In 2012, the BWSC entered into a Consent Decree which, among other things, requires developing and implementing GSI. This resulted in the Phase I BMP Implementation Plan to build pilot projects demonstrating GSI (CH2MHILL, 2013). Most notability in East Boston is the Central Square demonstration project located in the commercial district of East Boston schedule to be complete in 2017 which adds 11 GSI facilities including tree trenches and infiltration trenches along with environmental monitoring to quantify the effect.

Another component to this larger plan is adaptation to extreme events and climate changes spurred in part as a reaction to Hurricane Sandy which occurred October, 2012. BWSC has developed climate adjusted design storms recognizing climate change as a critical element to their long-term planning goals (BWSC, 2013)

Methodology

East Boston is a highly urbanized residential neighborhood (201 people per ha) (US Census Bureau, 2010) in Massachusetts on a peninsula surrounded by the Boston Harbor (Figure 4.1). It is serviced by both combined and separate sewers. The soil is classified as silty loam with a deep infiltration rate of 0.71 cm/hr and topographic slopes ranging from 3-15% (NCRS, 2017). The particular study area was chosen because its drainage network converges to one point where BWSC has monitored flow. In previous research, a calibrated SWMM model was developed for one large section (54 ha) in the combined sewer area based on physical sewer parameters obtained from the BWSC (Jeffers and Montalto, in preparation). A second calibrated model, created using the Artificial Network Generator (ANGel) developed by Ghosh and Hellweger (2012) based on artificial fractal geometries, was able to produce simulated results similar to as the physically based model (both models NSE>0.8 over the course of 1-month 5-minute interval observed sewer flow) (both models shown in Figure 4.2 and network properties in Table 4.1). A complete review of this model development can be found in this companion piece to the research. In this expansion of the model, LID controls are implemented under various levels and layouts to understand 1) the ability of artificial models to predict LID implementation, 2) the expected hydrologic benefits of a neighborhood scale GSI implementation project, 3) the role of GSI in climate change adaptation, and 4) spatial distribution dynamics related to GSI development. SWMM simulations were run under dynamic wave routing, Horton infiltration, 5-minute time steps routed at 5 seconds, dampen inertial terms, both normal flow criteria, and the Hazen-Williams force main equation.

GSI Scenarios

The land use of the neighborhood (Figure 4.1) was the primary factor for developing the GSI scenarios used in this study. Because 34% of the area is public ROW, a GSI strategy was selected to manage this part of the impervious area. The strategy selected was the 20’ x 5’ New York City Department of Environmental Protection (NYC DEP) Standard ROW Bioswale (ROWB) (NYC DEP, 2016). Though it was developed in NYC, the ROWB was used for a number of reasons: 1) it is designed to be installed on the sidewalk of the ROW eliminating the need to remove street parking spaces, 2) it is a standard publicly available design readily available for review, and 3) it has seen widespread implementation in New York City. To manage runoff from the 35% of the watershed that consists of rooftops, a green roof LID control was developed. An extensive green roof was assumed to minimize structural load considerations associated with deeper intensive green roofs.

The parameters used in these LID controls are shown in Table 4.2. Bioretention engineered soil was assumed for the ROWB based on a mixture of 20% clay, 50% sand, and 30% top soil. Parameters for the soil mixture were obtained from Carpenter and Hallam (2010) derived from field measurements. Green roof parameters were based on experimental results obtained from Palla and Gnecco (2015) who calibrated an SWMM green roof LID control using lab measurements. Other parameters were used as guided by the SWMM 5.1 User Manual (US EPA, 2017) based on the sources from Rawls, W.J. et al., (1983) and McCuen, R. et al. (1996).

Four GSI scenarios were developed. Case I assumed a maximum level of greening representing all of the rooftop area greened and a high level of ROWB implementation based on HLR. Typical municipal guidance documents recommend a HLR of 10:1 for infiltration based GSI (Philadelphia Water Department, 2016). Case II assumed only the maximum amount of rooftop greening, while Case III assumed only the high level of ROWB implementation (10:1 HLR). Case IV assumed a combination of green roofs and ROWB implementation. This combination was based on more reasonable budgets than the other two cases and resulted in 39% of the rooftops greened and a HLR of 40:1. In the fourth case, the same amount of money to install ROWBs at a HLR of 40:1 was used for green roofs resulting 39% of total roof area. In all cases, ROWBs were distributed evenly throughout each subcatchment based on a weighted average. A summary of these cases is shown in Table 4.3.

To compare the effect of GSI implementation in the physically based model and artificial model, the total volume and peak flow of each storm were plotted for each scenario. In a technical code of practice for hydraulic modeling of sewer systems, the Wastewater Planning Users Group (2002) developed criteria to assess model quality saying that the peak flow rates should be in the range of +25% and -15% while the total volume should be +20% and -10%

compared to observed flow. In this analysis, there was no observed flow, so the artificial model is compared to the physically based model under these guidelines.

The storms analyzed in the simulation were obtained from the BWSC and represent a typical year of 15-minute interval rainfall used by local water municipalities for modeling purposes (Figure 4.3). Monthly evaporation rates were based on historic rates at the nearby Logan Airport obtained through the National Stormwater Calculator (US EPA, 2017) and shown in Table 4.3**.** Four select hydrographs were illustrated to show the hydraulic response of the physical and artificial models. The effectiveness of GSI implementation was evaluated by assessing the reduction of total storm volumetric discharge and reductions in peak flow rates.

Effect of Climate Change

Because of the focus on GSI as part of the long term climate change adaption strategy by the BWSC, the effect of changing precipitation patterns was also simulated. The typical design year rainfall pattern was adjusted using SWMM-CAT for 2045-2074 median projected changes based on CMIP3 projections (US EPA, 2014). In addition to this design year, extreme precipitation events were simulated based on projections from BWSC obtained in the 2016 Climate Ready Boston report representing the 10-year 24 hour design storms forecast into 2100 (Table 4.4) (Climate Ready Boston, 2016). These projections were based on historic precipitation records and simulated using the SimCLIM software package to adjust CMIP3 precipitation projections to Boston assuming two greenhouse gas emission scenarios, B2 representing moderate cuts to emissions, and A1Fi representing the current trends or 'business as usual'. Using these rainfall depths, 24 hour SCS type III design storms were generated for simulation purposes.

Model Assumptions

Several simplifications and assumptions were made in this analysis. 1) Dry weather flow (DWF) was implemented into the model based on previous observed flow; however, DWF is only applied at the discharge point of the sewershed were sewer flow was observed and not throughout the model. 2) East Boston is situated close to Boston Harbor; however, tidal effects were not considered. This was justified because the particular section of East Boston is not immediately adjacent to water and a tide gate was installed in the receiving interceptor. In addition, no tidal effects were observed in the metered DWF. 3) Inlet design of the ROWBs was not considered and it was assumed that no bypass of the inlet occurred. 4) No clogging of the ROWB was modeled and it was assumed that the performance of the systems remained constant.

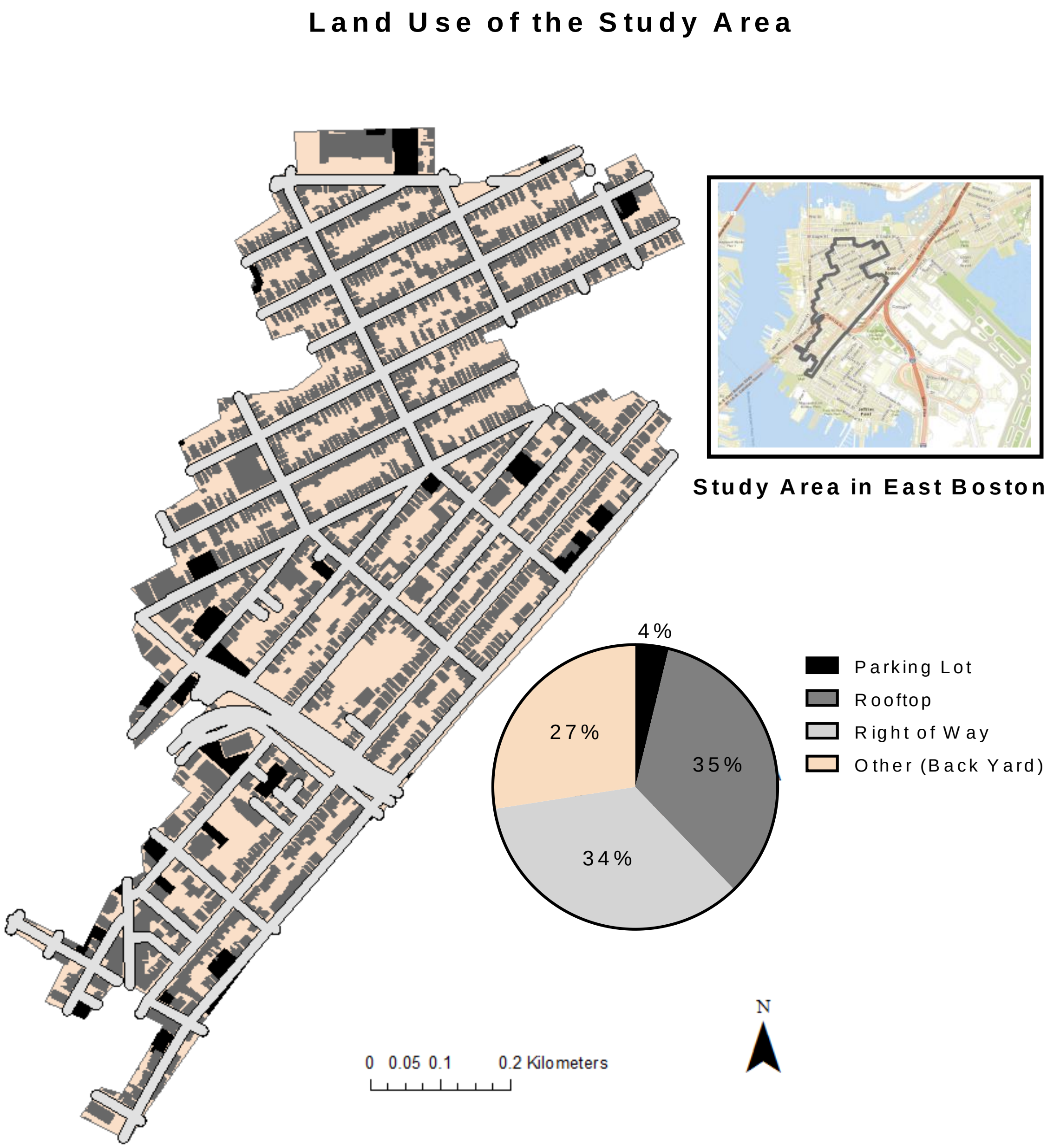

Figure 4.1: *Land use of the study catchment.*

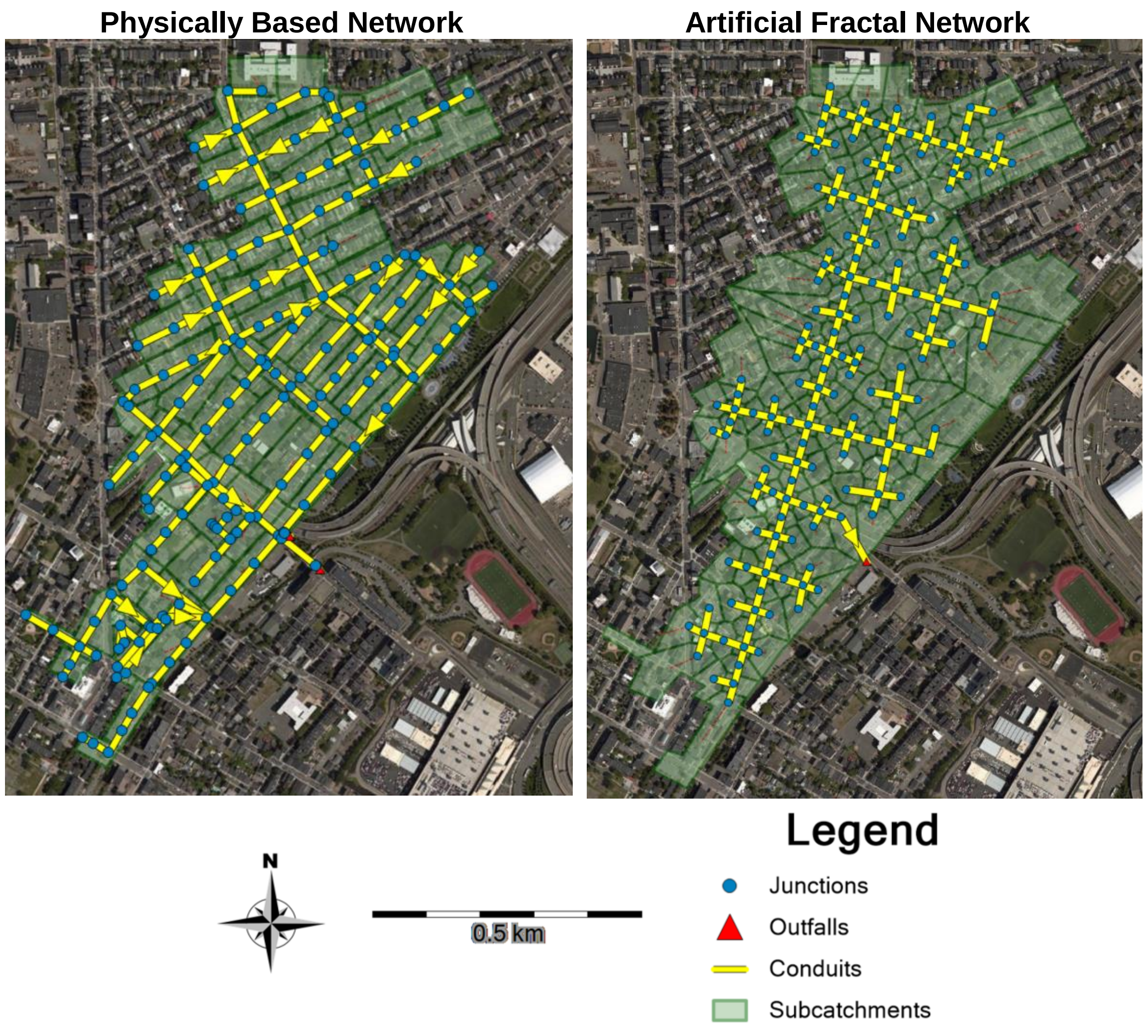

Figure 4.2: *Images from PCSWMM comparing the physically based (left) and artificial fractal (right) models*

Table 4.1: *Summary of the network geometries in the physically based and artificial fractal model.*

Network Summary

	Total Pipe Length (m)	# of Junctions	# of Subcatchments	Total Area (ha)	Longest Flow Path (m)
Physically Based	10502	183	128	54	1377
Artificial Fractal	6889	173	173	54	1234

Table 4.2: *SWMM LID Control Input Parameters*

	Right of Way Bioswale (Bio-Retention Cell)	
Parameter	**Value**	**Source**
Surface		
Berm height	15 cm	NYC DEP, 2016
Vegetation volume	0.2	McCuen, R. et al. (1996)
Surface roughness (n)	0.1	McCuen, R. et al. (1996)
Surface slope	1 %	Assumed
Soil	***Assuming 20% clay, 50% sand, 30% top soil***	
Thickness	91 cm	NYC DEP, 2016
Porosity	0.54	Carpenter and Hallam, 2010
Field capacity	0.283	Carpenter and Hallam, 2010
Wilting Point	0.047	Rawls, W.J. et al., (1983)
Conductivity	2.07 cm/hr	Carpenter and Hallam, 2010
Conductivity Slope	41	Rawls, W.J. et al., (1983)
Suction Head	2.40 in	Rawls, W.J. et al., (1983)
Storage		
Thickness	61 cm	NYC DEP, 2016
Void Ratio	0.4	AASHTO #57 Stone
Seepage Rate	0.71 cm/hr	NRCS, 2017
Clogging factor	0	Ignored
Underdrain		
Drain coefficient	0	No underdrain
Cost	$25,000/ROWB	NYC DEP, 2014
	Green Roof	
Parameter	**Value**	**Source**
Surface		
Berm height	0	-
Vegetation volume	0	-
Surface Roughness (n)	0	-
Surface slope	0	-
Soil		
Thickness	12 cm	Palla and Gnecco, 2015
Porosity	0.66	Palla and Gnecco, 2015
Field capacity	0.43	Palla and Gnecco, 2015
Wilting point	0.07	Palla and Gnecco, 2015
Conductivity	100 cm/hr	Palla and Gnecco, 2015
Conductivity slope	15	Palla and Gnecco, 2015
Suction Head		
Drainage Mat		
Thickness	2.5 cm	Palla and Gnecco, 2015
Void fraction	0.4	Palla and Gnecco, 2015
Roughness (Manning’s n)	0.02	Palla and Gnecco, 2015
Cost	$158.82/m^2	Cater and Keeler, 2008

Table 4.3: *Summary of Green Stormwater Infrastructure Implementation Scenarios*

	Scenario Summary			
	Case I	**Case II**	**Case III**	**Case IV**
Level of ROWB Implementation	10:1 HLR	0	10:1 HLR	40:1 HLR
% of Roofs Greened	100%	100%	0	39%
Construction Cost	$82,000,000	$32,000,000	$50,000,000	$25,000,000
Total Amount of Impervious Area Treated	69%	35%	34%	48%

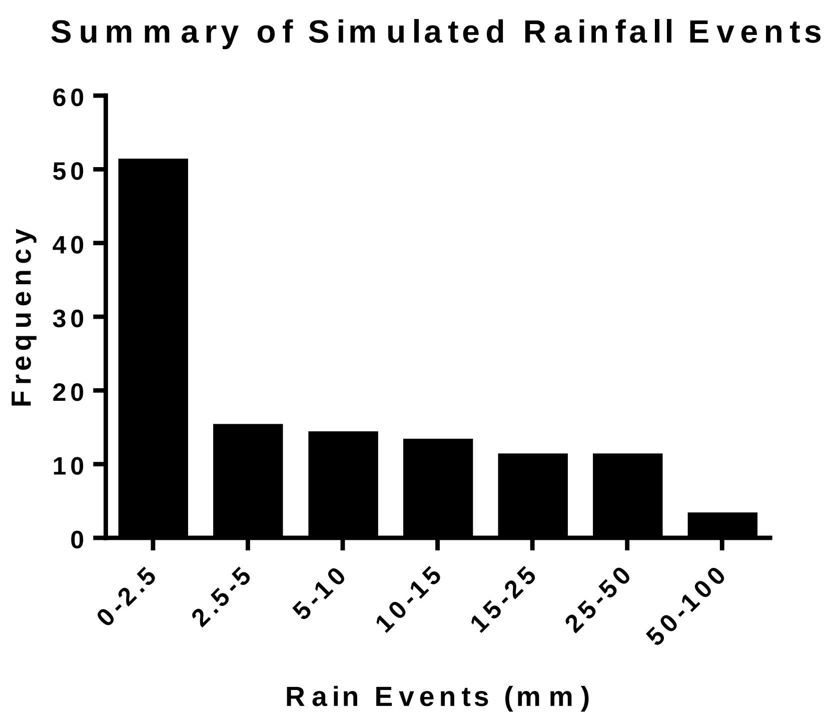

Figure 4.3: *Summary of rain storms simulated*

Table 4.4: *Evaporation Rates used in the simulation from Logan Airport*

Average Monthly Evaporation (mm/day)

Jan	Feb	Mar	Apr	May	Jun
2.03	2.79	3.81	5.33	6.10	6.35
Jul	Aug	Sep	Oct	Nov	Dec
6.86	5.84	4.83	3.56	3.05	2.54

Table 4.5: *Extreme Events projected for East Boston (Reproduced from Climate Ready Boston, 2016)*

	Baseline	2035	2060	2100
B2 (medium)	133 mm	141 mm	146 mm	154 mm
A1Fi (precautionary)	133 mm	142 mm	153 mm	169 mm

Results

The GSI scenario simulations were compared in the physically based model to the artificial model by total event volume, peak flow rates, and hydrographs over select storms. Total volume (Figure 4.4) in all of the GSI scenarios had an R^2>0.99 when comparing the artificial to the physically based model. All storms fit within the bounds of the Wastewater Planning Users Group (2002) criteria. The artificial model simulated peak flow in all scenarios (Figure 4.4) also showed a strong correlation (R^2>0.98) although more variability was observed in larger events. While most effects where within the bounds on the Wastewater Planning Users Group (2002) criteria for good fit, there was significantly more difference than the comparison in volumetric flow.

Select hydrographs (6.35mm, 12.7mm, 25.4mm, and 48.3mm events) for each scenario are shown in Figure 4.5 for each model with and without GSI. Case I demonstrates in both models that peak flow rates were significantly reduced in smaller events but in larger storms, peak flow rates were unaffected. In Case II, smaller events also had significant reductions in peak flow, however, larger event produced greater amounts of runoff under the influence of green roof LID controls. When this occurred, reductions in runoff were initially observed, however, over this effect diminished over the duration of the storm. Case III produced more modest reductions in peak flow for smaller events, however, the reductions were consistent even for larger storms. Case IV showed similar results to Case I in that the greatest reductions were seen in smaller event, however, greater peaks were observed in the largest storm similar to Case II. Differences between the artificial and physically based models without any influence of GSI were also observed but are discuss in greater detail in the companion piece to this research (Jeffers and Montalto, in preparation). Despite differences in the models without GSI implementation, in all cases the trend of the artificial and physically based hydrographs with GSI was consistent.

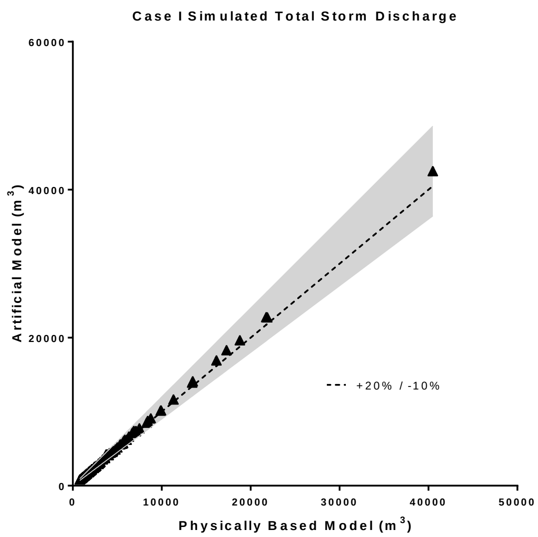
Case I Simulated Total Storm Discharge
Artificial Model (m3)
Physically Based Model (m3)
+20% / -10%
0
20000
40000
60000
10000
30000
50000

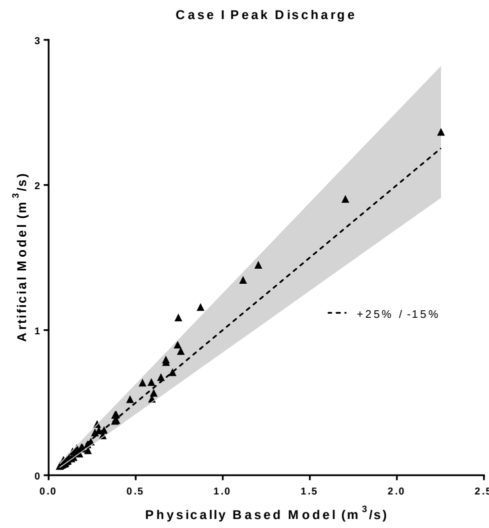
Case I Peak Discharge
Artificial Model (m3/s)
Physically Based Model (m3/s)
+25% / -15%
0.0
0.5
1.0
1.5
2.0
2.5

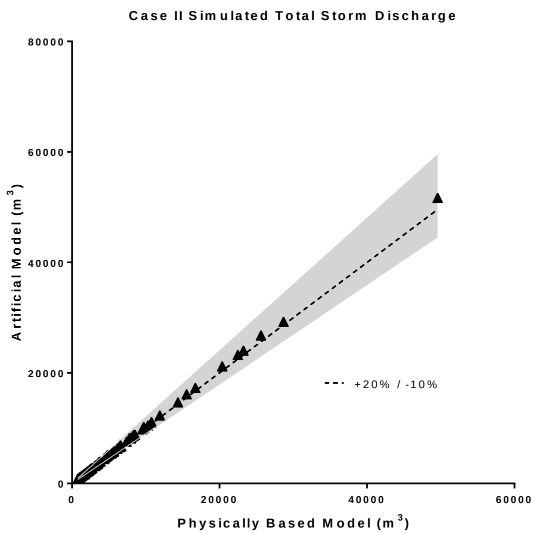
Case II Simulated Total Storm Discharge
Artificial Model (m3)
Physically Based Model (m3)
+20% / -10%
0
20000
40000
60000
80000

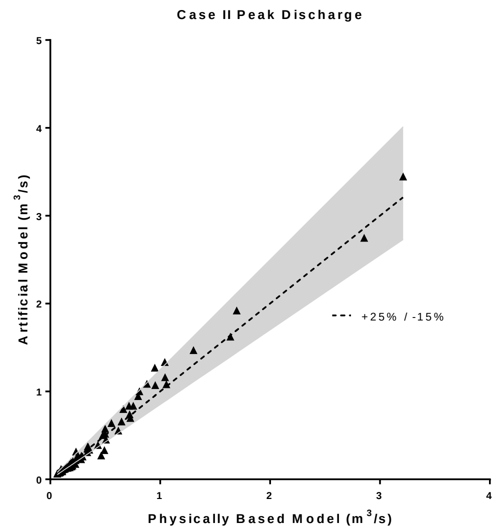
Case II Peak Discharge
Artificial Model (m3/s)
Physically Based Model (m3/s)
+25% / -15%
0
1
2
3
4
5

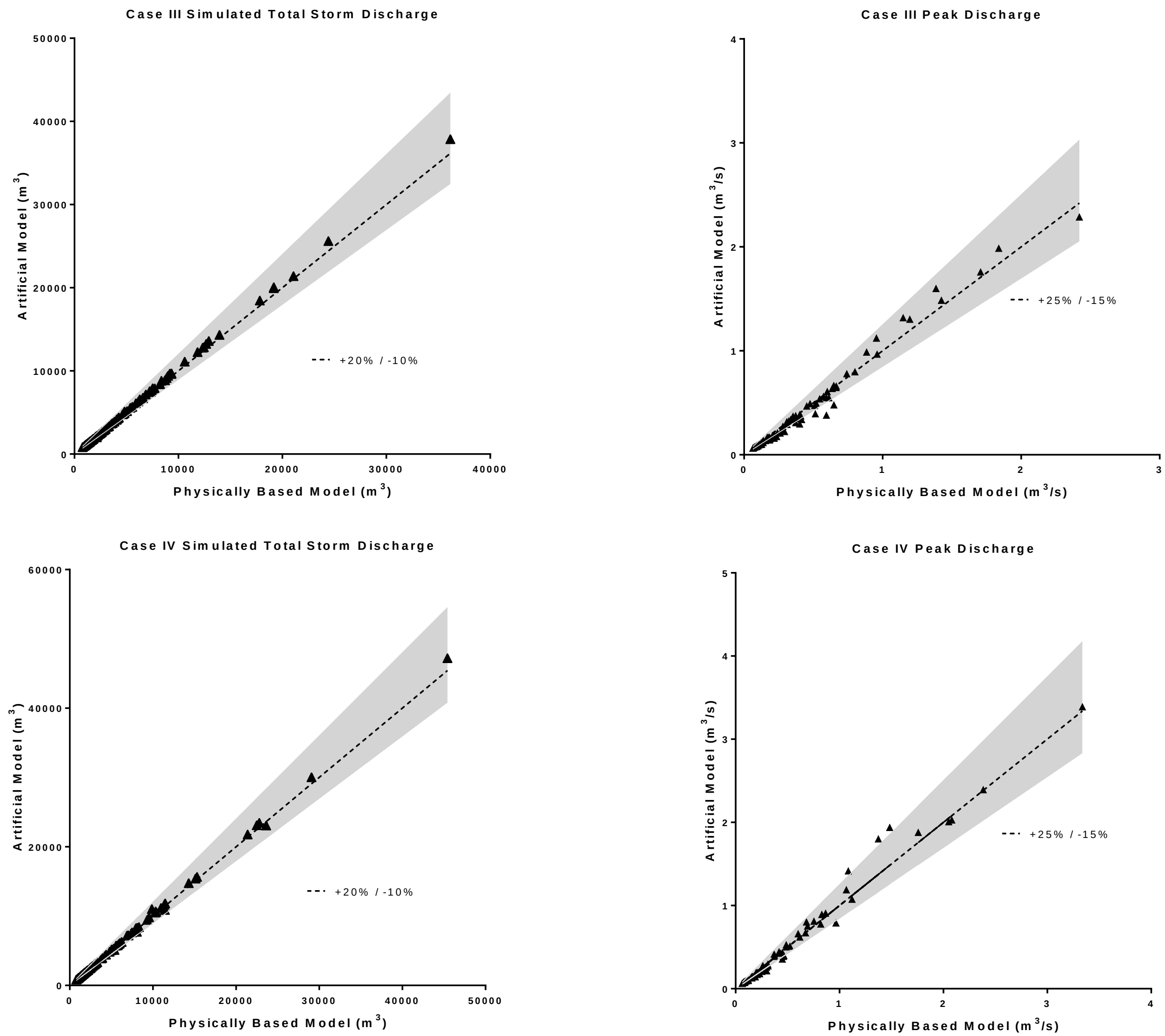

Figure 4.4: *Event based volumetric and peak flow reductions in the simulated GSI scenarios.*

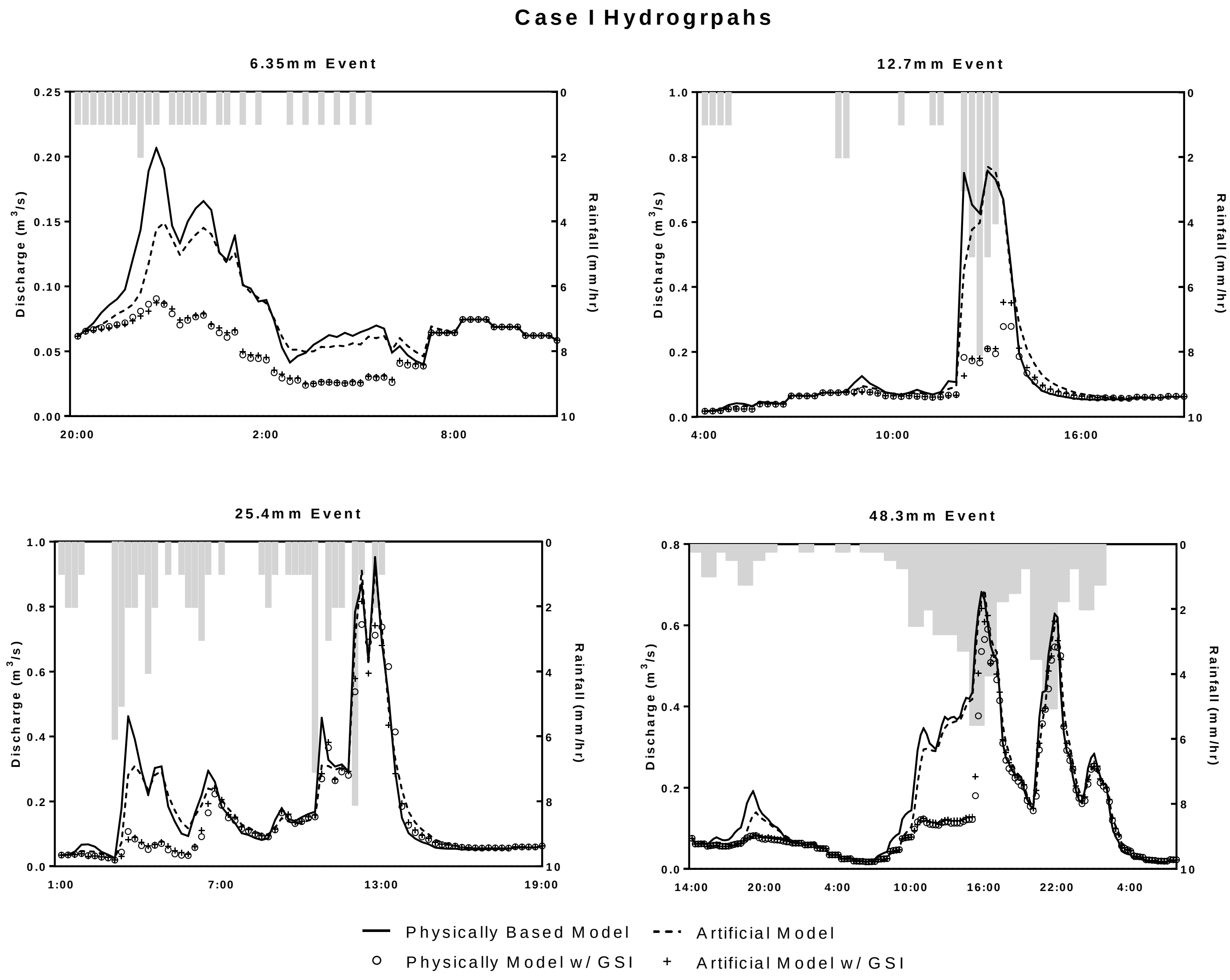
Case I Hydrogrpahs
6.35mm Event
12.7mm Event
25.4mm Event
48.3mm Event
Discharge (m3/s)
Rainfall (mm/hr)
0.25
0.20
0.15
0.10
0.05
0.00
20:00
2:00
8:00
4:00
10:00
16:00
1:00
7:00
13:00
19:00
14:00
20:00
4:00
10:00
16:00
22:00
4:00
Physically Based Model
Artificial Model
Physically Model w/ GSI
Artificial Model w/ GSI

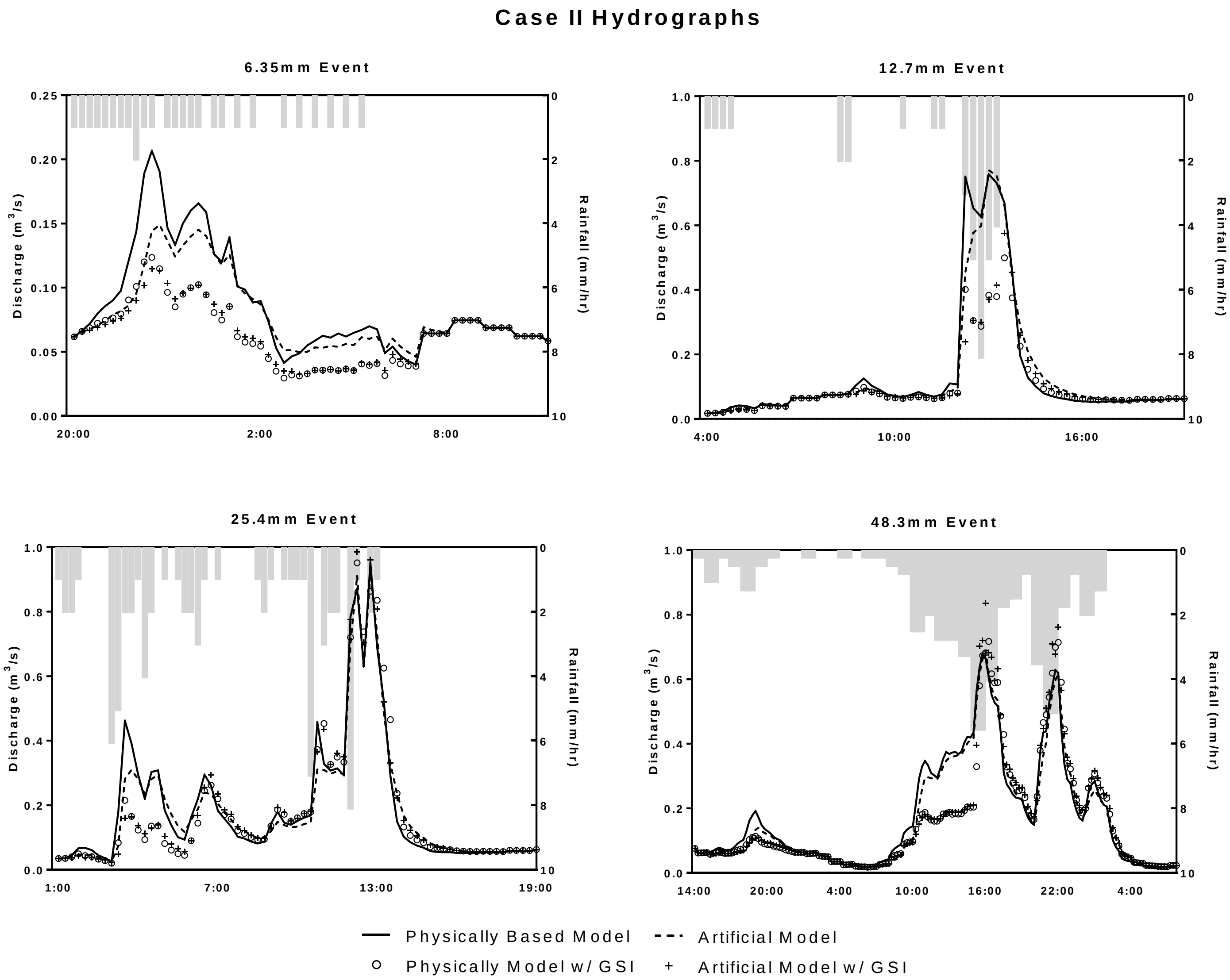
Case II Hydrographs
6.35mm Event
12.7mm Event
25.4mm Event
48.3mm Event
Discharge (m^3/s)
Rainfall (mm/hr)
0.25
0.20
0.15
0.10
0.05
0.00
0
2
4
6
8
10
20:00
2:00
8:00
1.0
0.8
0.6
0.4
0.2
0.0
4:00
10:00
16:00
1:00
7:00
13:00
19:00
14:00
20:00
4:00
10:00
16:00
22:00
4:00
Physically Based Model
Artificial Model
Physically Model w/ GSI
Artificial Model w/ GSI

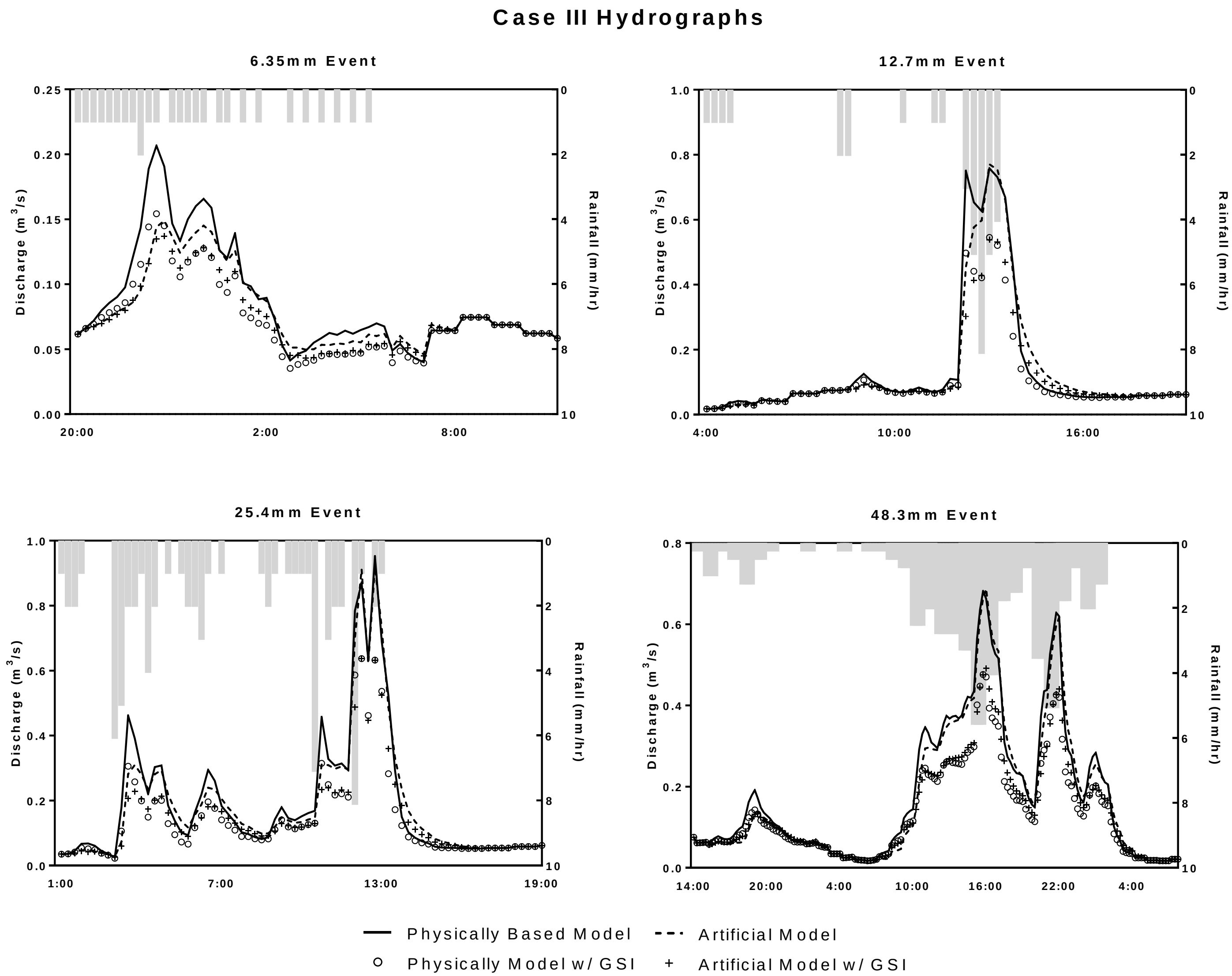
Case III Hydrographs
6.35mm Event
12.7mm Event
25.4mm Event
48.3mm Event
Discharge (m3/s)
Rainfall (mm/hr)
20:00
2:00
8:00
4:00
10:00
16:00
1:00
7:00
13:00
19:00
14:00
20:00
4:00
10:00
16:00
22:00
4:00
Physically Based Model
Artificial Model
Physically Model w/ GSI
Artificial Model w/ GSI

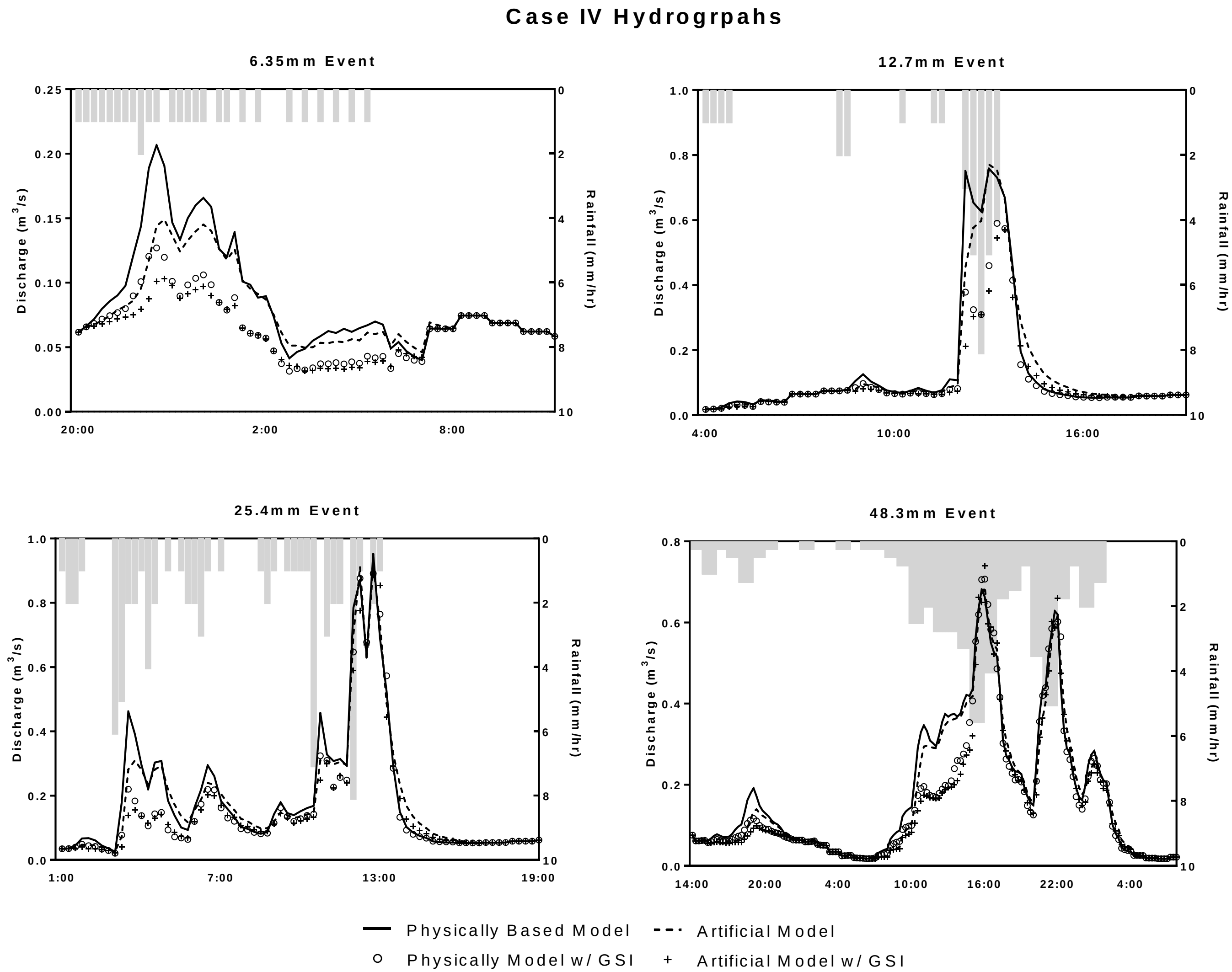

Figure 4.5: *Selected hydrographs the simulated GSI scenarios over varying rainfall depth*

Discussion

The artificial model was used to perform further analysis including comparing the GSI scenarios, spatial placement effects of GSI, and the impacts of GSI on climate change. The previous results suggest that the artificial model is an appropriate substitute for the physically based model.

GSI Scenarios

The GSI scenarios were simulated in the artificial model comparing each scenario in terms of volumetric and peak flow reductions binned by storm depth (Figure 4.6). Case I representing the maximum level of GSI implementation and a total estimated price of $82,000,000 was able to capture 54% of the total rainfall in the area. Because 69% of the total area had some form of GSI managing runoff, most small storms were nearly completely captured and peak flows greatly reduced. In Cases II and III, which each focused on one particular type of GSI, green roofs alone showed greater potential to manage runoff in smaller storms than ROWBs mainly because they completely covered 35% of the catchment reducing the overall imperviousness. In some larger events, Case II resulted in higher peak flow rates compared to baseline conditions (illustrated in the previous hydrographs). While the green roof was able to reduce the onset of the storm, once the green roof became saturated it became essentially hydrologically impervious. The increase in peak could be the result of latent water seeping from the green roof contributing to the peak, however, this effect was not expected and not fully understood. In contrast, the ROWBs in Case III showed consistent reductions across all storms and were able to manage larger storms more effectively. Annually, both cases had similar total volumetric reductions of 31% in Case II and 34% for Case III at an estimated cost of $32,000,000 and $50,000,000 respectively. Case IV was combination of green roofs installed on 39% of the roofs and ROWBs installed at a 40:1 HLR for a total cost of $25,000,000, the cheapest of all the scenarios. This scenario produced results similar to the Case II both in terms of volumetric and peak flow reductions and a total annual runoff reduction of 30%. By implementing some form of

GSI throughout the catchment, even at lower levels of implementation, significant levels of runoff reductions were achieved at a lower cost.

Spatial Analysis

Spatial effects of LID controls in the model were considered in order to investigate whether one particular layout of GSI was more effective than another. While this analysis could be accomplished using a physically based model, using artificial fractal models allows for quicker analysis with placement based on more perfect geometry. The amount of GSI simulated was based on Case IV described above. In one scenario, Case IVa, GSI was distributed only to the top subcatchments of the artificial sewershed. In another scenario, Case IVb, only one side of the sewershed received GSI. The layout of these configurations is shown in Figure 4.7. The scenarios were compared to the evenly distributed Case IV model described above.

The results of this analysis are shown in Figure 4.8 comparing the volumetric and peak flow reductions of each scenario binned by storm size. The results showed that in terms of volumetric reductions, evenly spacing GSI will produce the greatest benefits as this maximizes the amount of impervious space serviced by GSI. The same was generally true in terms of peak flow reductions; however, for storms between 15-50 mm, the two uniquely placed scenarios reduced peak runoff more than the evenly distributed scenario. This could be the result of a delay in peak flow expected from GSI implementation. Because the peak flow of the untreated parts of the catchments will occur before the treated parts, given certain rain events, this peak will have passed before the peak of the GSI treated subcatchments comes to concentration.

Effect of Climate Change

The effect of climate change on the annual design precipitation pattern was simulated under Case I, Case IV, and baseline conditions (Figure 4.9). Case I was highlighted in this regard to illustrate an upper bound of results to expect from GSI implementation and Case IV to illustrate a more reasonable level of GSI implementation. The climate change adjusted model produced 78 mm more annually than the baseline resulting in 7% more annual discharge. This annual increase resulted in 11% more annual discharge in the Case I scenario and 7% in Case

IV. Extreme rainfall events considered in this analysis ranged from 133-169 mm which were significantly larger than the events simulated over the typical 1992 annual rainfall year. Considering the 10-year 24 hour extreme events, Case I GSI implementation was able to reduce total storm discharge volumes by 12-19% and peak discharge rates 23-27% depending on the intensity of the storm (Table 4.6). This means that even the most aggressive GSI implementation strategy should only be considered a component of an adaptation strategy if the goal is to reduce flooding in the area.

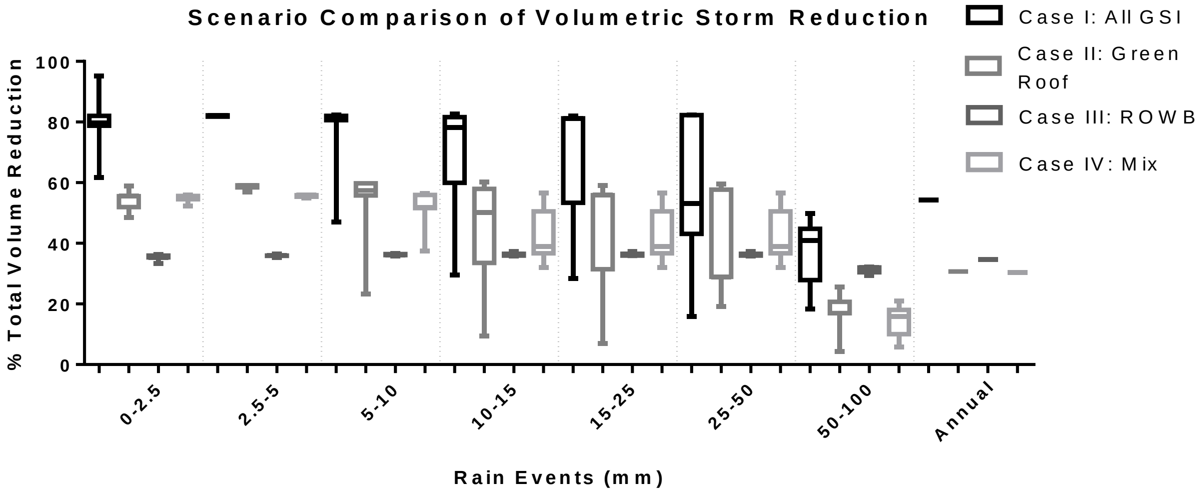

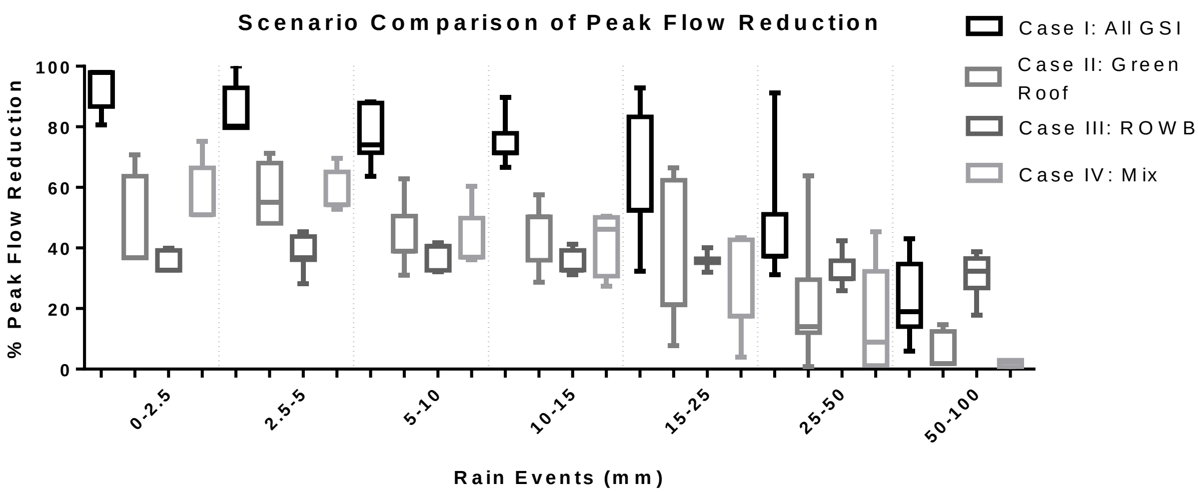

Figure 4.6: *Volumetric and peak flow reductions of the simulated GSI scenarios*

Spatial LID Control Scenarios

Case IVa:
LID focused at the top of the sewershed

Case IVb:
LID focused on one side of the sewershed

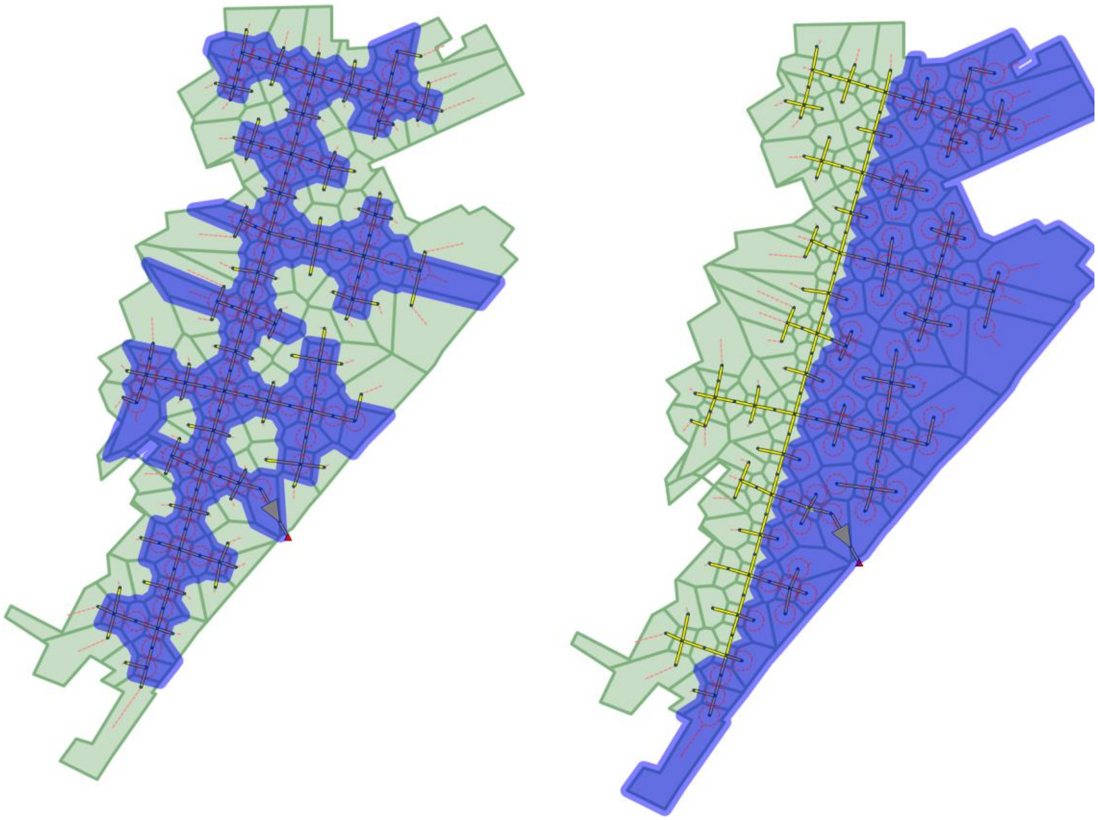

Figure 4.7: *Spatial configurations of LID controls simulated in the artificial network. Presence of LID is shown in the lighter region of the network. GSI concentrated at the top of the catchment (left) resulted in 41% of the impervious treated by GSI and when concentrated on one side of the catchment (right) resulted in 38% treated.*

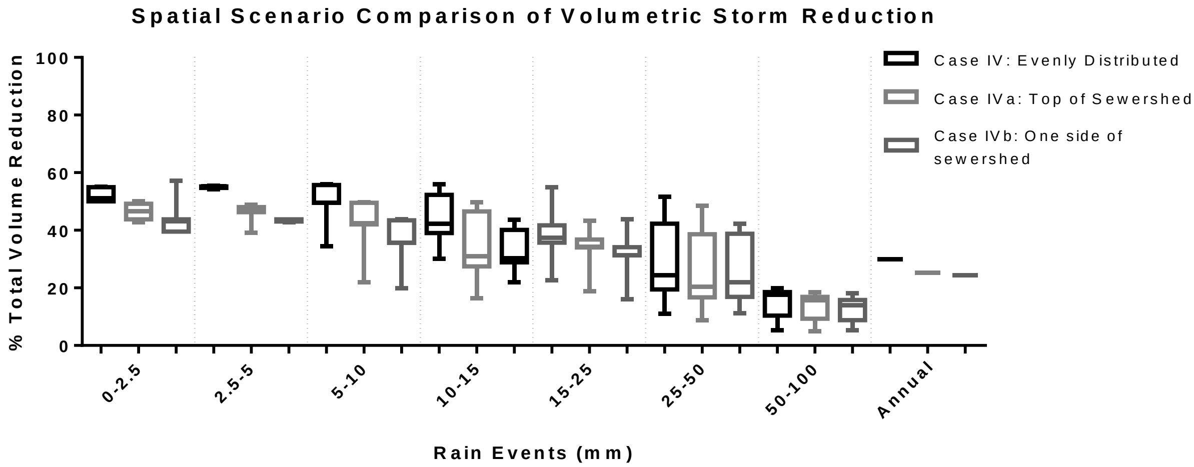

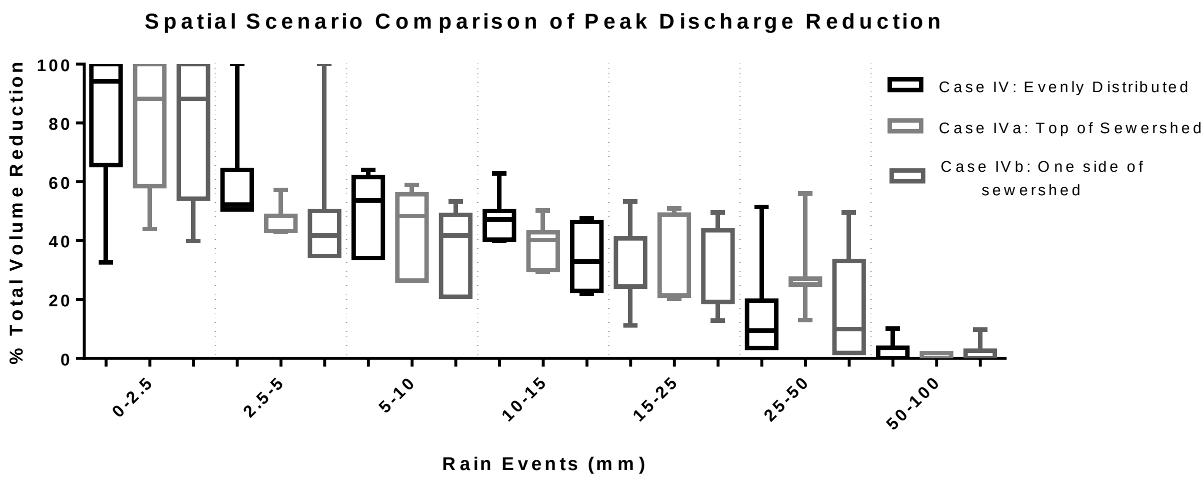

Figure 4.8: *Volumetric and peak discharge reductions of various LID spatial configurations*

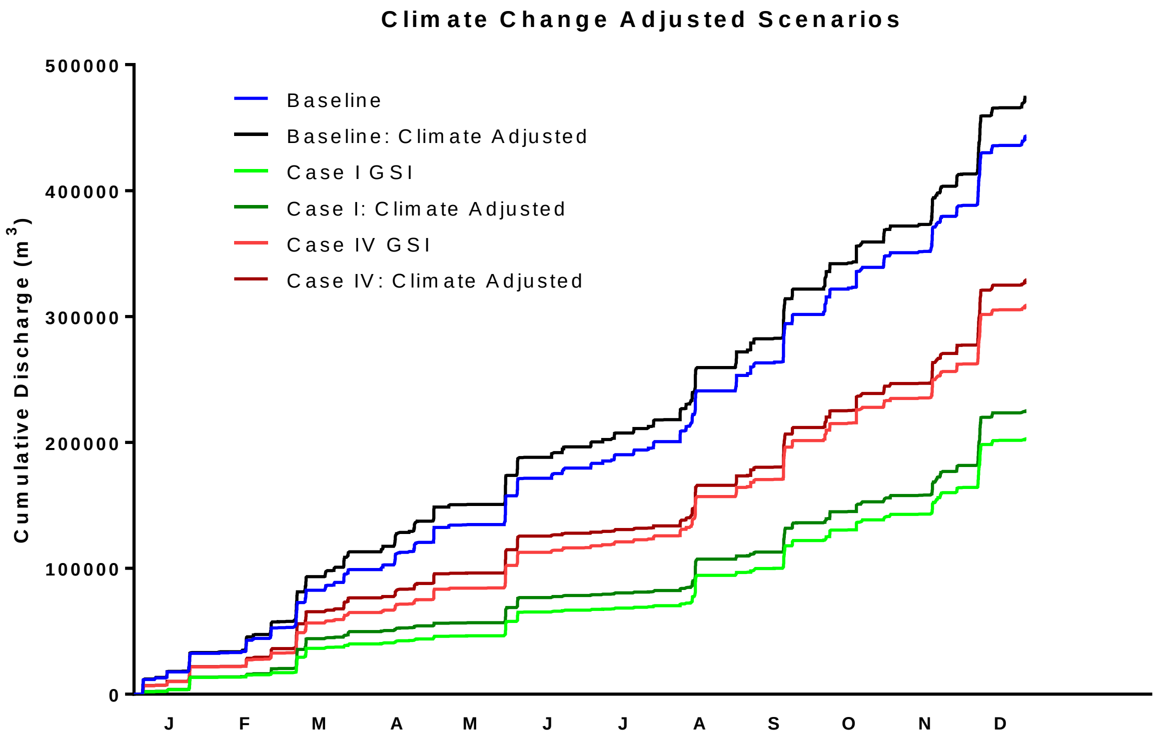

Figure 4.9: *Climate Adjusted Annual Rainfall under Case I and IV GSI scenarios*

Table 4.6: *Extreme event discharge reductions due to Case I greening scenario*

	Baseline		**2035**		**2060**		**2100**	
Emission Scenario	**B2**	**A1Fi**	**B2**	**A1Fi**	**B2**	**A1Fi**	**B2**	**A1Fi**
Storm Depth (mm)	133	133	141	142	146	153	154	169
% Volume Reduction	19%	19%	17%	17%	17%	16%	16%	12%
% Peak Reduction	27%	27%	28%	27%	28%	25%	26%	23%

Conclusions

The first aspect of this research was to assess the ability of an artificial model to model GSI relative to a physically base model. Overall, the model performance was comparable and in this circumstance artificial model GSI simulations are an appropriate substitute to the physically based counterpart. While both models were previous calibrated to observed flow without GSI, the main missing component of this analysis was a comparison to observed flow measurements with GSI to assess model accuracy. This, however, would be difficult given that multiple hypothetical scenarios were modeled.

The second aspect of this research was to demonstrate how the artificial models can be applied to address questions related to GSI planning and development. The analyzes performed highlight some of the ways that artificial networks could be utilized through a case study in East Boston. Comparing various GSI implementation scenarios for the study location, the most effective strategy in terms of costs and benefits is a combination of green roofs and ROWBs to maximize the amount of impervious area treated. To maximize total storm volume reductions, evenly distributing the GSI throughout the catchment provides the best results again, by maximizing the total the amount of impervious area serviced by GSI; however, other configurations could provide greater reductions in peak flows for larger events.

Related to the impact of climate change, the GSI scenarios simulated show that even small amounts of GSI implementation can manage the additional runoff projected in typical annual rainfall. When considering extreme events, however, GSI can only play a small in reducing total storm volume and peak flow if flood control is a priority. To better model the effect that GSI will have on urban flood control in the catchment, a digital elevation model (DEM) coupled with 2-D flood modeling could show location specific flood points. These types of models consider the effect of buildings and overland flow paths not considered in typical SWMM models. This would also enable a more tailored approach to GSI spatial placement concentrated in areas to reduce the flood burden on the most affected areas.

Roy et al. (2008) previously discussed that a key reason that GSI implementation has been slow in municipal drainage systems is because the engineers and planners responsible for these systems have not be fully convinced that GSI can provide relief from urban flooding or CSOs which they are typically under consent agreements to manage. While it is often required by the US EPA to have GSI as part of a larger sewer infrastructure plan, it can be seen as only a component to the larger stormwater management plan in conjunction with typical grey infrastructure. Understanding how GSI fits into that larger master plan in terms of the amount of GSI to build, the locations to implement, the longevity of the systems, how they will function over changing climates, and other uncertainties is part of ongoing research across the academic, municipal, and professional spectrum. Computer enabled modeling provides a powerful tool to address these uncertainties, but as Cantone and Schmidt (2009) point out, it is common for municipalities to rely of low resolution models that have been shown to misrepresent observed data. The reason for implementing these models is to reduce the time and monetary costs associated with the practice. The method described in this paper demonstrates a simple way to add higher resolution to a model and could theoretically be incorporated into existing municipal models.

List of References

Boston Water and Sewer Commission. (2013). *Boston Water and Sewer Commission 2014-2016 Capital Improvement Program,* .

Cantone, J., and Schmidt, A. (2011). "Improved Understanding and Prediction of the Hydrologic Response of Highly Urbanized Catchments through Development of the Illinois Urban Hydrologic Model." *Water Resour. Res.,* 47(8), W08538.

Cantone, J. P., and Schmidt, A. R. (2009). "Potential Dangers of Simplifying Combined Sewer Hydrologic/Hydraulic Models." *Journal of Hydrologic Engineering,* 14(6), 596-605.

Carpenter, D. D., and Hallam, L. (2010). "Influence of Planting Soil Mix Characteristics on Bioretention Cell Design and Performance." *J. Hydrol. Eng.,* 15(6), 404-416.

Carter, T., and Fowler, L. (2008). "Establishing Green Roof Infrastructure through Environmental Policy Instruments." *Environmental Management,* 42(1), 151-164.

CH2MHILL. (2013). *Phase I Stormwater Best Management Practices Implementation Plan,* Boston Water and Sewer Commission, .

City of New York Department of Environmental Protection Office of Green Infrastructure. (2016). "Standard Designs and Guidelines for Green Infrastructure Practices." .

Climate Ready Boston. (2016). *Climate Change and Sea Level Rise Projections for Boston,* .

De Sousa, Maria R C, Montalto, F., Spatari, S. (2012). "Using Life Cycle Assessment to Evaluate Green and Grey Combined Sewer Overflow Control Strategies." *Journal of Industrial Ecology,* 16(6), 901-913.

Ghosh, I., and Hellweger, F. L. (2012). "Effects of Spatial Resolution in Urban Hydrologic Simulations." *Journal of Hydrologic Engineering,* 17, 129-137.

Ghosh, I., Hellweger, F. L., Fritch, T. G. (2006). "Fractal generation of artificial sewer networks for hydrologic simulations." *Proc., Proceedings of the ESRI International User Conference, San Diego, California, August,* , 7-11.

Goldstein, A. (2011). "Comparison of a High and Low Spatial Resolution Model for an Urban Block and Implications for Depicting Low Impact Development." .

Jeffers, S., and Montalto, F. (in preparation). "Modeling Urban Sewer with Artificial Fractal Geometries." *Unpublished Material,* .

Jeffers, S., and Montalto, F. (in preparation). "Applying River Basin Scaling Laws to Urban Catchments." *Unpublished Material*.

Kansas City Water Services. (2013). *Kansas City's Overflow Control Program: Middle Blue River Basin Green Solutions Pilot Project Final Report,* .

Krebs, G., Kokkonen, T., Valtanen, M., Koivusalo, H., Setälä, H. (2013). "A High Resolution Application of a Stormwater Management Model (SWMM) using Genetic Parameter Optimization." *Urban Water Journal,* 10(6), 394-410.

McCuen, R. H., Johnson, P. A., Ragan, R. M. (1996). "Highway Hydrology: Hydraulic Design Series no. 2." *Highway Hydrology: Hydraulic Design Series no.2,* .

Moriasi, D. N., Arnold, J. G., Van Liew, M. W., Bingner, R. L., Harmel, R. D., Veith, T. L. (2007). "Model Evaluation Guidelines for Systematic
Quantification of Accuracy in Watershed Simulations." *American Society of Agricultural and Biological Engineers,* 50(3), 885-900.

National Resource Conservation Service. (2017). "Web Soil Survey." .

New York City Department of Environmental Protection. (2014). *NYC Green Infrastructure 2013 Annual Report,* .

Palla, A., and Gnecco, I. (2015). "Hydrologic Modeling of Low Impact Development Systems at the Urban Catchment Scale." *Journal of Hydrology,* 528, 361-368.

Philadelphia Water Department. (2016). *Pilot Program Final Report,* .

Pitt, R., Voorhees, J., Clark, S. (2010). "Integrating Green Infrastructure into a Combined Sewer Service Area Model " *World Environment Water Resource Congress 2010: Challenges of Change,* .

Rawls, W. J., Brakensiek, D. L., Miller, N. (1983). "Green-Ampt Infiltration Parameters from Soils Data." *J. Hydraul. Eng.,* 109(1), 62-70.

Rosa, D. J., Clausen, J. C., Dietz, M. E. (2015). "Calibration and Verification of SWMM for Low Impact Development." *JAWRA Journal of the American Water Resources Association,* 51(3), 746-757.

Roy, A. H., Wenger, S. J., Fletcher, T. D., Walsh, C. J., Ladson, A. R., Shuster, W. D., Thurston, H. W., Brown, R. R. (2008). "Impediments and Solutions to Sustainable, Watershed-Scale Urban Stormwater Management: Lessons from Australia and the United States." *Environmental Management,* 42(2), 344-359.

Selbig, W. R., and Balster, N. (2010). "Evaluation of Turf-Grass and Prairie-Vegetated Rain Gardens in a Clay and Sand Soil, Madison, Wisconsin, Water Years 2004-08." *U.S. Geological Survey Scientific Investigations Report 2010,* .

Smullen, J. T., Myers, R. D., Reynolds, S. K., Maimone, M. (2008). "A Green Approach to Combined Sewer Overflow Control: Source Control Implementation on a Watershed Scale " *11th International Conference on Urban Drainage, Edinburgh, Scotland, UK,* .

U.S. Census Bureau. (2010). "2010 Census." .

United States Environmental Protection Agency. (2017). "National Stormwater Calculator." (1.2), .

United States Environmental Protection Agency. (2014). *SWMM-CAT User's Guide,* .

US EPA. "Storm water management model (SWMM)." <https://www.epa.gov/water-research/storm-water-management-model-swmm> (Mar 22, 2017).

WASTEWATER PLANNING USERS GROUP. (2006). *GUIDE TO THE QUALITY MODELLING OF SEWER SYSTEMS;* .

Water Environment Federation. (2014). *Green Infrastructure Implementation,* WEF, .

Wayne C Huber. (2006). *BMP Modeling Concepts and Simulation;* .

Zellner, M., Massey, D., Minor, E., Gonzalez-Meler, M. (2016). "Exploring the Effects of Green Infrastructure Placement on Neighborhood-Level Flooding Via Spatially Explicit Simulations." *Computers, Environment and Urban Systems,* 59, 116-128.

Chapter 5: Conclusion

In the conclusion to this dissertation, the initial research questions will be presented along with the results and conclusions from each corresponding chapter. The original motivating question for this research was to answer the question “What impact will GSI have on urban hydrology?” In answering this fundamental question, three component questions were developed with subsequent associated hypotheses. The basic premise of the methodology to answer this larger question related to implementation of computer based modeling of artificial networks based on fractal geometries. The logic to apply this method was to first show that fractal geometries exist in urban drainage networks to build confidence that they could be modeled and simulated as such (Chapter 2). Based on these results, artificial models and the methodology associated with their implementation were developed in urban catchments (Chapter 3). The success of artificial models to simulate urban hydrology to observed flow enabled their use to simulate GSI in place of traditional physically based models and answer questions related to the practice (Chapter 4). The following will discuss these results in more detail and summarize the key points learned in each component of the work.

1) Are sewers fractals?
    a) Hack’s Law is valid in urban sewersheds.

Three urban catchments were analyzed using municipal sewer maps obtained in East Boston, Massachusetts (54 and 65 ha) and Bronx, New York (149 ha) by relating sewer length to its receiving drainage area. The relationship of length to drainage area fit the Hack’s Law prediction with an $R^2 > 0.86$ in each catchment. Stronger correlations were found in larger drainage areas, which is expected in natural river basins, the context in which Hack’s Law was originally developed.

    b) Existing sewersheds can be geometrically defined using Horton ordering.

One of the most defining characteristics of fractal geometries is scale invariance or self-similarity. Horton ordering is another method developed in natural river basins to assess how one order of a network relates to the other orders in the network. Perfect fractal geometries would have equivalent Horton ordering across all scales. On average, network bifurcation, the length-order ratio, the drainage density, the area-order ratio, and the pipe diameter-order ratio were all relatively consistent in the orders of the three catchments; however, the standard deviations were significantly high as would be expected in heterogeneous, often complex urban drainage networks in these two older United States cities. The most deviation from the trend was found in the highest part of the catchment (top of the sewershed). Another interesting finding of this analysis was that the fractal dimension of network (a measurement characteristic of the drainage density) was between 1.79-1.85 compared to 1.82 typical of natural river basins.

2) Can the sewershed be hydrologically modeled with artificial fractal geometries?
    a) Artificial networks can simulate urban hydrology as well as physically based models.

Artificial sewer networks based on fractal geometries were created and used to build SWMM models for two catchments (54 and 24 ha) in East Boston, Massachusetts. These models were compared to traditional physically based models that incorporated the actual sewer pipe locations, diameter, inverts, and realistic subcatchments at block scale resolution. The 54 ha model, along with its physically based counterpart, were calibrated to observed sewer flow, and both models were able to be calibrated with a NSE of 0.85 over the observed period encompassing 10 rain events between 0.5-12.7 mm. Both models predicted similar total event volumetric discharge and peak flow rates. A second analysis was done in the 22 ha catchment comparing an uncalibrated artificial model to an uncalibrated physically based model and, over an observed sewer flow period, resulted in NSE values of 0.75 and 0.85 respectively. Again, both models predicted similar volumes and peak flow rates, although in this case, the physically based uncalibrated model was more accurate.

b) Modeling a sewershed is more accurate using a high resolution fractal network than a lumped low resolution model.

Model resolution was also tested in the 54 ha catchment and showed that accurate simulations could be produced even in the lowest single subcatchment model. However, previous research has showed a much greater difference in lower resolution aggregated models. This could be because the catchment sizes in these studies were much bigger and had more pervious area. It is recommended the level of resolution employed in a model be a factor of the total catchment size. In this study, the catchment was 54 ha and 73% imperviousness so bigger catchments with less imperviousness could see these factors related to model aggregation can come into play. These potential issues can be avoided using artificial models.

3) Can GSI be modeled with artificial networks in urban catchments?

a) Artificial networks can simulate GSI as well as physically based models.

In the 54 ha urban catchment in East Boston, Massachusetts, GSI including infiltration based right of way infrastructure and green roofs were simulated in both an artificial fractal based model and a physically based model. Over the course of an annual 15-minute interval rainfall pattern, total rainfall event volumetric discharge was equivalent in both models. Peak event flow rates were also comparable, however, more variation was observed in larger events.

These questions were designed to build the case that artificial models can be used to analyze large scale GSI performance in an urban catchment and help address questions related to the practice. Chapter 4 of this dissertation largely serves as a case study and demonstration for their implementation. Below are a few of these questions that were discussed in this research:

1) What types of GSI are most effective?

Effectiveness in terms of GSI can be defined in many ways, but in this research it was defined by reductions in volumetric and peak event discharge and cost. Using literature reviewed GSI parameters as inputs into the calibrated SWMM in the 54 ha catchment in East Boston, various levels of green roof implementation and right of way infiltration based infrastructure were modeled using annual rainfall patterns. The results show that the most effective form of GSI to implement is related to the amount and type of space available to develop the systems. In the case of East Boston, the majority of the space was rooftops, so green roofs were a viable option (ignoring all other structure and political concerns). Using the right of way to install GSI is more likely a more feasible option as municipal entities have more control of how to use the space and can achieve significant results. This model, however, ignored design considerations of right of way GSI such as inlet design (which can result in bypass) and reductions in infiltration that can be expected over the lifetime of the systems, both of which can reduce system performance.

2) How much will various levels of implementations affect performance?

By looking at various levels of implementation of green roofs and right of way GSI, it was determined that the best way to effectively manage stormwater is to maximize the total amount of impervious area treated. In the case of green roofs, that means installing green roofs on the maximum amount of space. In the case of right of way GSI, that means installing systems to maximize the drainage areas that receive some form of treatment even it is means a higher hydraulic loading ratio for each system. This means that a combination of green roofs and right of way GSI is the best way to effect the most amount of impervious area.

3) Does the spatial position of GSI facilities throughout the catchment matter?

In line with the previous analysis, the most effective way to implement GSI found in this study catchment was to maximize the total amount of impervious area treated by GSI even if it means sacrificing low hydraulic low ratios in the infiltration based systems. When comparing the effect of clustering the systems at the top of the sewershed or clustering entirely on one side of the sewershed, it was shown that, although in some cases peak event rates can be reduced, overall performance is worse than an evenly distributed approach.

4) What role can GSI play to manage extreme precipitation events and changing rainfall patterns associated with climate change?

The effect of climate change in East Boston based on CMIP3 projections 30-60 years in the future predicted a 7% increase in annual precipitation. The various levels of GSI simulated in this analysis showed that total annual discharge would be reduced 30-54% annually, significantly more than the projected increased in precipitation. This means that GSI would be more than capable to maintain current baseline conditions in the system. In terms of extreme events, GSI was less able to address the concern. Even the most aggressive implementation strategy simulated (69% of impervious area treated) only reduced the projected 10-year design storms by 12-19% and the peak flows by 23-27% depending on climate trends. This analysis shows that GSI has a role to play in addressing extreme events; however, it should be considered a component in a larger strategy if the main objective is to reduce infrastructure vulnerability and flood control.

Significance

This research serves three purposes: 1) to bridge the gap between fractal river basin analysis and urban hydrology, 2) improve confidence in artificial networks for modelling urban drainage networks, and 3) demonstrate how artificial networks can be used to understand contemporary GSI implementation strategies. It provides a fundamental foundation for analyzing urban drainage networks by applying river basin scaling laws that have only been theorized or partially developed in previous work. While artificial network applications in modeling urban drainage networks have been done in the past, this research adds confidence in their application by basing the analysis in observed measurements and more thoroughly scrutinizing the model hydrologic response. In addition, this work demonstrates how artificial networks can be used to address contemporary stormwater management issues such as GSI applications and increasing precipitation patterns due to climate change.

Limitations / Future Work

While this research contributes to the scope of sewershed fractal geometry, in order to create general rules that could be applied universally, more sewer network should be analyzed to understand how these rules should be applied throughout different municipal systems. Further, it is important to determine the applicability of fractal artificial models in less urbanized areas or places with less homogenous topography. It may also be the case that newer cities have different fractal relations than older cities or that zoning and planning (or the lack thereof) influence the dynamics of the system.

The use of ANGel played a major role in the development of the artificial models. One of the features that was not fully explored was the ability to introduce irregularity to the network such that the fractal branches will branch at irregular angels rather than 90-degree bends (Figure 5.1). In addition, this irregularity can be stochastically or deterministically generated based on input into the ANGel program (Ghosh et al., 2006). Further analysis could make use of this tool to understand how this variability in artificial modelling should be adjusted to improve the performance. One way this could be accomplished it to stochastically generate several different networks and compare the hydrologic response in their associated SWMM models and observe statistical variability.

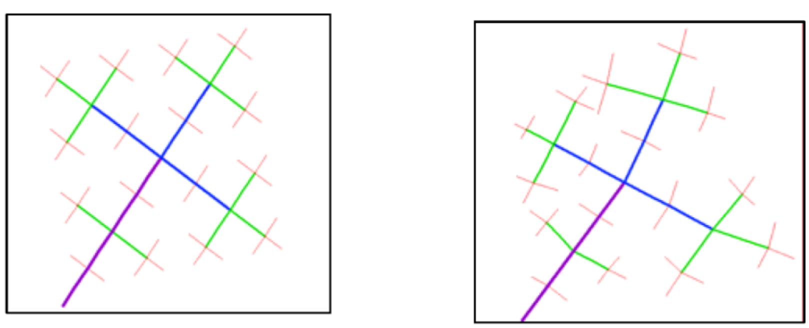

Figure 5.1: *The default fractal network (left) compared to the irregular network (right) (reproduced from Ghosh et al., 2006)*

A newer version of ANGel was in development that enables the network to be generated with Peano, H-Tree and NFB fractal geometries (Ghosh, 2010). When considering different topography and level urbanization, each type could be more application than another. In order to determine the most application fractal geometry to employ for a given area, future analysis is recommended. This type of study would individually vary parameters such as the topography, urbanization, and location for each fractal type (Table 5.1) to broaden the understanding of the best ways to implement artificial networks in future scenarios. It was stated that ANGel is in the public-domain (Ghosh et al., 2006), however, no public URL for download was found. It was obtained in this research by direct contact with the authors.

Table 5.1: *Parameters to consider in a future analysis*

Parameters to Adjust in Further Analysis	
	Parameter
Fractal Type	
	Tokunaga
	Peano
	H-Tree
	NFB
Topography	
	Slope
Urbanization	
	Population Density
	% Impervious
Location	
	Age of city
	Proximity to water
	Climate

One of the main critiques of the fractal models used in this study is that they do not incorporate topological characteristics of the catchment to define conduit and catchment slopes and widths. In this regard, Digital Elevation Models (DEMs) have shown promising applications in urban hydrologic modeling as they are able to take topographic information and create drainage networks based on elevation gradient (J. Schellekens et al, 2014). However, because urban drainage networks often do not follow the elevation gradient as is expected in natural river basins, generating a model based on a DEM can produce misleading results and requires information regarding the structure of the network. In one study built on applied fractal river basin analysis developed by Rodriguez et al. (2005), a DEM was implemented alongside sewer pipe location data to generate a model with accurate results for a large urban catchment in France (Rossel et al., 2014). Likewise, Blumensaat et al. (2012) developed a method to use DEM to generate artificial sewer pipe layouts that are relatively similar to actual layouts with assumed pipe diameters based on catchment characteristics with SWMM simulation results comparable to observed flow (NSE 0.51-0.73). It is possible that implementing a DEM alongside a fractal artificial sewer network generating tool such as ANGel would produce more realistic catchment parameters and conduit slopes and thus generate more accurate results particularly related to peak flow. In relation to GSI implementation and its role in urban flood mitigation, a digital elevation model (DEM) coupled with 2-D flood modeling could show location specific flood points. These types of models consider the effect of building and overland flow paths not considered in typical SWMM models. This would also enable a more tailored approach to GSI spatial placement concentrated in areas to reduce the flood burden on the most affected areas. It is recommended that future development of the methods and ideas discussed in this research incorporate DEMs and 2-D flood based modeling to develop new sophisticated, yet accessible ways to tailor GSI to municipal systems.

List of References

Blumensaat, F., Wolfram, M., Krebs, P. (2012). "Sewer Model Development Under Minimum Data Requirements." *Environ Earth Sci*, 65(5), 1427-1437.

Ghosh, I., Hellweger, F. L., Fritch, T. G. (2006). "Fractal generation of artificial sewer networks for hydrologic simulations." *Proc., Proceedings of the ESRI International User Conference, San Diego, California, August,* , 7-11.

Ghosh, I. (2010). "Characterizing and Understanding the Effects of Spatial Resolution in Urban Hydrologic Simulations." .

Rodriguez, F., Cudennec, C., Andrieu, H. (2005). "Application of Morphological Approaches to Determine Unit Hydrographs of Urban Catchments." *Hydrol. Process.,* 19(5), 1021-1035.

Rossel, F., Gironás, J., Mejía, A., Rinaldo, A., Rodriguez, F. (2014). "Spatial Characterization of Catchment Dispersion Mechanisms in an Urban Context." *Advances in Water Resources,* 74, 290-301.

Schellekens, J., Brolsma, R. J., Dahm, R. J., Donchyts, G. V., Winsemius, H. C. (2014). "Rapid Setup of Hydrological and Hydraulic Models using OpenStreetMap and the SRTM Derived Digital Elevation Model." *Environmental Modelling & Software,* 61, 98-105.

Vita

Scott Jeffers is a licensed Professional Engineer who believes in designing sustainable solutions for urban environments through green infrastructure and low impact design. He received a MS in Civil Engineering: Water Resources and MS/BS in Environmental Engineering graduating cum laude with distinction June 2012 from Drexel University. He has studied abroad at University of Sheffield Sheffield, UK in the Fall of 2008. He has worked as a consulting engineer at the Mott MacDonald Philadelphia, PA office since 2014 designing stormwater management systems in Philadelphia. Key projects include a neighborhood-wide stormwater sewer system that drains to surface green stormwater infrastructure practices and underground infiltration basins. Other responsibilities include presenting stormwater permit codes to clients and ensuring compliance. He has been a member of the Drexel Sustainable Water Resource Engineering Lab since 2011. He has taught at Drexel University as both an adjunct faculty and engineering teaching fellow since 2014 teaching Differential Equations, Hydrology, Hydraulics, Physics: Light and Wave Optics, Physics: Electricity and Magnetism, and the Freshman Engineering sequence. He a member of the Water Environmental Federation, the American Society of Civil Engineers, the American Water Works Association, and the American Water Resource Association. He has been awarded the Pennsylvania American Water Works Association Fresh Ideas Contest (2nd Place, 2014), a National Science Foundation Honorable Mention (2011), the A.J. Drexel Academic Scholarship (2007-2012), and obtained a Certificate in Toxicology and Industrial Hygiene from Drexel University (2012). His work has been presented at academic and professional conferences throughout the United States.